Dynamics of irregular wave ensembles in the coastal zone

Ekaterina Shurgalina

ÉCOLE CENTRALE MARSEILLE

THÈSE

pour obtenir le grade de
Docteur de l'École Centrale Marseille
École Doctorale (ED 353)

Sciences pour l'Ingénieur : Mécanique, Physique, Micro et Nanoélectronique
Discipline : Mécanique et Physique des Fluides

Dynamique de champs de vagues irréguliers en zone côtière

présentée par

Ekaterina SHURGALINA

Directeurs de thèse : Prof. Christian KHARIF et Prof. Efim PELINOVSKY

soutenue le 22 avril 2015 devant le jury composé de :

EZERSKY Alexander	(Rapporteur)	Professeur, Université Caen Basse Normandie
KHARIF Christian	(Co-Directeur)	Professeur, Ecole Centrale Marseille
KIMMOUN Olivier	(Examinateur)	MdC, Ecole Centrale Marseille
PELINOVSKY Efim	(Co-Directeur)	Professeur, Nizhny Novgorod State Technical University, Nizhny Novgorod
SHAMIN Roman	(Rapporteur)	Professeur, Peoples' Friendship University of Russia, Moscow
TALIPOVA Tatiana	(Examinateur)	Professeur, Institute of Applied Physics, Nizhny Novgorod

Acknowledgements

I would never have been able to finish my dissertation without the guidance of my committee members, help from friends, and support from my family.

Foremost, I would like to express my deepest gratitude to my Russian advisor Prof. Efim Pelinovsky for the continuous support of my PhD study and research, for his patience, motivation, enthusiasm, and immense knowledge. His guidance helped me in all the time of research and writing of this thesis. I could not have imagined having a better advisor and mentor for my PhD study.

I would like to express my sincere gratitude to my French advisor, Prof. Christian Kharif, for his guidance, caring, patience, and providing me with an excellent atmosphere for doing research during my stay in France.

My sincere thanks also goes to MdC Olivier Kimmoun for giving the knowledge about experimental work and for leading me working on the experiment devoted to the soliton generation in Ecole Centrale Marseille.

I would also like to thank my colleagues Prof. Tatiana Talipova, Phd. Alexey Slunyaev and Phd. Anna Sergeeva for the scientific conversations which helped enrich the knowledge and the scientific experience, the Head of the Chair of Applied Mathematics of Nizhny Novgorod State Technical University n.a. R.E. Alekseev, Dr. Andrey Kurkin, for giving me the opportunity to finish this thesis and to have a dissertation defense in time.

I would like to say special thanks to Evan Walters for his huge support with the translation of the dissertation into English.

Last but not the least, I would like to thank my family: my parents Gennady Shurgalin and Olga Osipova, and my elder sister Tatiana Shurgalina for supporting me spiritually throughout my life. My sincere thanks goes to my dear friend Sergey Zakharov, he was always supporting me and encouraging me with his best wishes.

ABSTRACT

Surface and internal gravity waves have an important impact on the hydrological regime of the coastal zone. Intensive surface waves are particularly interesting to study because they can be a serious threat to ships, oil platforms, port facilities and tourist areas on the coast; such waves hampered the implementation of human activities on the shelf. Nonlinear internal waves affect the underwater biosphere and cause sediment transport, they create washouts soil at the base of platforms and pipelines, affect the propagation of acoustic signals. Freak waves have a particularly strong impact, and they are studied in this thesis. Therefore, the study of freak wave formation in the coastal zone is relevant and practically significant.

The main goal of the thesis is the study of particularities of abnormal wave formation in coastal zones under different assumptions on the water depth and wave field form. In particular, it is demonstrated that the mechanism of dispersion focusing of freak wave formation "works" for waves interacting with a vertical barrier. It is shown that just before the maximum wave formation a freak wave quickly experiences a shape change from a high ridge to a deep depression. The lifetime of a freak wave increases with the growth of number of individual waves in anomalous wave packets, and the lifetime of a freak wave increases as water depth decreasing.

It is demonstrated that pair interaction of unipolar solitons lead to a decrease of the third and fourth moments of a wave field. It is shown that in the case of heteropolar soliton interactions the fourth moment increases.

The nonlinear dynamics of ensembles of random unipolar solitons in the framework of the Korteweg - de Vries equation and the modified Korteweg - de Vries equation is studied. It is shown that the coefficients of skewness and kurtosis of the soliton gas are reduced as a result of soliton collisions. The distribution functions of wave amplitudes are defined. The behavior of soliton fields in the framework of these models is qualitatively similar. It is shown that in these fields the amplitude of the large waves is decreased in average due to multi-soliton interactions.

A new breaking effect of solitons with small amplitudes and even changing of its direction in multi-soliton gas as a result of nonlinear interactions with other solitons is found in the framework of the modified Korteweg-de Vries equation.

It is shown that in heteropolar soliton gas abnormally large waves (freak waves) appear in the frameworks of the modified Korteweg - de Vries equation. With increasing of soliton gas density the probability and intensity of freak waves in such systems increases.

Keywords: freak waves, turbulence, soliton, model equations

RÉSUMÉ

« Dynamique de champs de vagues irréguliers en zone côtière »

Les vagues et les ondes internes de gravité ont un impact important sur l'hydrodynamique et l'hydrologie de la zone côtière. Les vagues extrêmes sont particulièrement intéressantes à étudier, car elles sont une menace sérieuse pour le transport maritime, les plates-formes pétrolières, les installations portuaires et les zones touristiques de la côte. Ces ondes entravent aussi les activités humaines développées à la côte. Les ondes internes non linéaires affectent la biosphère aquatique, notamment le transport de sédiments et créent des affouillements à la base des plates-formes et des pipelines. Elles affectent également la propagation des signaux acoustiques. Les vagues scélérates provoquent d'importants dégâts matériels et de nombreuses pertes en vies humaines. Par conséquent, l'étude de la formation des ondes scélérates dans la zone côtière est d'une importance capitale. L'objectif principal de la thèse est l'étude de la formation d'ondes océaniques anormales dans la zone côtières pour différentes profondeurs d'eau et différents champs d'ondes. Il est montré que le mécanisme de focalisation dispersive à l'origine de la formation d'ondes scélérates est pertinent quand les ondes interagissent avec une paroi verticale. Il est démontré que juste avant la formation de l'onde maximale, celle-ci change rapidement de forme, d'une haute crête vers un creux profond. La durée de vie de l'onde scélérate augmente avec le nombre d'ondes individuelles contenues dans le paquet d'ondes anormales et lorsque la profondeur de l'eau diminue.

Il est démontré que l'interaction de paires de solitons unipolaires conduit à une diminution des facteurs de dissymétrie et d'aplatissement du champ d'ondes. Il est prouvé que dans le cas d'interactions hétéropolaires de solitons, le facteur d'aplatissement augmente.

La dynamique non linéaire de champs de solitons unipolaires aléatoires est étudiée dans le cadre de l'équation de Korteweg - de Vries (KdV) et de l'équation de Korteweg - de Vries modifiée (mKdV). Il est montré que les coefficients de dissymétrie et d'aplatissement du gaz de solitons sont réduits à

la suite de collisions de solitons. Les fonctions de distribution des amplitudes des ondes sont obtenues. Le comportement des champs solitoniques dans le cadre de ces modèles est qualitativement similaire. Il est démontré que l'amplitude des ondes extrêmes diminue en moyenne en raison des interactions entre multi-solitons.

Dans le cadre de l'équation de Korteweg-de Vries modifiée, les interactions non linéaires entre le soliton de plus petite amplitude et les autres solitons du gaz ont pour effet de réduire sa célérité qui devient négative et de modifier ainsi sa direction de propagation.

A partir de l'équation de Korteweg-de Vries modifiée, il est prouvé que dans un gaz de solitons héteropolaires, des ondes scélérates peuvent se former. La probabilité d’occurrence et l’amplitude des ondes scélérates dans de tels systèmes augmente avec la densité du gaz de solitons.

Mots-Clés : soliton, turbulence, vagues scélérates, équations modèles

Table of contents

1 Introduction **10**

2 Linear interference of random waves and the appearance of abnormally large waves **15**

2.1 Introductory remarks……...……..16

2.2 Mechanism of dispersive focusing of freak wave appearance……..17

2.3 Various forms of freak waves in case of swell and wind wave interaction…..24

2.4 Wave interaction with a vertical barrier……....38

2.5 Conclusion……...…...…..45

3 Two-soliton interactions in nonlinear models of long water waves **46**

3.1 Introductory remarks…….47

3.2 Observation of solitons in the coastal zone and the basic equations……48

3.3 Two-soliton interactions in the framework of the Korteweg – de Vries equation …….64

3.4 Two-soliton interactions in the framework of the modified Korteweg – de Vries equation……..…66

3.5 Conclusion……76

4 Soliton turbulence in the framework of some integrable long-wave models **77**

4.1 Introductory remarks…….……78

4.2 Nonlinear dynamics of irregular soliton ensembles in the framework of the Korteweg – de Vries equation…….……79

4.3 Unipolar soliton gas in the framework of the modified Korteweg – de Vries equation…….……..89

4.4 Freak waves in soliton fields in the framework of the modified Korteweg – de Vries equation…….97

4.5 Conclusion……..…106

5 Conclusions **.107**

A Annexes **108**

A.1 Publication dans le journal “Natural Hazards and Earth System Sciences”..108
A.2 Publication dans le journal “Fundamental and Applied Hydrophysics”……117
A.3 Publication dans le journal “Fundamental and Applied Hydrophysics”……119
A.4 Publication dans le journal “Izvestiya, Atmospheric and Oceanic Physics”.121
A.5 Publication dans le journal “Physics Letters A”……123
A.6 Publication dans le journal “Fundamental and Applied Hydrophysics”…...128
A.7 Publication dans le journal “Radiophysics and Quantum Electronics”…….130
References **132**

Chapter 1

Introduction

Wind waves on the surface of natural water bodies is a complex and irregular system caused by interference and interaction of wave packets moving with different speeds and in different directions. The ability to forecast them is extremely important for navigation and the exploration of ocean resources. Operational forecasting of wind waves is based on the nonlinear kinetic equations of spectral wave intensity, and significant progress has been achieved there [Efimov et Polnikov, 1991; Lavrenov, 1998; Komen et al, 1994; Annenkov et Shrira, 2013, 2014; Badulin et al, 2005, 2007].

In a random wind wave field abnormally large waves (rogue or freak waves) may appear. Although in the past such waves have been the subject of maritime folklore, fairytales, and adventurous literature, over time this has changed to not simply be the case. These waves are particularly interesting to study because they can be a serious threat to ships, oil platforms, port facilities and tourist areas on the coast. Numerous observations of freak waves in different areas of the oceans are presented in monographs [Kurkin et Pelinovsky, 2004; Kharif et al, 2009, Dotsenko et Ivanov, 2006] and catalogues [Didenkulova et al, 2006; Liu, 2007, 2014; Nikolkina et Didenkulova, 2011, 2012].

Initially, freak waves have been studied in relation to waves in deep water, and the first descriptions of such waves were made by sailors. Later, instrumental data started to be accumulated with appearance of oil and gas platforms in a sea. The boom in the freak wave study happened after the registration of the abnormally large wave height of 26m (in a water depth of 70 m) on the wave platform "Draupner" in the North Sea on January 1, 1995, this wave is called the “New Year wave” [Haver et Andersen, 2000]. Physical mechanisms of freak wave generation in deep water include: 1) modulation instability, 2) interaction of waves with currents, 3) wind-wave interaction; these mechanisms are described in the books [Kurkin et Pelinovsky, 2004; Kharif et al, 2009] and reviews [Kharif et Pelinovsky, 2003; Dysthe et al, 2008; Slunayev et al, 2011; Didenkulova et Pelinovsky, 2011].

Dangerous waves near the coast are usually considered independently, and in the past it was believed that they stem from a different physical nature. Against the background of such catastrophic events such as tsunamis and storm surges, short-lived abnormal waves attracted less attention. Nevertheless, the number of observations of the abnormally large waves near the shore is growing, and these waves have been termed freak waves.

Such waves are quite a surprise to many people spending their holidays near the water. A 9m high wave washed two people from the pier in South Africa on August 26, 2005 [Kharif et al, 2009]. Another incident happened in October, 1998 when a group of students who were on a practice field on the small island of Diana, near Vancouver Island, Canada [Kurkin et Pelinovsky, 2004].

The students were on a cliff about 25 meters above the water. After 45 minutes, one student noticed a big wave that started crashing on the shore. He took a few pictures in intervals of about 2 seconds (Fig. 1). After 4 seconds, the wave reached them, and if it had been slightly higher the consequences would have been tragic. The analysis of observed data, collected in the catalogue [Nikolkina & Didenkulova, 2011, 2012], shows that the largest number of registered freak waves that led to the destruction and even death, occurs in the coastal zone: in the shallow part of the ocean (less than 50 m depth) and on the coast. Remarkably, in the 5 year period from 2006 to 2010, 50% of all events caused by the freak waves occurred on the coast, 38.5% - in shallow water and only 11.5% on the deep parts of the ocean and on the high seas.

Although these statistics are incomplete (excluding the instrumental data), they show the prevalence of the freak waves in the coastal zone and on the coast, and that they require special analysis. Although the physical mechanisms of freak waves in shallow water are partly the same as in deep water, there are different mechanisms associated their interaction with the bottom and coasts [Kurkin et Pelinovsky, 2004; Kharif et al, 2009; Slunayev et al, 2011; Akhmediev & Pelinovsky, 2010; Didenkulova et Pelinovsky, 2011].

Figure 1 – consecutive frames (2 second interval) of freak wave approaching to the coast, its height reached 25 m.

Therefore, the study of freak wave formation in the coastal zone is relevant and practically significant. It should be understood that the water depth near shore is not necessarily small (in comparison with the wavelength).

Many incidents of freak wave appearance near steep cliffs were recorded, where the water depth is large enough. The importance of investigating such cases is demonstrated in articles of scientists from Taiwan [Tsai et al., 2004] due to numerous victims among fishermen, who are sitting on the breakwaters and rocks. The photographs given above demonstrate the same class of freak waves.

In this case, the well-developed theory of waves on infinite or finite depth can be used. Thus, freak waves are studied in the framework of the nonlinear Schrödinger equation and its generalizations, and here are few references [Onorato et al, 2001, 2002, 2003, 2005; Dysthe et al, 2003; Dyachenko et Zakharov, 2008; Slunyaev et Sergeeva, 2011, 2012; Sergeeva et Slunyaev, 2013; Shemer et al, 2010; Slunyaev et al, 2013]. It is also important to mention the study of freak waves within the Euler equations in conformal variables [Zakharov et al., 2014; Shamin, 2009; Shamin et Udin, 2013; Shamin et al., 2013, 2014; Shamin et Udin, 2014] and new class of "vortex" freak waves associated with interactions in the atmosphere [Abrashkin et Soloviev, 203; Abrashkin et

Soloviev, 2013, Abrashlin et Oshmarina, 2014]. However, the presence of vertical barriers has not been considered in the theoretical models of freak wave generation.

If the water depth in the coastal area is small, the new effects related to the strong difference from quasisinusoidal waveforms which is characteristic for deep water started to be important. Nonlinear waves in the coastal zone often have soliton or quasi-soliton structures. More frequently, such waves occur when a tidal wave enters an estuary, where they transform into shock waves (hydraulic jumps) or undular bores [Chanson, 2012] and they can have a very irregular structure. The same situation is realized for tsunami waves, when they propagate into shallow water [Tsuji et al, 1994; Grue et al, 2008]. The soliton structure of the wave field in shallow water has already been mentioned in the article [Brocchini et Gentile, 2001]. Nonlinear wave theory in shallow water is well developed. The most famous model is the Korteweg-de Vries equation, derived in 1895 [Korteweg & de Vries, 1895]. The main specificity of this equation is its applicability for waves propagating in one direction only. Accounting for counter-propagation (or the more general problem of wave interactions propagating in various directions) has also been discovered a long time ago, and in this case many varieties of Boussinesq equations were derived; see., e.g., [Pelinovsky, 2007]. In the framework of shallow water models there are a few works about freak waves, based on the approximation of the narrowband wave packet [Onorato et al, 2003; Pelinovsky et Sergeeva, 2006; Sergeeva et al, 2011] or the Korteweg-de Vries equation [Pelinovsky et al, 2000]. At the same time, analysis of freak waves in soliton field has never been performed before.

It is important to mention that due to vertical water stratification by temperature and salinity, as well as flow velocity, internal waves exist in the coastal zone [Morozov, 1996; Konyaev et Sabinin, 2002]. Internal gravity waves have the same nature as surface gravity waves, but for them, gravity is almost balanced by the force of Archimedes. Weakly nonlinear theory of internal waves in the coastal zone is also based on the Korteweg-de Vries equation [Mitropolsky, 1981], however, here the following amendments of the nonlinearity become important and it leads to Gardner equation. In the framework of this equation for some type of stratification the effect of modulation instability is possible, which leads to the generation of "internal" freak waves [Grimshaw et al, 2005, 2010; Talipova, 2011]. And here we can say that the soliton structure of

internal waves, which always was noted in the observations [Ostrovsky et Stepanyants, 1989; Vlasenko et al, 2005], have not been yet taken into account in the analysis of freak waves.

Outline of the thesis

The remaining thesis is arranged as follows:

Chapter 2 is devoted to the mechanism of dispersive focusing. The freak wave appearance near the vertical barrier is studied in the framework of this mechanism. The interaction of swell and wind waves is also studied.

Chapter 3 is devoted to the two-soliton interaction in the framework of integrable models as elementary act of soliton turbulence.

Chapter 4 presents our numerical results concerning the dynamics of soliton fields. Soliton turbulence is studied in the framework of the Korteweg-de Vries equation and the modified Korteweg-de Vries equation. Freak waves appearance in the heteropolar soliton field is demonstrated.

Lastly, a thesis summary and concluding remarks are presented.

Chapter 2

Linear interference of random waves and the appearance of abnormally large waves

2.1 Introductory remarks

2.2 Mechanism of dispersive focusing of freak wave appearance

2.3 Various forms of freak waves in case of swell and wind wave interaction

2.4 Wave interaction with a vertical barrier

2.5 Conclusion

2.1 Introductory remarks

Water waves propagate with different velocities and in different directions; as a result of this complex interference, very irregular wave system containing weak and strong peaks is formed. Such large waves (freak waves) can be a serious threat to ships, oil platforms, port facilities and tourist areas on the coast. Mechanisms of abnormally large wave formation are described in the books [Kurkin et Pelinovsky, 2004; Kharif et al, 2009, Dotsenko et Ivanov, 2006] and numerous articles and reviews that will be cited in the thesis as needed. This chapter focuses on only one mechanism of large wave occurrence – the mechanism of dispersive focusing associated with the dispersion of water waves (dependence of the propagation velocity of the spectral components from their frequency). This mechanism is very popular for the freak wave generation in the laboratory, where their reliable reproducibility is necessary [Brown et Jensen, 2001; Johannesen et Swan, 2001; Clauss, 2002; Kurkin et Pelinovsky, 2004; Kharif et al, 2008, 2009, Shemer et al., 2007; Shemer et Dorfman, 2008; Shemer et Sergeeva, 2009].

Particular attention will be paid to the study of kinematics and statistics of large waves in linear random wind wave fields. Paragraph 2.2 is based on basic equations of water waves and a description of dispersive focusing mechanisms is also presented. Examples of single freak wave appearances in the framework of this mechanism are given. The interaction of simultaneously moving swell waves with weak wind waves in the framework of potential theory is considered in paragraph 2.3. It is noted that in the case of variable wind, swell waves can be focused at a distance from the original area - in a storm area, forming an abnormally large wave (or "freak wave"). An investigation of the visibility of freak waves of different shapes from a background of wind waves is made. The formation of "freak waves" at vertical barrier (rock or cliff) is studied in paragraph 2.4.

2.2 Mechanism of dispersive focusing of freak wave appearance

Suddenly appearing short-lived abnormal waves on the sea surface (freak waves) attract the attention of specialists because they can be a serious threat to ships, oil platforms, port facilities and tourist areas on the coast.

Numerous observations of freak waves in various areas of the oceans are presented in books [Lavrenov, 1998; Kurkin et Pelinovsky, 2004; Kharif et al, 2009] and in articles [Lavrenov, 1985; Lopatuhin et al., 2003; Divinsky et al., 2004; Badulin et al., 2005; Didenkulova et al, 2006; Liu, 2007; Nikolkina et Didenkulova, 2011, 2012]. Through the mechanisms of freak wave generation in the open sea there are [Kharif et al, 2009]: a) superpositions of a large number of individual spectral components moving with different velocities and in different directions (geometrical and dispersive focusing); b) nonlinear mechanisms of modulation instability; c) interactions of waves with the bottom and currents.

Each of these mechanisms has its own specificity, which manifests in the corresponding probability of freak wave appearance and its lifetime. Each mechanism leads to different waveforms of freak waves and different scenarios of their manifestation. All of these important features have not been sufficiently studied yet.

In this paragraph the scenario of the appearance of freak waves in the sea, based on dispersive focusing of wave packets propagating in the same direction, is considered. When the group wave velocity depends on the frequency, this mechanism “works” for dispersive waves of all physical natures. In this case, the faster waves overtake the slower ones. It is obvious that for a significant focus of wave energy, the convergence of large numbers of quasi-monochromatic packets is necessary.

This mechanism "works" for deterministic and for random waves, leading to a natural or accidental occurrence of abnormally high waves. It can occur in both linear and nonlinear theory of water waves, but of course, nonlinearity leads to its features in the wave field [Pelinovsky et Kharif, 2000; Pelinovsky et al., 2003; Kharif et al, 2001; Pelinovsky et al, 2000; Shemer et al., 2007; Shemer and Dorfman, 2008].

Theoretical (analytical) results on wave packet focusing in water are obtained mainly using linear theory, specifically in the framework of the parabolic equations for

wave packet envelopes [Clauss et Bergmann, 1986; Magnusson et al., 1999; Shemer et al., 2002; Pelinovsky et al., 2003; Shemer et Dorfman, 2008].

The parabolic equation for wave packets can be derived for weakly modulated waves in waters of any depth, not necessarily infinitely deep. However dispersion decreases in shallow water, and processes of dispersion convergences occur over very long times (distances), which can exceed the physical dimensions of water reservoir. Therefore, the main application of parabolic equations is associated with the finite but not the small depth. One exact solution of this equation is Gaussian impulse [Clauss et Bergmann, 1986; Magnusson et al, 1999; Pelinovsky et Kharif, 2000], which demonstrates the process of the emergence of abnormally high waves and their disappearance. The description of the process of single freak wave generation will be given in this paragraph.

In this chapter, the following will be assumed:

1. The liquid is assumed to be ideal, incompressible and unstratified.

2. We will consider two-dimensional potential wave motion (both a horizontal and vertical coordinate).

3. The water depth is constant and there is no water filtration through the "solid" bottom.

4. The action of the wind flow is neglected, and the atmospheric pressure is constant.

In this case, the original equations are two-dimensional Euler equations:

$$\frac{\partial u}{\partial t}+u\frac{\partial u}{\partial x}+w\frac{\partial u}{\partial z}+\frac{1}{\rho}\frac{\partial p}{\partial x}=0, \tag{2.1}$$

$$\frac{\partial w}{\partial t}+u\frac{\partial w}{\partial x}+w\frac{\partial w}{\partial z}+\frac{1}{\rho}\frac{\partial p}{\partial x}+g=0, \tag{2.2}$$

$$\frac{\partial u}{\partial x}+\frac{\partial w}{\partial z}=0, \tag{2.3}$$

where u, w – horizontal and vertical components of fluid velocity, ρ – density, p – pressure, g – acceleration due to gravity, x – horizontal coordinate, z – vertical coordinate

and t - time. Fluid is limited by fixed horizontal bottom. $z=-h$, there is a free surface with equilibrium position of $z=0$ (Fig. 2.1).

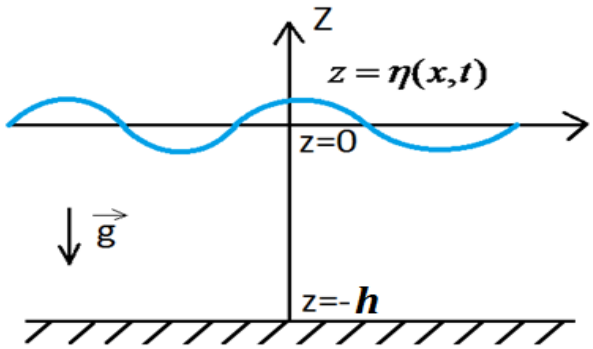

Figure 2.1 - geometry of the problem.

Equations (2.1)-(2.3) must be supplemented by boundary conditions. Conditions of fluid nontransmission through the solid boundary (bottom) is

$$w=0 \qquad \text{at} \qquad z=-h\,. \tag{2.4}$$

On the free surface the kinematic condition must be satisfied

$$w=\frac{\partial\eta}{\partial t}+u\frac{\partial\eta}{\partial x} \qquad \text{at} \qquad z=\eta(x,t)\,. \tag{2.5}$$

and dynamic condition on the surface

$$p=p_{atm} \text{ at } z=\eta(x,t) \tag{2.6}$$

where $\eta(x,t)$ is a vertical displacement of the free surface, and p_{atm} is constant atmospheric pressure.

Taking into account that the motion of the fluid is assumed to be irrotational, we can use the velocity potential $\Phi(x,z,t)$, determined by the formula

$$u=\frac{\partial\Phi}{\partial x}, \qquad w=\frac{\partial\Phi}{\partial z}\,. \tag{2.7}$$

After substituting (2.7) into (2.3) we come to the Laplace equation:

$$\frac{\partial^2\Phi}{\partial x^2}+\frac{\partial^2\Phi}{\partial z^2}=0\,. \tag{2.8}$$

The boundary condition at the bottom (2.4) is transformed into:

$$\frac{\partial \Phi}{\partial z} = 0\,, \qquad z = -h \tag{2.9}$$

and kinematic condition (2.5) into

$$\frac{\partial \eta}{\partial t} + \frac{\partial \Phi}{\partial x}\frac{\partial \eta}{\partial x} = \frac{\partial \Phi}{\partial z}\,, \qquad z = \eta(x,t) \tag{2.10}$$

To transform the dynamic boundary condition equation (2.6), the Bernoulli integral must be used, which is obtained from equation (2.2), after integrating by vertically

$$\frac{p}{\rho} + gz + \frac{\partial \Phi}{\partial t} + \frac{1}{2}\left(\frac{\partial \Phi}{\partial x}\right)^2 + \frac{1}{2}\left(\frac{\partial \Phi}{\partial z}\right)^2 = \text{const}\,, \tag{2.11}$$

where *const* may be a function of *x* and *t*. Taking into account that the potential is defined with precision up to any function of time, the integral or equation (2.11) with equation (2.6) as a condition on the free surface then converts into

$$g\eta + \frac{\partial \Phi}{\partial t} + \frac{1}{2}\left(\frac{\partial \Phi}{\partial x}\right)^2 + \frac{1}{2}\left(\frac{\partial \Phi}{\partial z}\right)^2 = 0\,, \quad \text{at} \quad z = \eta(x,t) \tag{2.12}$$

Thus, we have a closed system for two functions $\eta(x,t)$ and $\Phi(x,z,t)$. It is a linear Laplace equation (2.8) with linear (2.9) and nonlinear (2.10), and (2.12) boundary conditions. The function $\eta(x,t)$ could be neglected with the help of (2.12) and a closed nonlinear boundary value problem for the potential could be obtained. The derivation of this system can be found in many textbooks of hydrodynamics and it is presented here in a shortened form. In any case, this is a complex system, which is why the number of analytical solutions for water waves are seldomly found.

In the case of linear wave motions in a reservoir of finite depth, the Euler equations can be simplified by transferring boundary conditions from the unknown free surface $z = \eta(x,t)$ to the plane $z = 0$. Additionally, all nonlinear terms in the kinematic and dynamic boundary conditions can be omitted. The basic equation for wave motion is the Laplace equation (2.8) which, of course, remains unchanged.

The kinematic condition (2.10) takes the following form

$$\frac{\partial \eta}{\partial t} = \left.\frac{\partial \Phi}{\partial z}\right|_{z=0}, \tag{2.13}$$

correspondingly the dynamic condition is

$$\eta = -\frac{1}{g}\left.\frac{\partial \Phi}{\partial t}\right|_{z=0}. \tag{2.14}$$

It is convenient to exclude the function $\eta(x,t)$ by substituting equation (2.14) into (2.13) and obtaining a single boundary condition at the free surface

$$\frac{\partial^2 \Phi}{\partial t^2} + g\frac{\partial \Phi}{\partial z} = 0, \qquad (z = 0). \tag{2.15}$$

As a result, we obtain a closed linear boundary value problem for the potential, consisting from the Laplace equation (2.8) with linear boundary conditions (2.9) and (2.15).

Because of homogeneity of the boundary value problem with respect to the transformation of the horizontal coordinate and time, the solution of this boundary value problem can be found by separation of variables

$$\Phi(x,z,t) = \Psi(z,k)\exp[i(\omega t - kx)], \tag{2.16}$$

where the parameters ω and k are free. A brief solution of the boundary value problem is presented below. After substituting (2.16) into the Laplace equation (2.8), it is transformed into an ordinary differential equation for the function Ψ and can be easily solved

$$\Psi(z,k) = C_1\exp(kz) + C_2\exp(-kz). \tag{2.17}$$

The constants can be found from the boundary conditions. Taking into account the boundary condition at the bottom (2.9), it then takes the following form (assuming $k > 0$)

$$\Psi(z,k) = C_1\cosh[k(z+h)]. \tag{2.18}$$

After substituting (2.18) into (2.15) with (2.16), the dispersion equation for waves in the fluid of finite depth can be found:

$$\omega^2 = gk\tanh(kh). \tag{2.19}$$

The dispersion relation indicates the relationship of spatial and temporal scales of water surface oscillations, determined by a specified balance of forces for given type of waves. This is the fundamental difference of wave fields from turbulent fields, for which there is no such link.

The expression of potential takes the following form:

$$\Phi(x,z,t)=\left[\frac{-i\omega C_1}{k\sinh(kH)}\right]\cosh[k(z+h)]\exp[i(kx-\omega t)]\,. \qquad (2.20)$$

With the help of (2.14) the solution of water surface displacement can be written as

$$\eta(x,t)=A\exp[i(\omega t-kx)], \qquad A=-\frac{i\omega C_1}{g} \qquad (2.21)$$

where A is wave amplitude. This solution describes a traveling monochromatic wave to the right. The expression for the wave propagating to the left can be written similarly. General solution of the linear potential problem can be written with the help of elementary solutions such as Fourier integral

$$\eta(x,t)=\int_{-\infty}^{+\infty}A(k)\exp[i(\omega t-kx)]dk+\int_{-\infty}^{+\infty}B(k)\exp[i(\omega t+kx)]dk\,, \qquad (2.22)$$

where the conjugation condition on the spectral amplitude must be imposed

$$A^*(k)=A(-k), \qquad B^*(k)=B(-k). \qquad (2.23)$$

We consider the waves moving in only one direction below ($x > 0$). In this case, the displacement of the water surface is described by only one integral

$$\eta(x,t)=\int_{-\infty}^{+\infty}A(k)\exp[i(kx-\omega t)]dk\,, \qquad (2.24)$$

where $A(k)$ is the complex Fourier spectrum determined by the initial perturbation corresponding to the traveling wave, $\eta_0(x)$:

$$A(k)=\frac{1}{2\pi}\int_{-\infty}^{+\infty}\eta_0(x)\exp(-ikx)dx\,. \qquad (2.25)$$

Under certain initial conditions within the solution (2.24) large waves can appear at some moment. However, such adequate initial conditions are difficult to find. Therefore a different approach is used [Kurkin et Pelinovsky, 2004; Kharif et al, 2009]: the Cauchy problem for the initial conditions corresponding to the expected abnormal wave is solved, and then the resulting solution is inverted in space. As a result, there are possible forms of the wave packet, and their evolution leads to the formation of abnormal waves in a finite time with subsequent transformation back into a wave packet.

Scenario of a single freak wave appearance in the framework of the mechanism of dispersive focusing is given in the article **Pelinovsky E., Shurgalina E., and Chaikovskaya N. The scenario of a single freak wave appearance in deep water – dispersive focusing mechanism framework. Nat. Hazards Earth Syst. Sci., 2011, 11, 127-134.**

Let us say a few words about the manifestation of the same effect in a fluid of finite depth. If the waves are long enough, they all propagate with the same velocity ($c(k) = \sqrt{gH}$) and hence they cannot overtake each other. Thus, in purely shallow water the effect of dispersion focusing is impossible. Freak waves in nonlinear traveling (Riemann) waves are also absent [Didenkulova et Pelinovsky, 2011]. Then other effects must play a role here. In the case of water with small but finite depth, the velocity of spectral component propagation in the approximation of the linearized Korteweg-de Vries equation takes the following form:

$$c(k) = \frac{\omega}{k} = \sqrt{gh}\left(1 - \frac{k^2 h^2}{6}\right) \qquad (2.26)$$

and shorter components may overtake each other. This process is considered in the articles [Pelinovsky et al, 2000; Talipova et Pelinovsky, 2009] taking into account nonlinear effects. It is important to emphasize that due to small dispersion the overtaking process takes a long time, thus the lifetime of the freak waves in shallow water in the framework of mechanisms of dispersion focusing is greatly increased. In this sense, it decreases the risk because such a wave can appear at a great distance from the ship or from the shore, thus preparations for the meeting with the danger wave can be done.

2.3 Various forms of freak waves in case of swell and wind wave interaction

A large number of photos and eyewitness stories of freak waves in the ocean has been accumulating during the past decade. Available collected data proves the existence of freak waves of various forms [Kurkin et Pelinovsky, 2004, Faulkner, 2000, Kharif et al., 2009]. In literature there are descriptions of abnormally large waves in the form of "white wall", "single tower", "three sisters" (a group of several individual waves).

Sometimes in front of freak waves there are depressions of several meters deep - "hole in the sea". Oftentimes these waves have sharp fronts and are asymmetric, indicating the nonlinear character of freak waves. Typical records of abnormal waves, including one and two "sisters" are shown on Fig. 2.2.

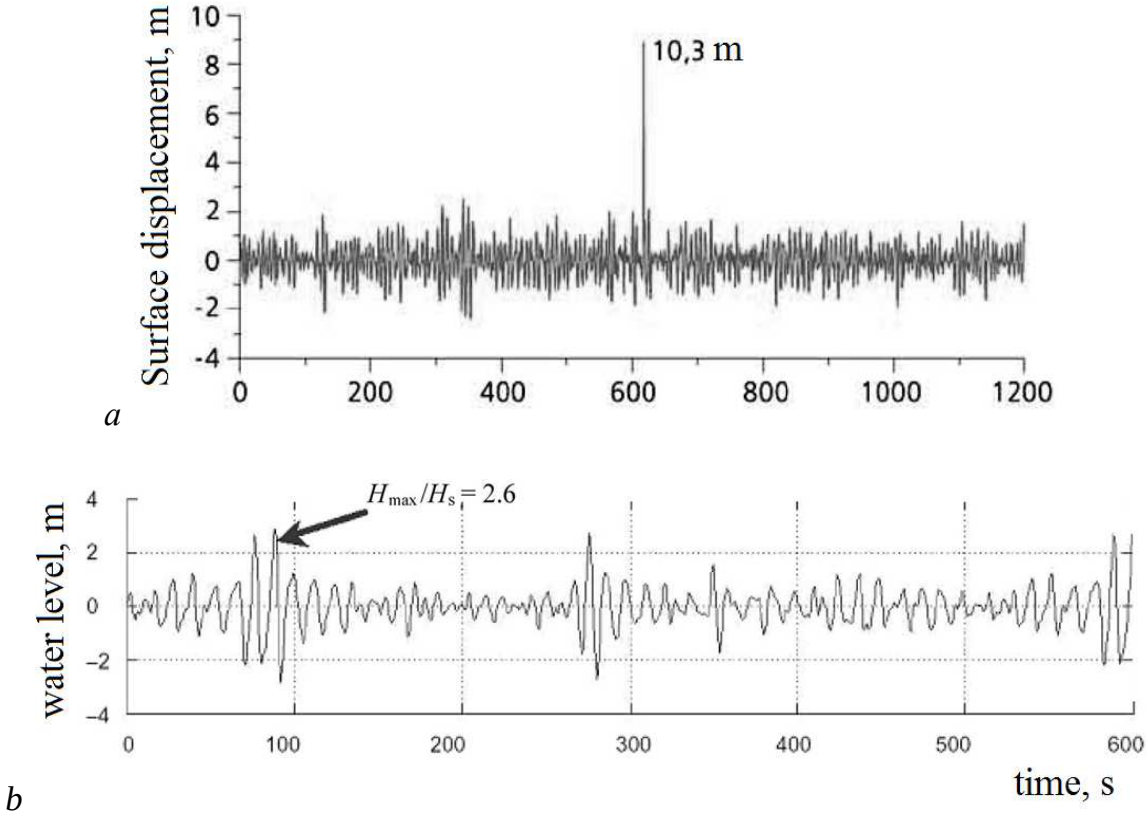

Figure 2.2 Temporary record of abnormally high wave in the Black Sea (a), received on 22 November 2000 [Divinsky et al., 2004], and a group of abnormally large waves (b) in the Sea of Japan [Mori et al., 2002] – 24 January 1987.

One of the mechanisms of freak wave formation is a combined effect of geometric (spatial) and dispersive wave focusing in case of imposition of waves moving in different directions (“crossing sea”). One reason is that wave superposition can be the interaction of swell, coming from a storm area, with wind waves in the area of local storm. Usually for wind waves description statistical methods are used, and for swell description at large distances from the storm deterministic methods are used. Water waves are dispersive, and out of the storm area swell is a frequency-modulated packet and longer waves with greater velocity of propagation are ahead of the shorter ones. This fact has already been used in practice to determine the distance to the storm zone by changing swell current frequencies [Snodgrass et al, 1966]. Wind in storm area is not constant, and it leads to wave packet generation with a very complicated law of frequency changing with time, including the generation of packets when short waves propagate ahead of long ones. It is obvious that such packets will focus in the anomalous wave due to dispersion, and then spread out over large distances from the storm area. Thus, at intermediate distances from the storm area, we can expect the appearance of abnormally large swell waves (freak waves), which will interact with a random wind wave field associated with a local storm. The main purpose of this section is to estimate the lifetime of abnormally large swell waves in wind wave fields.

To simplify the problem, we will assume that the anomalous swell wave is already formed at the initial time and stands out against a background of wind waves. It could have a different shape, as was mentioned in the beginning, thus we consider several possible freak wave forms. Spreading of abnormally large swell waves on an unperturbed (smooth) water surface and the interaction of swell with a random wind wave field will be studied.

The following class of modulated waves with a Gaussian envelope will be modeled:

$$\eta_{freak}(x) = a \exp\left(-\frac{x^2}{l^2}\right)\cos(K_0 x), \tag{2.27}$$

where l – characteristic size of the wave packet (envelope) and K_0 – carrier wave number. In all cases considered below K_0 = 0.07 m^{-1}, it corresponds to the length of individual wave of approximately 90 m.

By changing *l*, we actually change the number of waves ("sisters") in the abnormal group.

The parameter *a* in the linear theory plays a role of a normalizing factor that helps to "keep" the amplitude of the wave packet the same. Various forms of abnormally large waves are shown in Fig. 2.3, and their evolution will be discussed in this section. There are one, two, three, and four "sisters" (the number of "sisters" corresponds to the number of crests above the zero water level). It is important to mention that deep troughs can be considered as freak wave of negative polarity. The length of wave packets is changing from 200 to 800 m in our calculations, and its positive amplitude is equal to 0.6 m. The steepness of the anomalous wave in this case is sufficiently small (0.042), which is why such waves can be considered in the frameworks of linear theory.

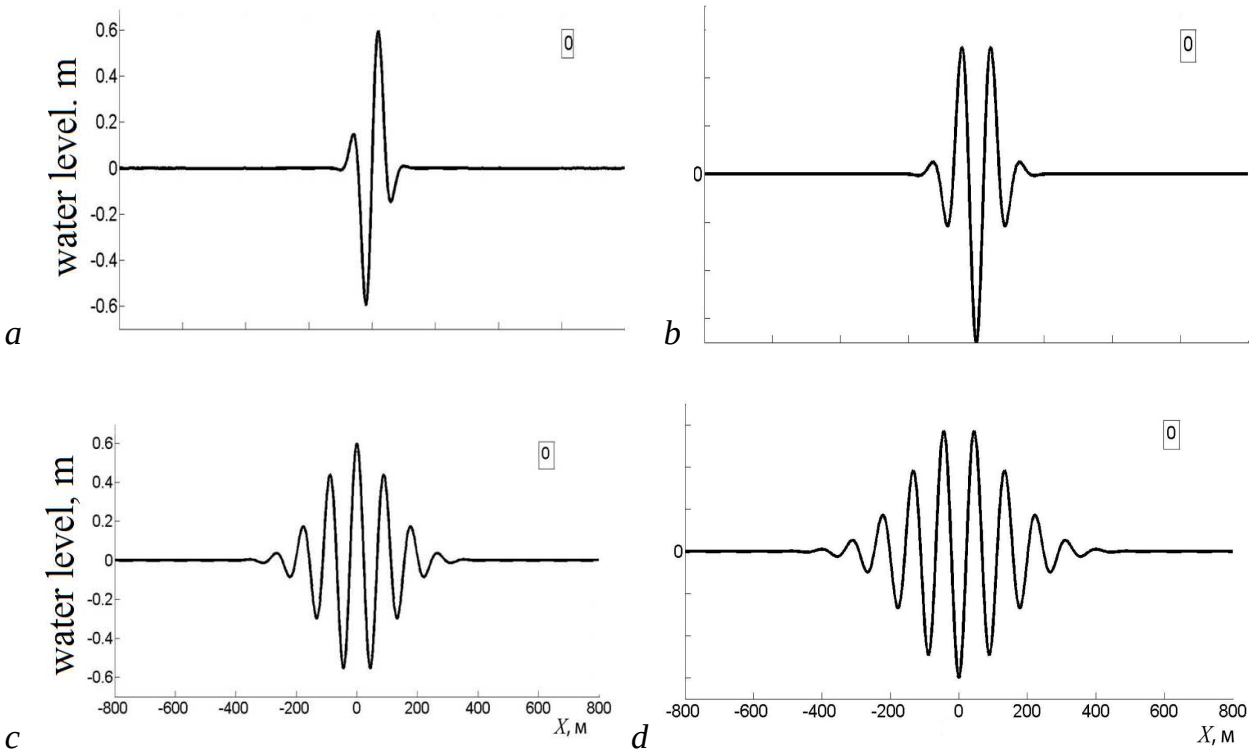

Figure 2.4 – initial forms of abnormal wave packets

a – «one sister» (a = 0.72 m, l = 50 m); b – «two sisters» (a = 0.8 m, l = 80 m); c – «three sisters» (a = 0.59 m, l = 160 m); d – «four sisters» (a = -0.62 m, l = 200 m).

During the time the perturbation (2.27) is transformed into a wave packet due to dispersion of water waves, as shown in Fig. 2.5 for a time moment of 50 seconds. The wave packets for different initial perturbations behave similarly. Wave trains are stretched in space due to dispersion, the number of individual waves increases linearly

with time, and packet amplitude decreases with time (at large times as $t^{-1/2}$ [Uizem, 1977**]**).

At the initial times due to interference processes the maximum positive amplitude of the packet may even grow up and be changed monotonically (Fig. 2.6). "Three sisters" are spreading out into space slower than "one sister" due to a decrease of dispersion. From these considerations the lifetime is growing with increasing wave numbers in the group.

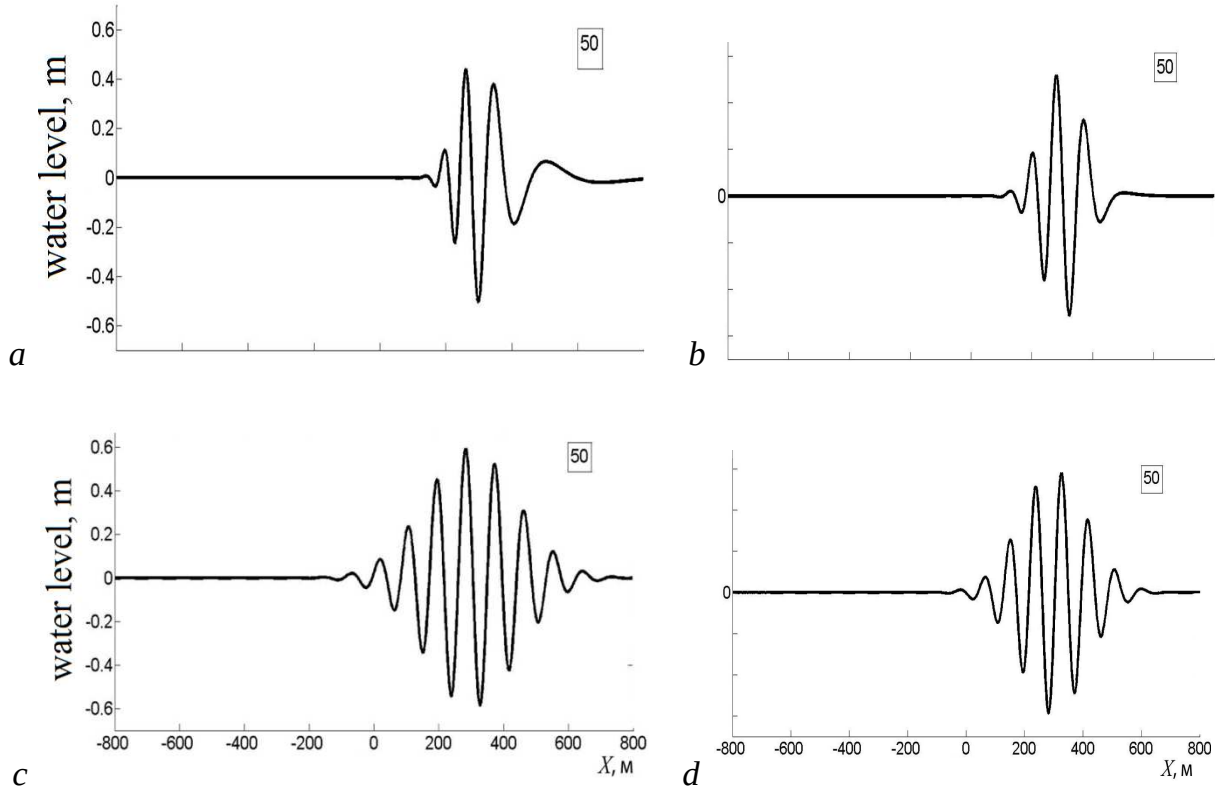

Figure 2.5 – Shape of different wave packets in the moment of 50 seconds.

a – «one sister», b – «two sisters», c – «three sisters» d – «four sisters».

The obtained above solutions show the evolution of the wave packet on a perfectly smooth surface. In this case, formally the lifetime of freak waves are equal to infinity. If it is assumed that there is a threshold of water wave visibility, the lifetime becomes finite. For example, consider three critical values of the wave amplitude when the wave becomes "invisible": 0.3, 0.4 and 0.5 m (a more accurate determination of the minimum observed wave heights should take into account the background wind waves - see. below). It is obvious that the lifetimes of abnormal waves will also be changed.

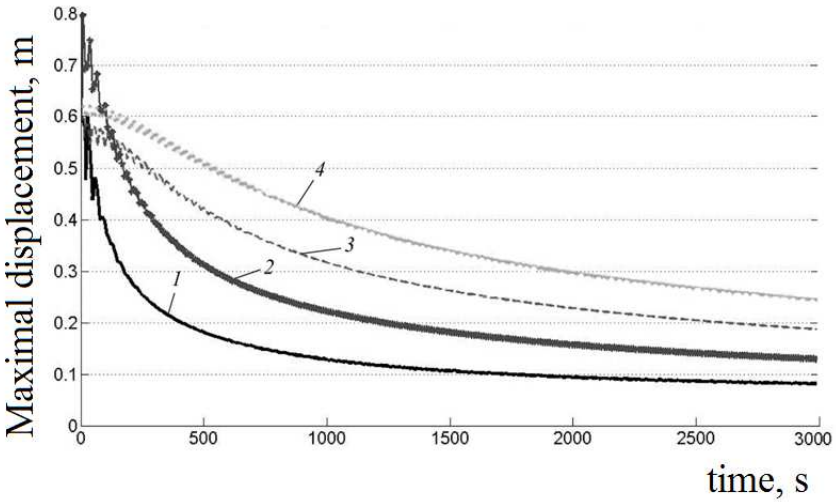

Figure 2.6 – The changing of the maximum positive displacement of water surface over the time, 1 – «one sister», 2 – «two sisters», 3 – «three sisters», 4 – «four sisters».

Fig. 2.7 shows that with increasing the number of waves in the initial group's wave lifetime increases with the square of the average number of waves; more precisely the exponent in the regression curves vary from 1.7 to 1.8.

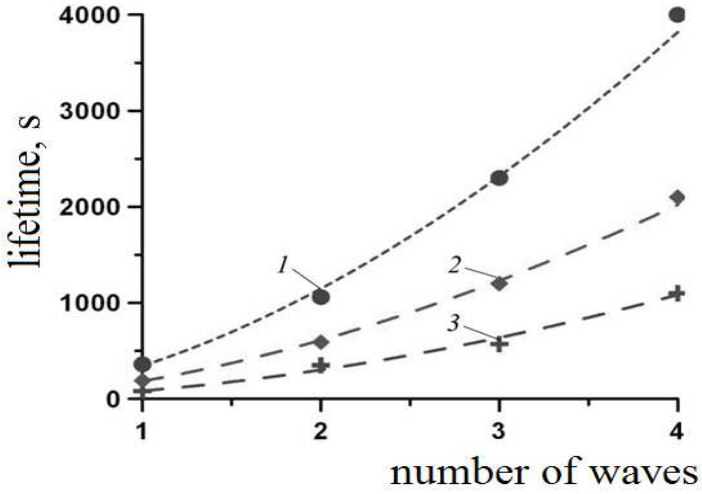

Figure 2.7 – Dependence of freak wave lifetimes and the number of waves for different critical threshold values of visibility (the critical amplitude of the "visible" waves, m: 1 - level of 0.3, 2 - 0.4, 3 - 0.5. The dashed lines are regression curves).

The value of freak wave lifetimes in the framework of deterministic problems strongly depends their "level of visibility". It is more important to understand the influence of nonlinearity on the value of the lifetime and the applicability of linear theory to the description of the formation of abnormal waves. In the article [Shemer et al, 2007],

there are descriptions of a laboratory experiment and numerical simulations of the dispersive focusing of the wave packet in the framework of the nonlinear theory. It is shown that the freak wave lifetime is about of 1-3 minutes (steepness is 0.2-0.3). The same estimation follows from our results for a single wave. Taking this into account we hope that our estimations of lifetimes of abnormal waves of different shapes (from fig. 2.7) are the same for nonlinear theory.

Swell waves propagate in the background of wind waves caused by the action of local wind. We assume that the wind is weak enough and it generates waves with small amplitudes, thus that abnormal swell waves are visible in the background. The interaction time of wind with waves is large enough (it is determined by the ratio of the water density to the air density, which could takes hours) [Kharif et al. 2008, 2009] and it is much longer than the lifetime of freak waves (a few minutes, as we will see below). Thus we will not take into account winds in the model.

However, wind determines the distribution of wave elements, in particular, the spectrum, amplitude, and the carrier frequency. As an approximation of the spectrum of wind waves here we use the Pearson-Moskowitz spectrum for developed waves, it depends only on the wind speed [Trubkin, 2007]. The Pearson-Moskowitz spectrum describes the frequency spectrum at any point, but we need a spatial spectrum. In the case of small amplitude unidirectional waves, the spatial spectrum is easy to calculate from the frequency spectrum by using the dispersion relation

$$S(k) = \frac{\alpha}{2k^3}\exp\left[-\frac{\beta g^2}{U^4 k^2}\right], \qquad (2.28)$$

where $\alpha = 8.1\cdot 10^{-3}$; $\beta = 0.74$; U – wind velocity. The spatial spectrum of wind waves for wind speed of 4.3 m/s is presented in fig. 2.8.

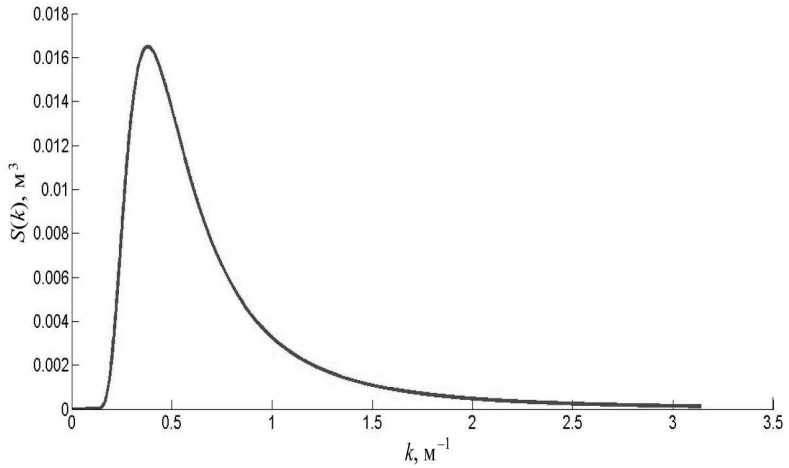

Figure 2.8 - spectrum of wind waves for wind speed of U = 4.3 m/s.

In this case, random wind wave fields are defined in the same way as the previous paragraph. Thus there is no need to go into further detail here. Wind waves are characterized by the significant wave height, which is defined as the average height of the largest one third of the waves. In the approximation of a Gaussian distribution of wind waves the significant wave height can be defined as [Kurkin et Pelonovsky, 2004; Kharif et al, 2009]

$$H_s = 4\sigma, \tag{2.29}$$

where σ is a dispersion, founded from

$$\sigma^2 = \int_0^\infty S(k)dk = 2.74 \cdot 10^{-3} \frac{U^4}{g^2}. \tag{2.30}$$

This implies the following approximate formula for the significant wave height

$$H_s = 0.2 \frac{U^2}{g}. \tag{2.31}$$

Our calculations will be done for the wind velocity U = 4.3 m/s, when the linear theory can be applied (the corresponding estimates are discussed below). The significant wave height is H_s = 0.38 m for such velocity. It is more convenient to use significant wave amplitude: $a_s = H_s/2$ = 0.19 m.

The central wavenumber in wave spectrum is k_0 = 0.4 m^{-1} corresponds to a wavelength of λ_0 = 15.7 m (substantially smaller than swell wavelength).

The fundamental wave steepness, defined by a significant amplitude ($k_0 a_s$ = 0.076), is small enough in the framework of the Pearson-Moskowitz, hence linear theory can be applied.

The process of freak wave evolution in wind waves is considered below. Length of wind waves and swell waves differ about 6 times, making it easy to separate them by the methods of spectral analysis. Group velocities differ as well (in about 2.5 times), thus during the time these wave systems overlap each other several times with different phases and amplitudes.

The amplitude criteria are chosen as a criteria of freak waves [Kurkin et Pelinovsky, 2004; Kharif et al, 2009]

$$a_{fr} > 2a_s = H_s, \tag{2.32}$$

all the waves with an amplitude greater than 38 cm are considered as freak waves, regardless of their origin (swell or wind wave).

The superposition of deterministic swell waves (2.27) with a random wind wave is shown in Fig. 2.9 for a fixed set of phases for the time moment 0 s (the moment of freak wave formation).

The swell waves transform into wave packets due to dispersion, the number of individual waves grows, and the amplitudes are reduced. Freak waves in wind wave fields can appear as well (as shown below), and their amplitudes exceed a critical value a_{fr} = 0.38 m.

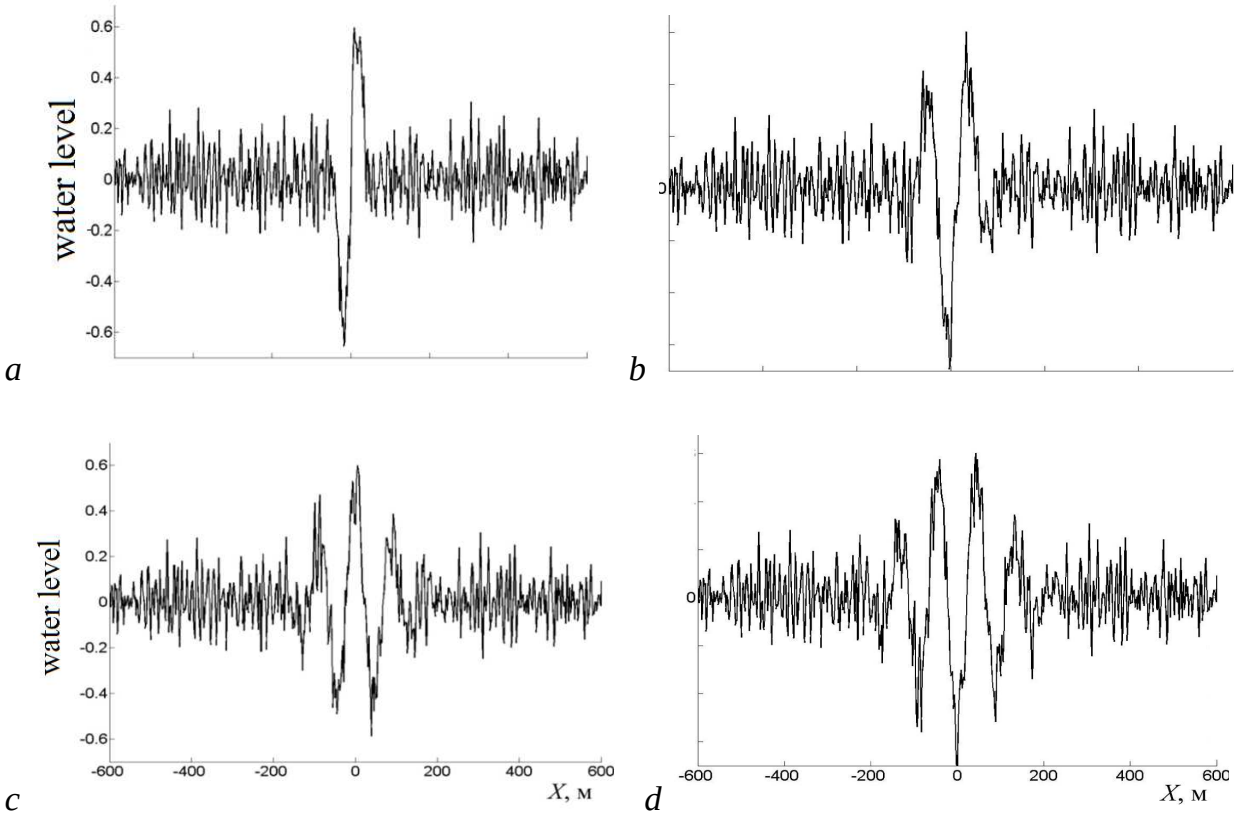

Figure 2.9 – freak waves in a wind wave field (t=0).
a – «one sister», l = 35 m; b – «two sisters», l = 70 m; c – «three sisters», l = 110 m; d – «four sisters», l = 140 m (l – characteristic value of the wave-packet envelope).

Space-time (*x* - *t*) diagrams are a good way to study the wave evolution since they make it easy to separate swell and wind waves moving with different speeds. This method is widely used for the analysis of dispersive wave packets. Space-time diagrams for all considered forms of abnormal swells are shown in Fig. 2.10. The planes of wave fields exceeded the amplitudes of freak waves a_{fr} = 0.38 m are presented in the diagrams. The clearly observed bright line starting from the origin of the coordinate system corresponds to the anomalous swell wave transforming in the wind wave field. This line is extended from the moment of time 4000 s at *x* = 0 (in cases c and d) due to the periodic boundary conditions used in the calculation, yet as previously mentioned, we will not analyze such long times. A significant number of randomly appearing single points and short lines appeared outside of bright line. The slope of these lines and single points differ from the slope of the main line, thus freak waves appear mainly in wind wave field.

It is important to mention that the "natural" freak waves in the wind wave field occur frequently in accordance with the predictions of the linear statistical theory based on the Rayleigh distribution. Space-time diagrams show that the number freak waves depends on the computational domain size - which is still poorly investigated. Lastly, the diagrams are similar qualitatively for different initial set of random phases.

The "right" and "left" diagrams in Fig. 2.10, correspond to two realizations of wind waves, which differ slightly in general. While the localization of abnormal waves in the background is varied, "lines" of freak waves have almost the same intensity. The space-time diagrams can be used for the estimation of freak wave lifetimes. Lifetimes of freak waves are random due to the random nature of wind waves. Even the lifetime of abnormal swell wave is also changing because the bright, almost continuous line time becomes discontinuous after some time (Fig. 2.10).

Using the amplitude criteria in equation (2.32), we found that the anomalous wave "one sister" disappears in about 4-8 minutes, "two sisters" - 30-40 minutes, "three sisters" - 60-70 min, and "four sisters" - more than 2 hours.

These values are higher than the lifetimes of deterministic signals, where the threshold of visibility was selected artificially. However, the tendency of increasing of freak wave lifetimes with the growth of number of individual waves in the wave packet is saved in both cases. The values of freak wave lifetimes are unreal in some sense, because the lifetime depends on the ratio between the swell height and wave background. In our case, the amplitude of the anomalous swell was chosen to be sufficiently large (0.6 m), and a_{fr} / a_s is about 3.2.

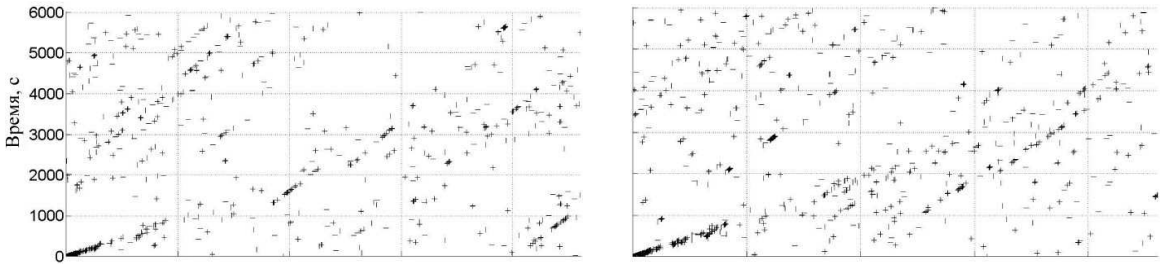

a

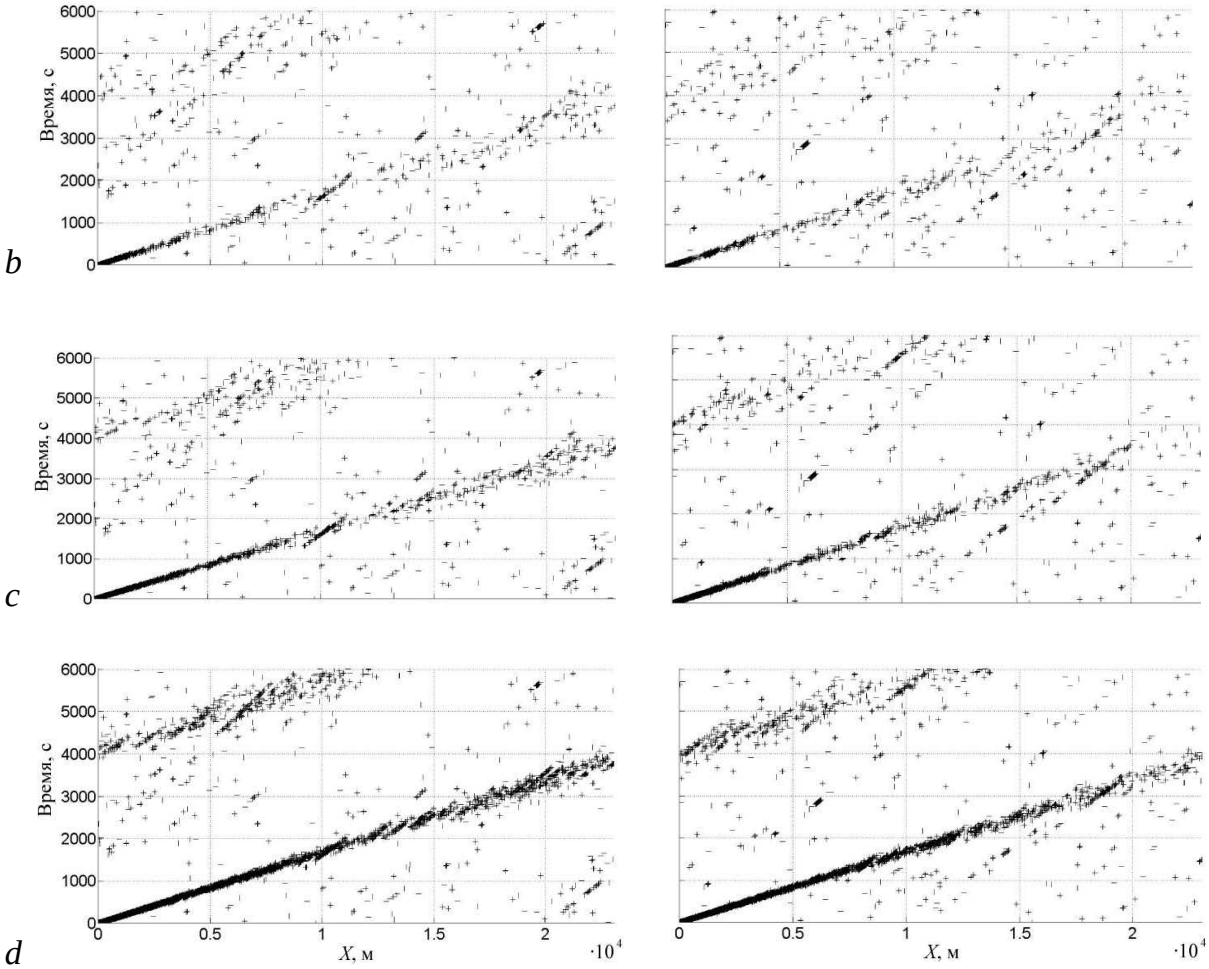

Figure 2.10 – space-time diagrams

a – «one sister»; b – «two sisters»; c – «three sisters»; d – «four sisters».

The left and right diagrams correspond to two different realizations of wind waves.

Such waves are rarely observed on the ocean surface. If we consider only wave amplitudes that are very large, three times higher than large amplitude waves, the number of such waves is much less on the space-time diagram (Fig. 2.11). Virtually all "natural" freak waves disappear, and only noticeable blurring anomalously large swell.

The number of waves which exceed the significant wave height by three times is sufficiently small in the space-time diagrams (Fig. 2.11). All "natural" freak waves disappear, and only the transforming of abnormal swell waves remains. Freak waves with a/a_s = 2.2, 2.7 should be observed more frequently. Fig. 2.12 shows the cuts of the wave field (on the level of a/a_s=2) in the case of evolution of "one sister" for three different

swell amplitudes at the initial moment, corresponding to the formation of freak waves. The larger initial amplitude which will be longer exceed the threshold a_{fr}.

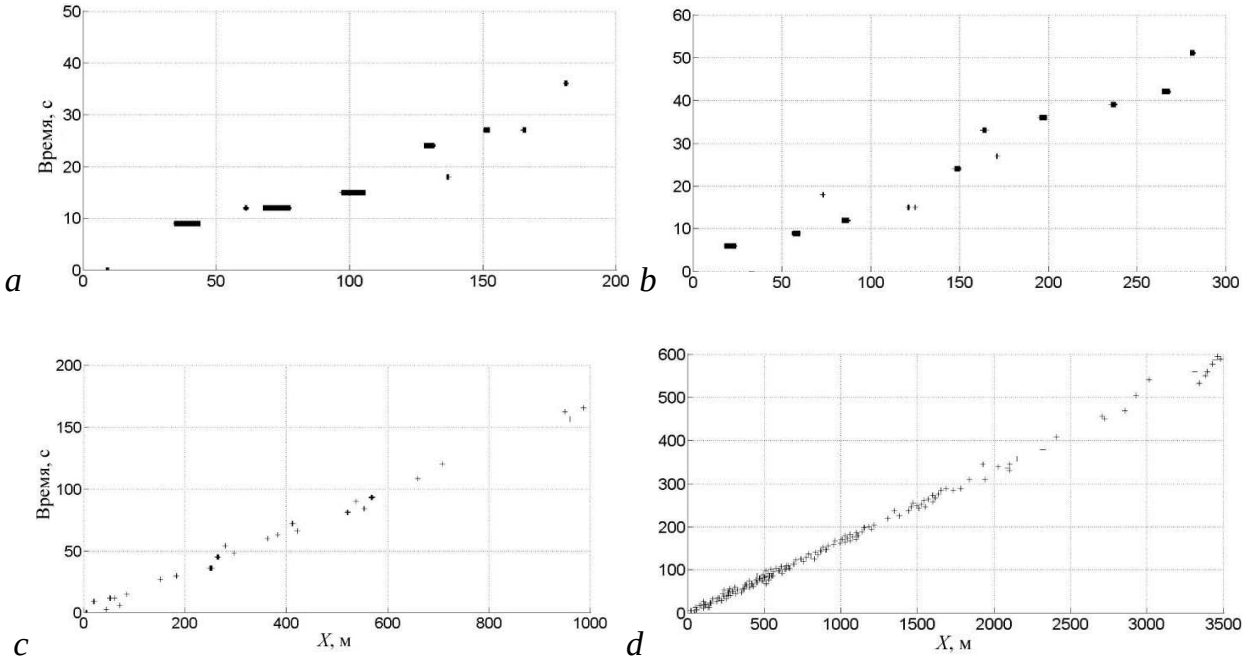

Figure 2.11 – 2D projection (u(x,t) = const) of wave field at the level of $3a_s$,

a – «one sister»; b – «two sisters»; c – «three sisters»; d – «four sisters».

It is difficult to say that when the freak wave is disappeared in wind wave field, which has its "own" freak waves, we can estimate its lifetime. Thus, when a/a_s = 2.2 (Fig. 2.12*a*), the time at which the freak wave disappears is 1–2 min, in case of a/a_s = 2.7 (Fig. 2.12*b*) – 2–3 min, and in the case of a/a_s = 3.2 (Fig. 2.12*c*) – 6–7 min.

The same figures can be given for abnormal swell of the forms of "two, three and four sisters". They have the same dynamics; just intensity and width of lines will be changed.

In case of “two sisters” for the ratios of a/a_s =2.2, 2.7 and 3.2 the average times of freak wave disappearances are 9, 15 an 35 minutes respectively; in case of «three sisters» – 15, 50 and 80 minutes, in case of «four sisters» the lifetime exceeds 2 hours, and such long-living waves are difficult to call abnormal.

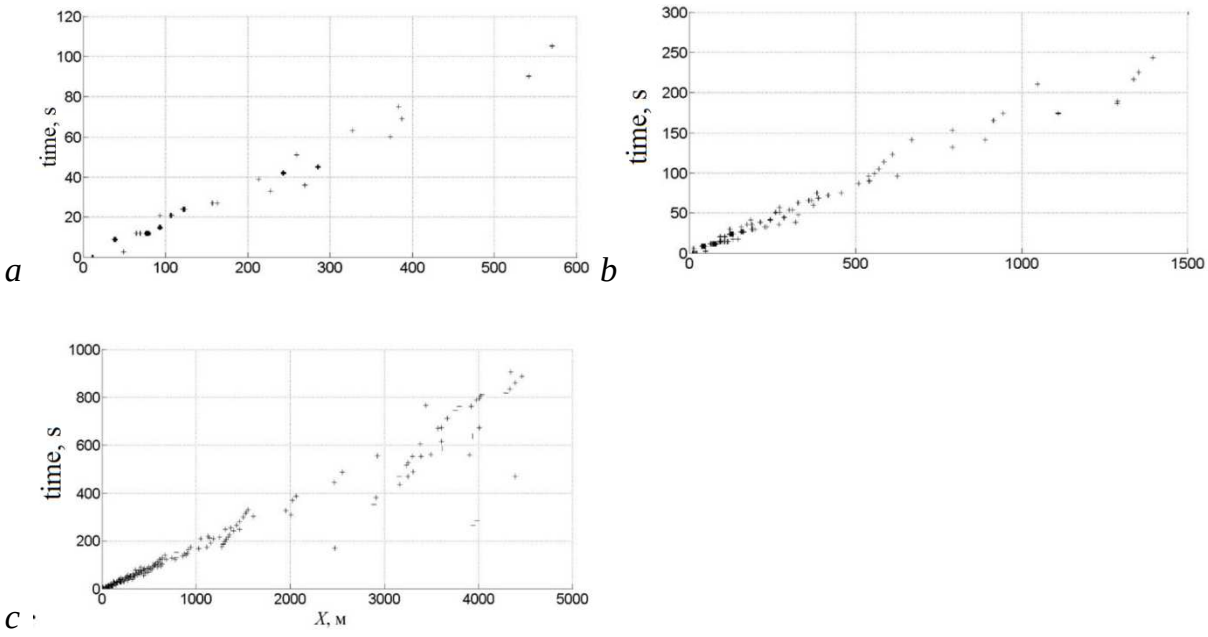

Figure 2.12 - 2D projections of wave field in case of «one sister» evolution for different values of a/a_s*:* $a - a/a_s = 2.2$; $b - a/a_s = 2.7$; $c - a/a_s = 3.2$.

The data of freak wave lifetimes are taken from the descriptions of the sailors who report from what distance they can see the abnormal wave. This is inconsistent because it is obvious that the visibility from a ship depends on the weather conditions. Thus we assume that a freak wave may be visible at a distance of 500 meters from the ship.

Then, according to the diagrams, the total lifetime (appearance + wave disappearance) of all types of swell waves is about 4 minutes (this estimation is made based on the condition that the ship is located at a distance of 500 m from the wave formation). Swell speed, calculated from the slope on the space-time diagrams, is approximately 5.8 m/s. Standard formula for the group velocity of the wave packet in deep water

$$c_{gr} = 0.5\sqrt{g/k_0}\,, \tag{2.33}$$

gives the value equal to 6 m/s, it is close to the direct estimation of swell speed.

The wave covers a distance of 1000 m (500 m – before wave apogee and 500 m – after), in approximately 3 minutes. Which is smaller than visual estimation of 4 min. The lifetime may vary depending on the ship position in relation to the wave "epicenter". For example, at a distance of 20 km swell wave packet is already quite wide and a 1 km freak

wave passes for 15 min (Fig. 2.10d, left side). Thus, if the ship is close to the "epicenter", the abnormal waves propagate with the largest amplitude, but they have a shorter duration; conversely, if the ship is far from the "epicenter", the amplitude of the freak waves are relatively small, but the ship will shake for much longer (at large distances wave packet will be wider due to dispersion).

It is important to mention that when the depth decreases the lifetime of the freak wave increases, and it gives a hope for the possibility of early detection in coastal areas.

Estimations of the lifetimes of abnormally large swell waves in wind wave fields of wind waves are given in the article **E.G. Shurgalina, E.N. Pelinovsky Manifestation of abnormal swell on weak wind waves Fundamental and Applied Hydrophysics. 2012, Vol. 5, № 1, 77–88.**

2.4 Wave interaction with a vertical barrier

Presently the possibility of freak wave appearances near the coast provokes particular interest. Such waves are quite a surprise to many people spending their holidays near the water. A wave of about 9 feet washed two people off from the pier in South Africa on August 26, 2005 [Kharif et al., 2009] (Fig. 2.13). On February 14, 2010, 13 people were washed off from a concrete parapet into the ocean by two large waves, and many of them got fractures and bruises. It happened near San Francisco (Half Moon Bay), where about 200 spectators were watching a windsurfing competition (Fig. 2.14) (http://www.ireport.com/docs/DOC-409122?hpt=T2).

Figure 2.13 Photo of a freak wave washing two people off from a pier in South Africa

Figure 2.14 The sudden appearance of a large wave on the shore near San Francisco (14 February 2010).

One of possible scenarios of freak wave appearance near a vertical barrier based on the mechanism of dispersive focusing will be considered in this paragraph.

Usually the problem of freak waves is discussed regarding the open ocean due to the obvious danger to ships and oil and gas platforms. However freak waves are found in the coastal zone as well, and their statistics and geographical distribution during 2006-2010 can be found in [Nikolkina & Didenkulova, 2011, 2012]. Thus particular interest must be devoted to the possibility of freak waves appearing near steep coast, cliffs or special protective walls, where people do not expect the emergence of dangerous waves.

The geometry of this problem is shown in Fig. 2.15. The wave approaches the wall from the right. The water depth is large enough to consider the waves as linear.

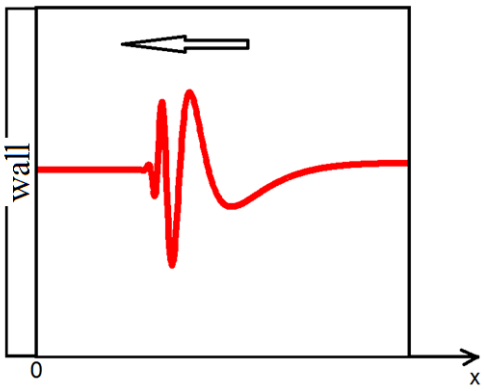

Figure 2.15 – geometry of the problem.

A mathematical model of this problem is similar to the model described in section 2.2. Since waves reflect from the wall, it is necessary to consider the superposition of the opposing waves, thus their horizontal velocity at the wall is equal to zero.

$$\eta(x,t) = \int_{-\infty}^{+\infty} [A(k)\sin(\omega t) + B(k)\cos(\omega t)]\cos(kx)dk\,. \qquad (2.34)$$

Expressions for the components of the particle velocity, can be found from potential $\Phi(x,z,t)$:

$$w(x,z,t) = \int_{-\infty}^{+\infty} \omega[A(k)\cos(\omega t) - B(k)\sin(\omega t)]\cos(kx)\exp(|k|z)dk\,, \qquad (2.35)$$

$$u(x,z,t) = \int_{-\infty}^{+\infty} \omega[A(k)\cos(\omega t) - B(k)\sin(\omega t)]\sin(kx)\exp(|k|z)dk\,, \qquad (2.36)$$

From equation (2.36) it is clearly seen that the horizontal velocity at the wall is zero at any time; and it is used in equation (2.34).

Solutions to equations (2.34) - (2.36) for a fixed frequency describe a standing wave. Fourier superposition of standing waves can also describe a complex system of the wave approaching the wall, and after its reflection. The formula could be rewritten (2.34), introducing amplitude and phase spectrum

$$\eta(x,t) = \int_{-\infty}^{+\infty} [C(k)\sin[\omega t - \varphi(k)]]\cos(kx)dk\,, \tag{2.37}$$

$$\eta(x,t) = \frac{1}{2}\int_{-\infty}^{+\infty} C(k)[\sin[\omega t + kx - \varphi(k)] + \sin(\omega t - kx - \varphi(k)]dk\,. \tag{2.38}$$

The terms appearing in (2.38), have a clear physical meaning, the first of them

$$\eta(x,t) = \int_{-\infty}^{+\infty} A(k)\sin[\omega t + kx - \varphi(k)]dk \tag{2.39}$$

represents a wall approaching to the vertical wall (here $A = C/2$), and the second one

$$\eta(x,t) = \int_{-\infty}^{+\infty} A(k)\sin[\omega t - kx - \varphi(k)]dk \tag{2.40}$$

is a reflected wave. Both waves can be written in a more compact form

$$\eta_{\pm}(x,t) = \int_{-\infty}^{+\infty} A(k)\exp(\omega t \pm kx)dk\,. \tag{2.41}$$

From a physical point of view, the interaction of waves with a wall is equivalent to the interaction of two identical waves, or wave packets, moving towards each other. In this case, the boundary condition on the wall (the equality of horizontal velocity to zero) is performed automatically.

As in the previous sections, the initial conditions for the time of freak wave formation on a wall can be set and the process of its decay into two waves propagating in different directions can be considered. The resulting solution in the half-space of $x > 0$ after inverting time and space will demonstrate the formation of freak waves.

A Gaussian impulse will be chosen as an anomalous wave near the vertical wall. In fact, the "half" of the Gaussian pulse ($x > 0$) is expected to be a freak wave near the

wall. The shape of the wave packets at different dimensionless times are shown in Fig. 2.16.

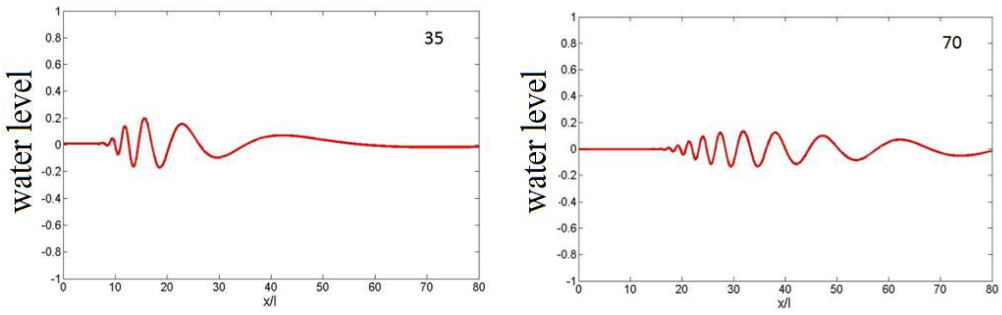

Figure 2.16 - the evolution of the initial Gaussian impulse in deep water after a long time (the numbers are the dimensionless times).

The integral (2.41) is a superposition of waves moving in opposite directions and is calculated numerically. Evolution of the waveform at short times is shown on Fig. 2.17. Initially, a positive pulse (crest) is transformed into sign-variable wave and then into a wave trough (depression), and then into wave train.

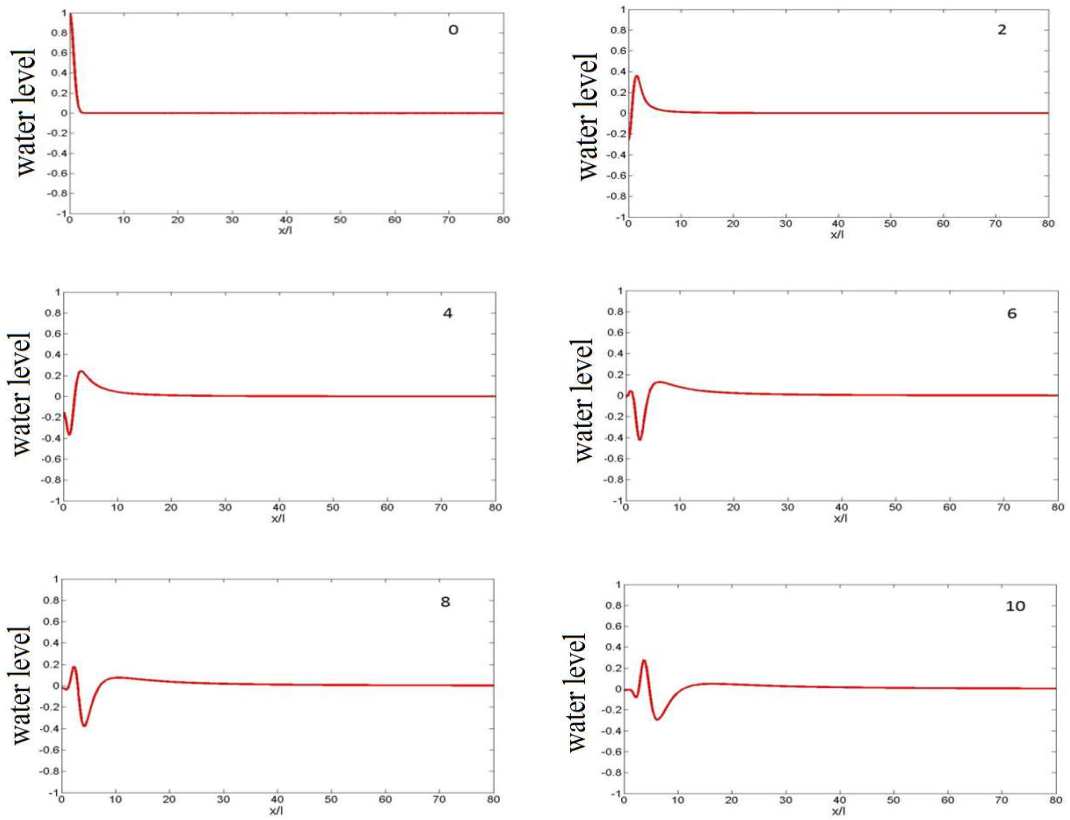

Figure 2.17 - Evolution of the Gaussian impulse at short times (numbers are dimensionless times).

Let us suppose that in a random wave field there is a deterministic frequency-modulated packet of small amplitude, as described above. In this case, a random disturbance does not change its energy average, and the probability of large wave occurrence is small in relatively small times. As a result, the initial wave field "looks" like purely random, and then a high ridge grows and over time disappears into random waves again. Such processes of interference of deterministic and random fields have already been discussed in paragraphs 2 and 3, but not for a single wave formation at the wall in deep water. Non-linearity, if it is small, cannot prevent dispersion focusing of a deterministic wave packet, thus at the first stage it is neglected. The wind wave field will be presented by already known scenario, so is it not necessary to go into detail.

Superposition of deterministic and random components of the wave field at different times is illustrated in Fig. 2.18, where time is measured in seconds from the moment of freak wave formation. The abnormal wave exists about 1 minute after its formation at the wall. Taking that into account, a similar process occurs when waves approach the wall (for this it is necessary to consider the figures in the opposite direction in time), thus the lifetime of the anomalous wave is about 2 minutes. Hence it is clear that forecasting freak waves is very difficult because there is no time to prepare for their appearance on such short notice.

If a person is located on a pier, the big crest is the only danger for him. This crest is visible several times (2 - 4 times) for about 10 seconds before it arrives on the coast. It is unlikely that in this case the first low ridges will attract a man's attention, and in fact the freak wave will be visible for about 30 seconds before the largest wave’s arrival on the bank.

Only directly before the pier can the observer see that wave consists of crests and troughs and that the large wave changes often its polarity, so a person will feel that a freak wave is not coming to the shore, but suddenly appears directly in front of the wall, epitomizing the eyewitness descriptions.

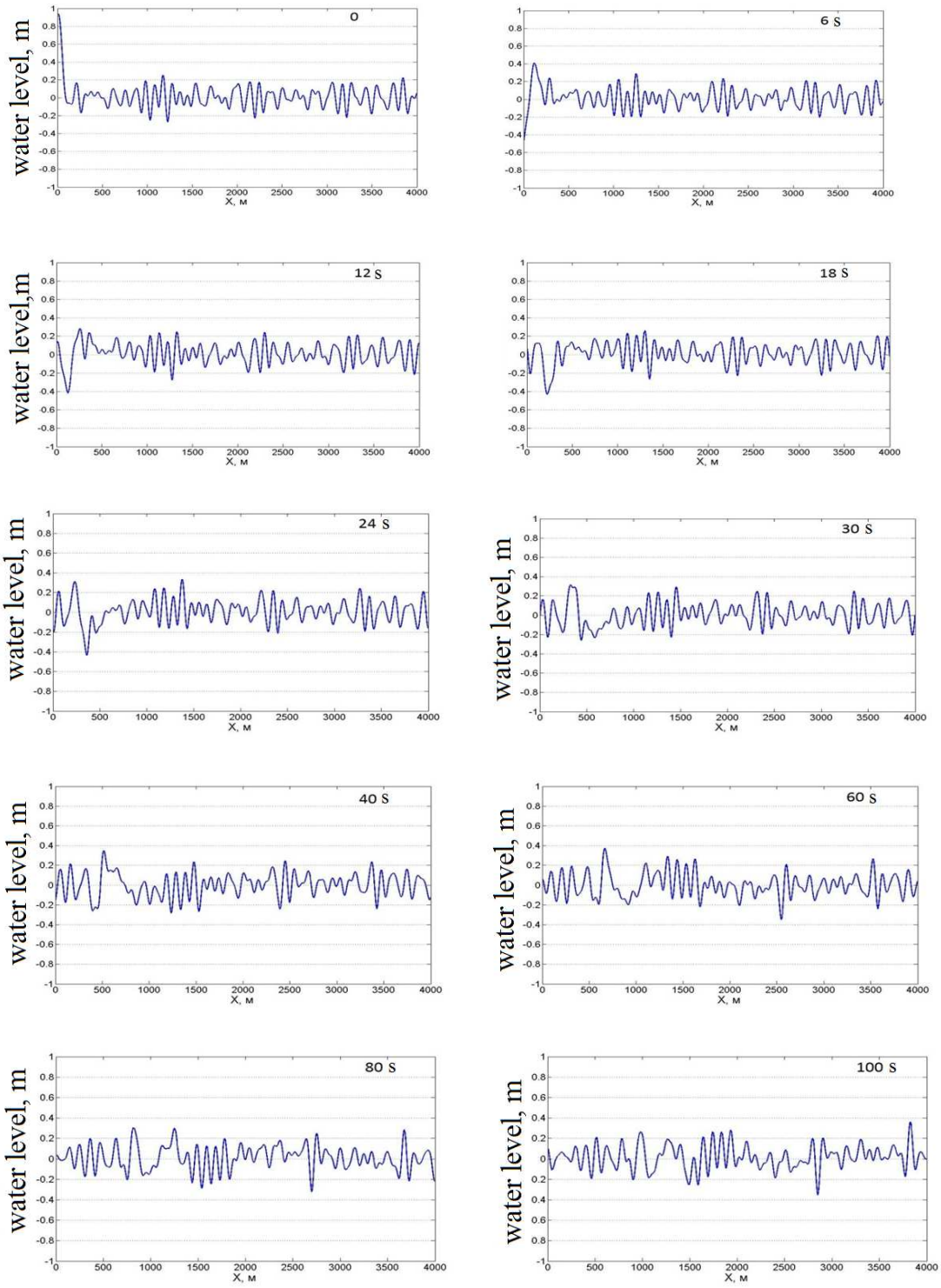

Figure 2.18 – spatial realizations of wave field at different times.

The same holds true for when ships and freak waves collide at sea. This is why the typical descriptions are: "The crews of ships do not have time to prepare for a meeting with the danger" (Kurkin et Pelinovsky, 2004). The fact of the sudden appearance of the freak waves requires mental preparation of the person. This analysis is performed by PhD N. Chaikovskaya, co-author of our work [Pelinovsky et al, 2011]. She specified the

specific, purely psychological factors, such as sthenic or asthenic emotions, the ability to anticipate of life situations, etc. According to [Rogovin et Karpova, 1985], activity preparation to external stimuli occurs 0.5 - 2 seconds later (or even slower), so there is no time to run off the bank. Therefore, it is a very important task to study the psychological characteristics of human behavior in case a freak wave is encountered.

The freak wave's lifetime given in Fig. 2.19, which shows the maximum crest height and trough depth in the area of 5 km after reflection from the wall. There is a significant variation of wave height during 40 - 60 seconds (similar time – for waves approaching the wall), thus a value of 1.5 - 2 minutes can be taken as the lifetime of anomalous wave.

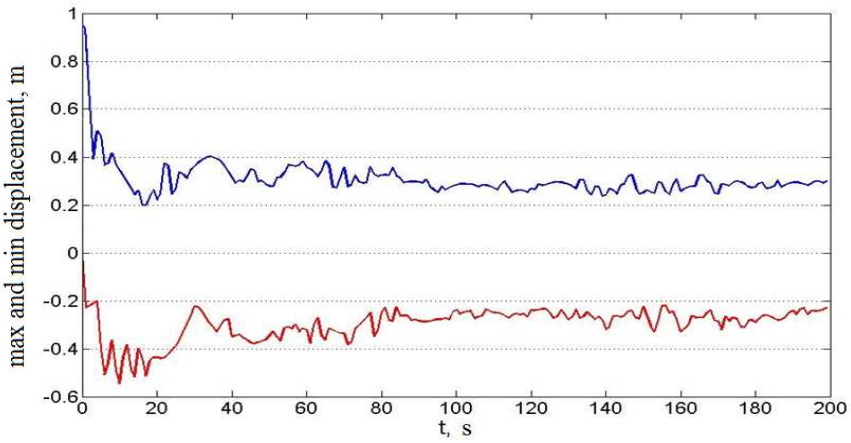

Figure 2.19 – the maximal and minimal displacement.

Freak waves can become long-lived with decreasing depth. Even if dispersion is not considered, freak waves are formed due to the nonlinear interaction of waves with the wall [Pelinovsky et al, 2008]. If bottom changing (slope) is taken into account, the interaction of the waves with the bottom will play the role as well [Didenkulova et Pelinovsky, 2011]. Thus, the characteristic portrait of freak wave appearance near the vertical barrier depends on a number of factors. The mechanism described above is implemented in case if the depth near the cliff is big enough.

One possible scenario of freak wave appearance near a vertical barrier based on the mechanism of dispersive focusing is presented in **E.N. Pelinovsky, E.G. Shurgalina. Abnormal wave amplification near a vertical barrier. Fundamental and Applied Hydrophysics, 2010, No. 4 (10), 28-37.**

2.5 Conclusion

In this chapter, the classical mechanism of dispersion focusing in the linear theory is considered. One of the scenarios of single freak wave appearance in the framework of this mechanism is presented. It is demonstrated that the characteristic lifetime of a single freak wave is about two minutes for typical conditions at sea. It is noted that during this time the wave quickly (in about 10 seconds) changes its shape from the hump to depression and vice versa. That is why the difficulty of freak wave forecast is obvious even if it is seen at a relatively large distance. The lifetimes of freak waves of different shapes - "one, two, three and four sisters" are analyzed in the framework of dispersion mechanisms focusing of wave packets.

Scenarios of freak wave appearances near vertical cliff are discussed. In shallow water, a wave’s shape is changing slower than in deeper water because of small dispersion. This means that an observer will see a freak wake approaching the coast, increasing the height and almost conserving its shape. In this case, it seems that prediction of freak wave appearance is possible as it parallels tsunami wave prediction methods. Waves are usually highly nonlinear in shallow water, and this will be considered in the next chapter.

Chapter 3

Two-soliton interactions in nonlinear models of long water waves

3.1 Introductory remarks

3.2 Observation of solitons in the coastal zone and the basic equations

3.3 Two-soliton interactions in the framework of the Korteweg – de Vries equation

3.4 Two-soliton interactions in the framework of the modified Korteweg – de Vries equation

3.5 Conclusion

3.1 Introductory remarks

The dynamics of waves in shallow water are fundamentally different than the behavior of waves in deep water. From a physical point of view, this is due to decreasing of dispersion roles provided that the individual waves live long enough. On the other hand nonlinearity becomes very strong in shallow water, since the wave height is comparable to the depth. This is especially noticeable in case of wave runup on the shore. Solitary waves (solitons), which are often observed in the coastal area, provoke particular interest.

This chapter is devoted to the features of two-soliton interactions in the framework of the Korteweg de - Vries equation and the modified Korteweg de - Vries equation which are used to describe the surface and internal gravity waves in shallow water. Some data observations of soliton groups (undular bores) and internal solitons in natural bodies are presented in §3.2. The criterion of transition of breaking bore to undular bore, formerly known only in the literature of laboratory data, is analyzed.

Known in the literature of laboratory data, the criterion of transforming of breaking bore to undular bore is particularly analyzed. Here we analyze the field data to test the validity of this criterion in natural waters. This criterion is necessary for the selection of an adequate physical and mathematical model of wave motion. Two-soliton interactions in the framework of the Korteweg - de Vries equation are studied in §3.3.

In this classical problem of theoretical physics and nonlinear wave theory, we focused on the study of the moments of the wave field, which has not been done in previously, and therefore cannot be found in previous literature. Features of two-soliton interactions in the framework of the modified Korteweg - de Vries equation, commonly used in the theory of internal waves, are shown in §3.4. These two-soliton interactions are elementary acts of soliton turbulence and they play a significant role in multi-soliton field dynamics, which will be demonstrated in Chapter 4. Then the results are summarized in the conclusion.

3.2 Observation of solitons in the coastal zone and the basic equations

In the coastal zone wind waves are often presented as asymmetrical waves and their crests are separated by extended troughs. From the point of view of the shallow water theory (Korteweg-de Vries equation or a system of Boussinesq) [Zakharov et al., 1980, Newell, 1985, Lamb, 1983; Kudriashov, 2008], such waves are called cnoidal and when the distance from the crests is large enough, cnoidal waves consist of a sequence of solitary waves called solitons. Frequently they can be observed when a tidal bore enters a river estuary and transforms into a braking bore (hydraulic jump) or an undular bore.

Wonderful photos of such bores are collected in the book [Chanson, 2012] and a few of them are shown on Fig. 3.1. Some of them have a very regular structure, but others are irregular (see instrumental record on Fig. 3.1, taken from the article [Brocchini and Gentile, 2001]). The soliton nature of the wave fields in the coastal zone, where waves with sufficiently large amplitudes can appear, has already been mentioned in this article. This example shows the existence of freak waves in a soliton field, and to explain them a special approach is required.

a) *Tidal bore on Selyun River (France), 19 September 2008. There is a "wavy" transverse profile of the tidal wave caused by the presence of shoals and bars. Propagation direction - from the left to the right.*

b) Undulating bore on the river Dordogne (France), 27 September 2000.

c) Tidal bore on the river Severn (UK), February 11, 2009. There are various forms of the bore: the breaking part near the coast and in the shallows, and undular bore on deeper water.

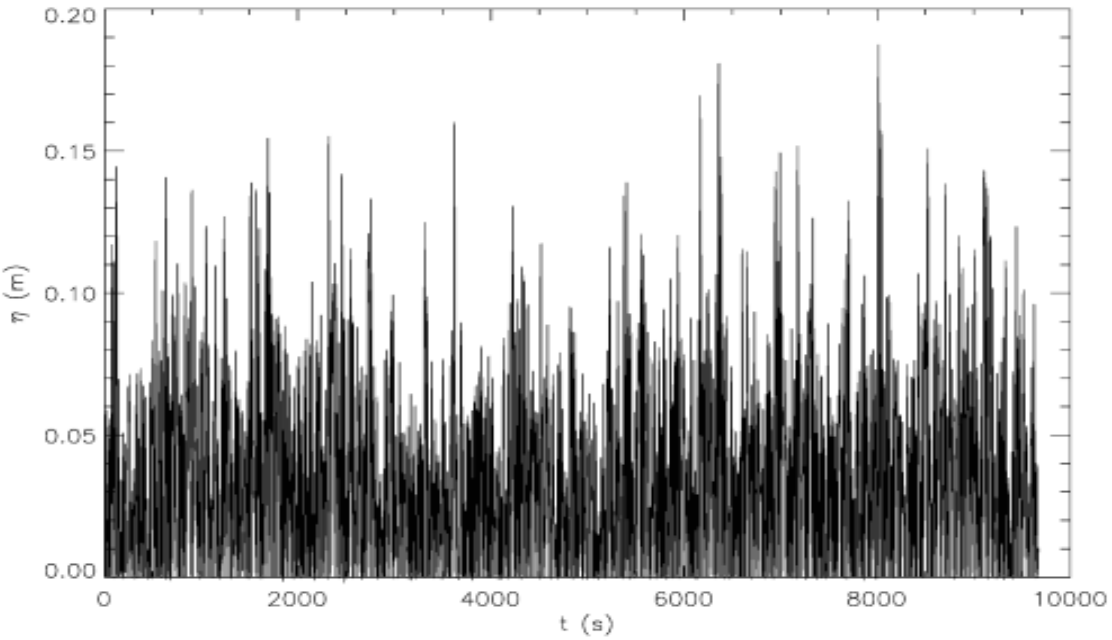

d) Instrumental wave record in the coastal zone.

Figure 3.1 – wave forms in the coastal zone.

However, in addition to undular bores (represented by a set of solitons) in shallow water breaking bores can exist naturally as well. Frequently, they are found close to each other in one place, as illustrated in the Fig. 3.2, taken from the site (www.surfalaska.net).

Figure 3.2 Photo of the bore in Cook Inlet, Alaska.

If in the center where the depth is greater there is an undular bore, closer to the shores there is a changing regime with breaking bore appearance. The formation of both types of bores is clear from physical considerations. If the wave non-linearity is small enough, then dispersion prevents breaking of the tidal wave and promotes the formation of undular oscillations. This process is qualitatively well described by the known solutions of the Korteweg-de Vries equation [Zakharov et al., 1980, Newell, 1985, Lamb, 1983]. If the nonlinearity is large enough, the dispersion can neither prevent the rapid steepening of the wave front nor its breaking. This process is also well understood in the framework of a hyperbolic system of shallow water [Stocker, 1959].

Unfortunately, the most well-known applied numerical models of wave dynamics in the coastal zone cannot take into account both of these effects. Shallow water equations are commonly used to describe tidal waves and tsunami waves.

The breaking bores can be described by the numerical model CLAWPACK [Pelinovsky et Rodin, 2012]. In other models, for example TUNAMI and AMI DANCE, the smoothing of the wave front is carried out by introducing horizontal viscosity (diffusion); while in real waters the spatial step is large enough which is why the nonlinear wave deformation is not that noticeable [Zahibo et al. 2006]. On the other hand, in new models of nonlinear dispersive theory (Boussinesq equation of different order) the undular bore is well-prescribed, particularly, during the 2004 Indian Ocean Tsunami [Dao & Tkalich, 2007; Grue et al, 2008], but wave breaking was not observed there. Nonlinear dispersive models do not have significant performance and, hence, they are rarely applied to the tsunami problem.

This is precisely why a simple criterion of legitimacy to use a particular model for describing the real situation is needed. Such criteria are known in the results of numerous laboratory experiments under idealized conditions of dimensional flow [Stocker, 1959; Docherty & Chanson, 2010; Favre, 1935; Nakamura, 1973; Teles Da Silva & Peregrine, 1990].

However these criteria have not been tested by the field data of wave processes in the coastal zone. Therefore the analysis of field data, which allows one to conclude the applicability of the criteria obtained in the laboratory conditions, will be carried out

further. It may help to perform a preliminary zoning of a water reservoir by the type of waves propagating there.

There is a fairly large collection of tidal bores which form when tidal waves enter a river. The classical tidal bore example is a bore on the river Severn in England downstream from the city of Gloucester, which has a height above two meters during spring tide. Tidal bores are periodic, and this makes it relatively easy to collect a large amount of data. Many of them are presented in the book [Chanson, 2011] with quantitative parameters. Field data of recorded tidal bores all over the world is collected and presented in Table 3.1.

Table 3.1 Field data of tidal bores (Brealing - B*, undular* - U*).*

№	River, date	h, m	H, m	H/h	Bore type	Reference
1	Seine River, France	1	1.9	1.9	B	[Chanson, 2008]
2	Sélune River, France, 24/09/10	0.38	0.72	1.89	B	[Mouaze et al., 2010]
3	Sélune River, France, 25/09/10	0.33	0.74	2.25	B	[Mouaze et al., 2010]
4	Garonne River, France, Podensac, 10/09/10	3.1	4.2	1.35	U	[Bonneton et al., 2011]
5	Garonne River, France, Podensac, 4/09/10	1.85	2.1	1.13	U	[Bonneton et al., 2011]
6	Qiantang River, China, October 2007	1	4	4	B	[Cun-Hong and Hai-Yan, 2010]
7	Rio Mearim, Brazil, 30/01/91	1.8	2.7	1.5	U/B	[Kjerfve and Ferreira, 1993]
8	Dee river, Great Britain,	0.8	1.05	1.3	U	[Simpson et al., 2004]

	15/05/2002					
9	Garonne river, France, Arcins channel, 10/09/10	1.74	2.3	1.32	U	[Simon et al., 2011]
10	Dee river, Great Britain, 22/09/72	1	1.8	1.8	U	[Chanson, 2009]
11	Dordogne river, France, 26/04/90	1.12	1.602	1.43	U	[Chanson, 2011]
12	Daly river, Australia, 2/06/2003	1.5	1.78	1.19	U	[Chanson, 2011]
13	Qiantang River, China, 19/09/09	7.12	7.90	1.1	U	[Zhu, 2011]
14	Garonne River, France, 7/06/12	2.65	3.17	1.2	U	[Reungoat et al., 2014]
15	Garonne River at Arcins, France, 19/10/13	2.05	2.35	1.15	U	[Reungoat et al., 2014]
16	Dee River, Great Britain, 6/09/03	0.72	1.17	1.63	B	[Simpson et al., 2004], [Reungoat et al., 2014]
17	Sée River, France, 7/05/12	0.9	1.46	1.62	U	[Reungoat et al., 2014], [Furgerot et al., 2013]

Similar measurements around the same place, date, and conditions that were approximately the same were excluded. Therefore, we hope that our sample is representative. Input parameters are the bore type, bore height from the bottom (H), and the water depth in front of bore (h).

The total number of data points is 17, including 5 cases of breaking bores, 11 cases of undular bores, and one intermediate.

The criteria available in the literature are based on various parameters of the wave stream and the simplest of them use the ratio of bore height measured from the bottom (H), to the undisturbed water depth (h). In this paper [Favre, 1935] the following criterion exists: H/h <1.28 corresponding to the undular bore, H/h> 1.75 corresponding to the breaking bore (hydraulic jump). The intermediate regime lies between these cases, when both effects may occur – the breaking and dispersive transformation.

In the book [Stocker, 1959] there is a more general criterion which does not include any intermediate regime: $H/h < 1.5$ corresponding to the undular bore, $H/h > 1.5$ corresponding to the breaking bore. In the experimental work of Nakamura [Nakamura, 1973] one more condition is added to the Stocker criteria: $H/h > 9$ corresponding to the case of a parabolic wave (dam destruction).

In the work [Teles Da Silva & Peregrine 1990] the intervals of criterion are shifted a little bit: $H/h < 1.3$ corresponding to the undular bore, $H/h > 1.7$ corresponding to the breaking bore. Undular bores with breaking may be observed between these criterion.

The field data from the Table 3.1., can be checked by these criteria (Fig. 3.3).

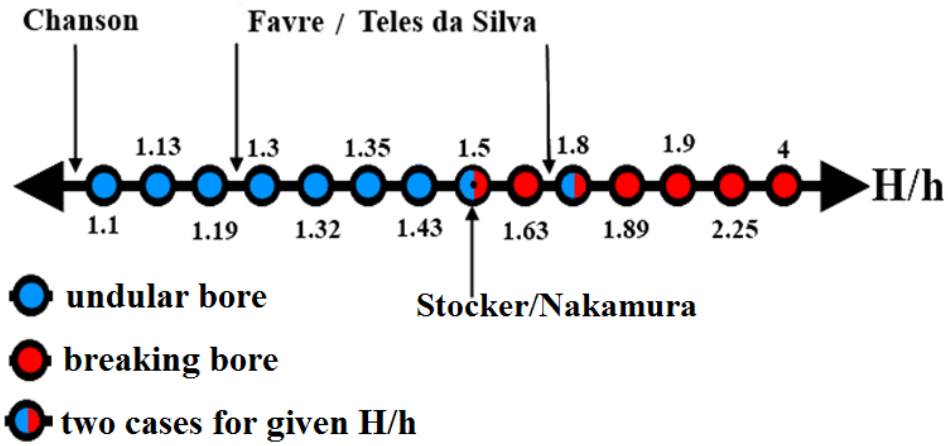

Figure 3.3 Distribution of observed data by the parameter H/h.

As we can see, undular and breaking bores are well separated by threshold H/h=1.5, except for one case with H/h=1.8, which is on the threshold of the interval of Favre - Teles da Silva. In general we can say that the criterion H/h=1.5 may be used for a rough assessment of the wave motion type, and accordingly, a suitable choice of the numerical model to describe the wave dynamics. We will also assume that H/h <1.5, and

even $H/h << 1.5$, which allows study of the undular bore containing small-amplitude solitons. This statement applies to the surface waves on a shallow sea.

This study is published in the following article: **E.N. Pelinovsky, E.G. Shurgalina, Rodin A.A. On the criteria of the transition from breaking bore to undular bore. Izvestiya, Atmospheric and Oceanic Physics, 2015, 51 (2).**

Solitons, however, exist not only on the water surface, but also inside the fluid if it is stratified. This situation is typical for natural reservoirs when the effects of turbulent mixing are weak. Internal gravity waves are of the same nature as surface gravity waves, but for them the gravity is almost balanced by the Archimedes force, thus the reduced gravitational acceleration is approximately three orders of magnitude less than for surface waves. Internal waves exist in the case of stable ocean stratification, where the average water density increases towards the bottom. Internal waves have been described theoretically in the middle of the XIX century, and found in the ocean in the early XX century, but it took nearly another century to understand the importance of internal waves in the ocean [Miropolsky, 1981; Konyaev and Sabinin, 1992].

The height of a typical oceanic internal wave is usually much larger than the typical height of a surface ocean wave; it becomes larger when the stability of density water stratification becomes less. Internal waves observed in the ocean have amplitudes around 5-20 m, but sometimes they can be greater. Thus the internal solitons in the Andaman Sea have speeds up to 2.0 m/s and amplitudes up to 60 m [Osborne & Burch, 1980]. Although there are other mechanisms of internal wave generation such as wind circulation and unstable flows, the main mechanism of strong internal wave generation is the transformation of the barotropic tidal current on the sharp drop depth (edge of the continental shelf).

In the presence of strong tidal current, large amplitude waves occur exactly at the edge of continental flow. In the vertical plane such waves look like a single variation of the pycnocline depth (areas of the most dramatic changes of water density) of sufficiently large value (up to 15-20 m). Their velocities are about 0.6-1.0 m/s. Then the vertical distribution of density is restored within a few hours and the initial perturbation, propagated along the pycnocline, is divided into a number of consecutive solitons, forming a train consisting of leading soliton - the largest and the quickest wave in the

wave train, and the wave tail - a group of small dispersive waves in the end of the train (undular bore or solibor).

Various satellite images of internal waves are shown on Fig. 3.4 - 3.7.

Figure 3.4 Internal waves in a freshwater Lake Ladoga in the radar image of spacecraft "Almaz-1» (26.06.91, 04:54 UTC). © NGO engineering.

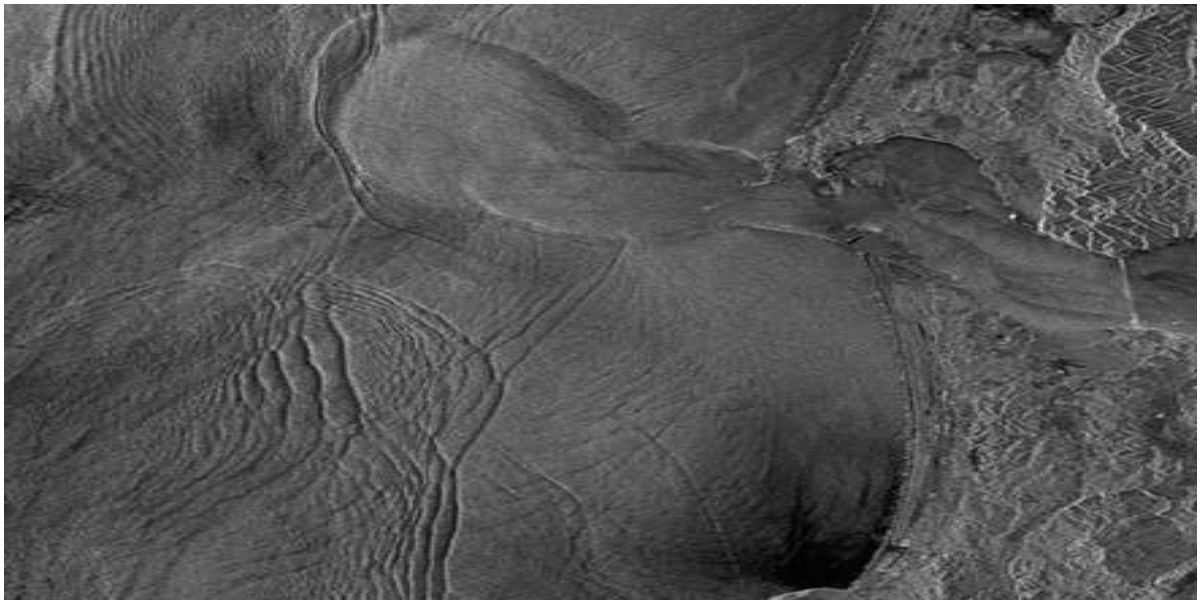

Figure 3.5 Internal waves in the Pacific Ocean near the west coast of the United States (Washington) on radar imagery of satellite Radarsat (9.08.1999, 01:55 UTC). There are two types of internal waves: one is generated by the tide and propagates towards the shore, the other – by a powerful motion of Colombia River and propagates into the open ocean. © CSA

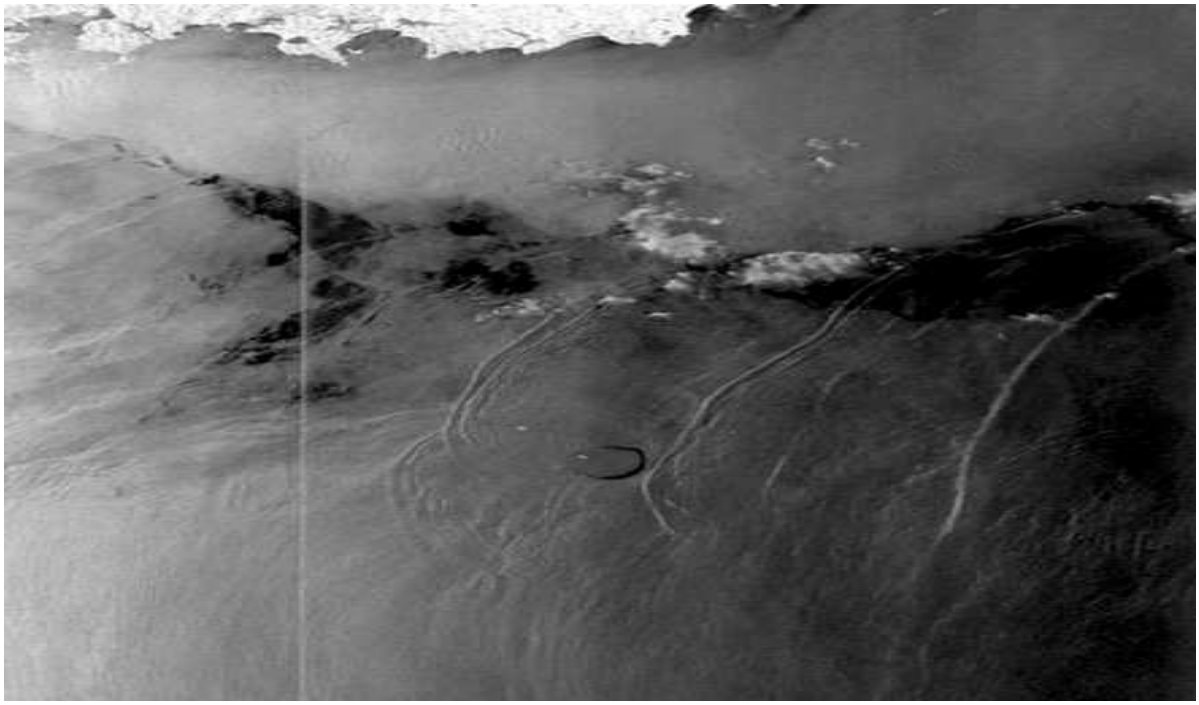

Figure 3.6 Eight packages of internal waves in the South China Sea on radar images of Radarsat (26.04.1998) © CSA

Figure 3.7 Internal waves in Dongsha Atoll in the South China Sea on the radar images ERS-2 (23.06.1998, 14:41 UTC). © ESA

Although a large amount of experimental material is collected, internal waves have not been studied enough. Particularly the mechanisms of generation of various internal waves, the conditions of their propagation and transformation, dynamic stability and energy dissipation are not yet clear. Satellite and radar measurements allow us to understand the spatial characteristics of internal waves, their evolution, and their dynamics. Due to remote methods the role of nonlinear effects in internal wave evolutions becomes obvious.

Currently, the atlases and catalogs of internal waves are created based on satellite records (see. eg, [Atlas, 2004]). Several reviews of internal solitons are published [Ostrovsky & Stepanyants, 1989, 2005; Apel et al., 2007]. This confirms that the solitons are an integral part of the wave dynamics on the surface and inside of the ocean. Therefore, the study of solitons and their interactions is an important task.

Let us briefly present the basic equations describing solitons in a shallow sea. Our analysis will be based on the family of the Korteweg-de Vries equation. For surface waves it was derived in 1895 in the pioneering work of Korteweg and de Vries, and then rewritten again in [Korteweg & de Vries, 1895; Karpman, 1973]. The Korteweg - de Vries equation has the following form

$$\frac{\partial \eta}{\partial \tau} + \alpha\eta\frac{\partial \eta}{\partial x} + \beta\frac{\partial^3 \eta}{\partial x^3} = 0, \tag{3.1}$$

$$\alpha = \frac{3}{2h}c_0, \qquad \beta = \frac{c_0 h^2}{6}, \tag{3.2}$$

where $c_0 = \sqrt{gh}$ (h is a constant water depth), $\eta(x,\tau)$ is a displacement of water level, x is a coordinate and τ is time.

The coefficients α and β are called the coefficients of nonlinearity and dispersion. As seen from (3.2) with depth decreasing the nonlinearity grows while dispersion decreases, thus the nonlinear effects are most strongly manifested in shallow water.

The canonical form of the Korteweg - de Vries equation could be obtained by using the following substitutions:

$$t = \beta\tau, \qquad u = \frac{\alpha\eta}{6\beta}, \tag{3.3}$$

and then the equation (3.1) takes the following dimensionless form

$$\frac{\partial u}{\partial t} + 6u\frac{\partial u}{\partial x} + \frac{\partial^3 u}{\partial x^3} = 0. \tag{3.4}$$

In the majority of mathematical and physical papers devoted to the dynamics of weakly nonlinear waves in weakly dispersive media the Korteweg - de Vries equation is written in present form [Zakharov et al., 1980; Lamb, 1983, Newell, 1985].

The Korteweg - de Vries equation can also describe the distribution of weakly nonlinear internal waves close to the long-wavelength limit. However for internal waves the situation is much richer. In this case the physical meaning of the wave function $\eta(x,\tau)$ in (3.1) is as follows: in the zero-order perturbation theory, which describes the linear internal waves without dispersion, the variables are separated [Pelinovsky et al., 2000; Grimshaw et al., 2002] and the vertical displacement of isopycnals (lines of equal density) can be represented in the form:

$$\zeta(x, y, \tau) = \eta(x, \tau)\Phi(y). \tag{3.5}$$

There is a new vertical coordinate y and $\Phi(y)$ is a modal function defining the distribution of waves with the depth. It is found from the solution of the boundary value problem (Sturm-Liouville problem) with zero boundary conditions at the bottom ($y = -h$) and on the free surface ($y = 0$):

$$\frac{d^2\Phi}{dy^2} + \frac{N^2(y)}{c^2}\Phi = 0, \quad \Phi(0) = \Phi(-h) = 0, \tag{3.6}$$

where h is a water depth (the origin of coordinates is associated with the water surface), $N(y)$ is a Brunt-Vaisala frequency (buoyancy), which is determined by the vertical distribution of the water density $\rho_0(y)$:

$$N(y) = \sqrt{-\frac{g d\rho_0}{\rho_0 dy}}, \tag{3.7}$$

c – eigenvalues of the Sturm - Liouville problem (3.6), which determines the linear approximation of the long internal wave propagation speed. It is easy to show that the boundary value problem (3.6) has a discrete spectrum with different eigenvalues [Mitropolsky, 1981]. In this model, each mode of internal waves propagate independently, thus we will not continue to use the index to select a specific mode of internal waves. Schematic representations of the buoyancy frequency with the depth in the ocean are shown on Fig. 3.8. The eigenfunctions, calculated according to (3.6), describing the distribution of isopycnals with the depth (modes) taken from [Talipova et al., 1999] are also shown.

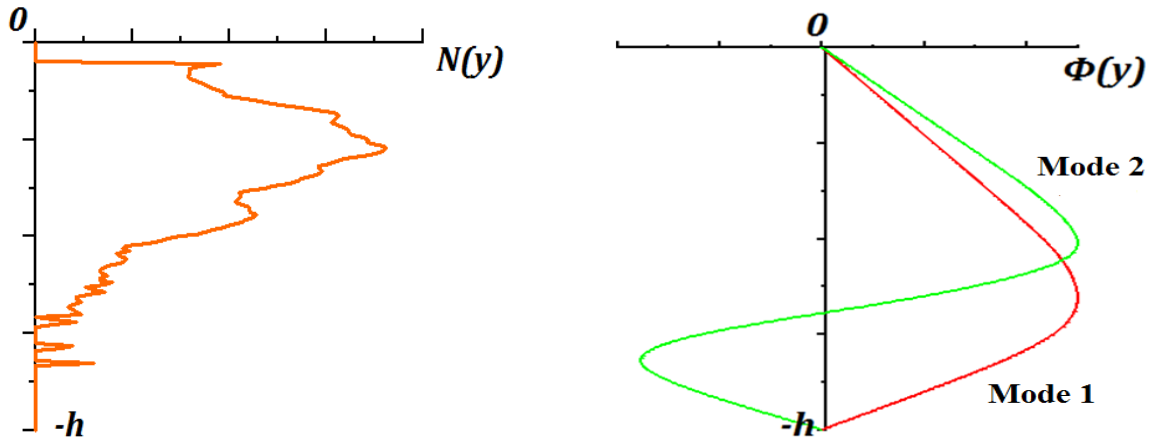

Figure 3.8 Buoyancy frequency and mode functions of internal waves (two modes).

The normalization condition on the function $\Phi(y)$: $\Phi_{max} = 1$ is used, thus the function $\eta(x,t)$ describes the vertical isopycnal displacement at the maximum mode (these maxima may be at different depths for different modes). The Korteweg-de Vries equation (3.1) is obtained for this function, but now its coefficients are expressed by integral expressions [Benney, 1966; Mitropolsky, 1981; Pelinovsky et al., 2000]:

$$\alpha = \left(\frac{3c}{2}\right)\frac{\int_{-H}^{0}(d\Phi/dy)^3\,dy}{\int_{0}^{H}((d\Phi/dy)^2\,dy}, \tag{3.8}$$

$$\beta = \left(\frac{c}{2}\right)\frac{\int_{-H}^{0}{}^{2}\Phi^2 dy}{\int_{-H}^{0}(d\Phi/dy)^2\,dy}. \tag{3.9}$$

In the special case of two-layer liquid and the Boussinesq approximation (water density changes are small) the coefficients on the surface (3.1) will take the simple form of [Ostrovsky & Stepanyants, 1989]

$$c = \sqrt{\frac{g\Delta\rho}{\rho}\frac{h_1 h_2}{h_1 + h_2}},\ \beta = \frac{c h_1 h_2}{6},\ \alpha = \frac{3c}{2}\frac{h_1 - h_2}{h_1 h_2}, \tag{3.10}$$

where $\Delta\rho / \rho$ - density jump between the upper layer of thickness h_1 and the lower layer of thickness h_2.

The transition to the canonical Korteweg-de Vries equation is similar to equation (3.3). However, there is one fundamental difficulty. In contradistinction to surface waves the coefficient of quadratic nonlinearity can change sign, and even vanish, while the dispersion coefficient is always positive. This is evident from the general expression (3.8), and from the special case of two-layer liquid. In the second case it is evident that the zero value of nonlinearity is achieved if the thicknesses of the layers are identical. But in this case the balance between nonlinearity and dispersion is disrupted, but they must have the same order in the frameworks of Korteweg-de Vries equation.

To obtain the nonlinear evolution equations, in this case it is necessary to modify the asymptotic scheme. In this case the non-linearity must be considered up to the cubic order. In the case when the coefficient of the quadratic nonlinearity is equal to zero, the modified Korteweg-de Vries equation (mKdV) is obtained for the internal waves [Grimshaw et al, 1997]. This equation differs from the Korteweg-de Vries equation by the nonlinear term and has the following form:

$$\frac{\partial \eta}{\partial \tau} + \alpha_1 \eta^2 \frac{\partial \eta}{\partial x} + \beta \frac{\partial^3 \eta}{\partial x^3} = 0. \tag{3.11}$$

The coefficient of cubic nonlinearity is defined by the integral expression

$$\alpha_1 = -\frac{3c}{2}\frac{\int [2(d\Phi/dy)^4 - 3(dT/dy)(d\Phi/dy)^2]dy}{\int (d\Phi/dy)^2 dy} \tag{3.12}$$

which includes the function *T(y),* and this function is a solution of the inhomogeneous boundary value problem

$$c^2 \frac{d^2T}{dy^2} + N^2(y)T = \frac{3c^2}{2}\frac{d}{dy}\left[\left(\frac{d\Phi}{dy}\right)^2\right] \tag{3.13}$$

with zero boundary conditions at the bottom and free surface, and with normalization of $T = 0$ at the depth where the function $\Phi = 1$. The physical meaning of the function $T(y)$ is a nonlinear correction to the mode, thus the vertical displacement of isopycnals is defined by the more complicated expression

$$\zeta(x, y, \tau) = \eta(x, \tau)\Phi(y) + \eta^2(x, \tau)T(y). \tag{3.14}$$

Taking into account the normalization of the functions Φ and T, the wave function $\eta(x,t)$ still describes the vertical isopycnal displacement at the maximum mode.

The sign of cubic nonlinearity coefficient is unclear from the integral equation (3.12). If we re-use the two-layer approximation for the density, and when quadratic nonlinearity coefficient is equal to zero ($h_1=h_2$), the coefficient of cubic nonlinearity is [Ostrovsky & Stepanyants, 1989]:

$$\alpha_1 = -\frac{3c}{h_1^2} \tag{3.15}$$

In this case it is negative (in fact it is negative at any ratio of the layer thicknesses). In the three-layer "symmetric" flow (upper and lower layers have the same thickness h_1 and the same density difference between layers), the coefficient of the quadratic nonlinearity vanishes, and the coefficient of cubic nonlinearity becomes [Grimshaw et al, 1997]

$$\alpha_1 = -\frac{3c}{4h_1^2}\left(13 - \frac{9h}{2h_1}\right). \tag{3.16}$$

The cubic nonlinearity coefficient is negative for $h_1 > 9h/26$ (when the middle layer is thin and the stratification is close to two-layer stratification), and it is positive in the opposite case (when the middle layer is large). Calculations of the coefficients of quadratic and cubic nonlinearity for the real stratifications of the Ocean are made in [Grimshaw et al, 2007].

Thus, in the framework of the modified Korteweg - de Vries equation (3.11), the dispersion coefficient is always positive, and the coefficient of cubic nonlinearity can have any sign or even be vanished for the internal wave.

If the cubic nonlinearity coefficient is not zero, then a substitution similar to (3.3)

$$t = \beta\tau, \qquad u = \sqrt{\frac{|\alpha_1|}{6\beta}}\eta, \tag{3.17}$$

allows us to get the modified Korteweg-de Vries equation in a canonical form

$$\frac{\partial u}{\partial t} \pm 6u^2 \frac{\partial u}{\partial x} + \frac{\partial^3 u}{\partial x^3} = 0 \tag{3.18}$$

where the sign of a nonlinear term coincides with the sign of the coefficient of cubic nonlinearity. From a mathematical point of view the modified Korteweg-de Vries equation with any sign of cubic nonlinearity coefficient can be studied as well, being fully integrable over the Korteweg-de Vries equation [Zakharov et al., 1980; Lamb, 1983; Newell, 1985].

However, nonlinear dynamics are quite different for different signs of the coefficient of cubic nonlinearity. Particularly, the equation (3.18) with a negative "cube" doesn’t have limited solutions (solitons) at the zero pedestal, while in the case of the positive "cube", such solutions are available. The dynamics of quasi-sinusoidal waves is also different in these equations, particularly, with a positive "cube" effects of modulation instability are possible [Grimshaw et al, 2010; Talipova, 2011], and they lead to the appearance of direct and inverse cascades of the spectrum [Dutykh & Tobish, 2014a, b].

Primary attention will be paid to the interaction of two solitons in the framework of equations (3.4) and (3.18) with a positive "cube" in this chapter. All solitons in these equations have exponential tails tending to zero (pedestal). With the help of well-known two-soliton solutions and numerical simulation new properties of such interactions affecting the moments of the wave field will be predicted.

3.3 Two-soliton interactions in the framework of the Korteweg – de Vries equation

The Korteweg - de Vries equation is completely integrable, and the Cauchy problem can be solved for this equation. Proposed in [Gardner et al, 1967] method of the inverse scattering problem is very popular now and it is presented in a number of books [Newell, 1985; Zakharov et al., 1980]. Two operators called a Lax pair form the basis for the Korteweg - de Vries.

$$\hat{L}\psi = \lambda\psi,\ \hat{A}\psi = \psi_t, \tag{3.19}$$

where

$$\hat{L} = -\frac{\partial^2}{\partial x^2} + u(x,t),\ \hat{A} = -4\frac{\partial^3}{\partial x^3} + 6u\frac{\partial}{\partial x} + 3\frac{\partial u}{\partial x}. \tag{3.20}$$

The first equation in (3.19) is a stationary one-dimensional Schrödinger equation with the potential *u(x,t)*, depending on the parameter that has a sense of time *t*. The second equation describes the time dependence of the solution. In the framework of the inverse problem method, the spectrum of the Schrödinger equation does not depend on time and can be found with the initial condition for the Korteweg - de Vries equation. Discrete spectra (which are always real), if they exist, determine the soliton amplitudes that arise from given initial conditions.

The continuous spectrum describes the dispersion packets which also arise from the initial conditions. Although the scheme of soliton finding in the frameworks of stationary Schrödinger equation is quite simple; a solution in explicit form (eg, soliton phases, and the amplitude of the wave packets) is not a trivial task. The task of finding the particular multi-soliton solutions of the Korteweg-de Vries equation is easier in some sense, especially if various transformations like Backlund transformation, Hirota, and Darboux are used [Lamb, 1983, Newell, 1985].

It is important to emphasize that solitons are resistant wave formations and their shape is preserved after the interaction with each other and with wave packets. This is why solitary waves are called solitons, emphasizing the wave-particle dualism.

Soliton research has become an independent task, and these waves can be isolated in measurements of wave fields. Here we consider one of the classical problems in the theory of solitons - the interaction of two solitons. The description of this process is given in many articles, and the main results were obtained in the 70s [Zakharov et al., 1980; Lax, 1968]. Nevertheless, a number of important features of this interaction, which are necessary for the understanding of soliton turbulence, were lost. They are discussed in the article: **Pelinovsky E.N., Shurgalina E.G., Sergeeva A.V., Talipova T.G., El G.A., Grimshaw R.H.J. Two-soliton interaction as an elementary act of soliton turbulence in integrable systems. Physics Letters A, 2013, 377 (3-4)**, **272–275.**

3.4 Two-soliton interactions in the framework of the modified Korteweg – de Vries equation

We have already mentioned the applicability of the modified Korteweg-de Vries (mKdV) to internal waves in the ocean previously. The modified Korteweg-de Vries is also used to describe wave propagation in isotropic media (for example, acoustic waves in the plasma) [Perelman et al., 1974; Pelinovsky and Sokolov, 1976; Grimshaw et al, 2005; Ruderman et al, 2008].

This family of nonlinear waves is much richer, and instead of solitons there are breathers - nonlinear wave packets [Lamb, 1983; Clarke et al, 2000]. Meanwhile, the analysis that we did in the article mentioned in the previous paragraph was not made for the modified Korteweg-de Vries equation. The simple interaction of two solitons has not yet been studied. It is obvious that the pair interactions play a definitive role in the dynamics of multi-soliton fields in the framework of the modified Korteweg - de Vries equation because of its complete integrability. This is why in this paragraph we focus on the study of the contribution of two-soliton interactions to the wave field moments in the framework of the modified Korteweg - de Vries equation. A new feature in comparison to Korteweg-de Vries equation is the existence of solitons with both polarities.

We will use the canonical form of the mKdV equation (3.11) with a positive sign of the coefficient of cubic nonlinearity. The exact solution of this equation is a soliton:

$$u(x,t) = sA\,\mathrm{sech}[A(x - ct - x_0)], \qquad c = A^2 \tag{3.21}$$

where A is an amplitude of soliton, $s = \pm 1$ determines the soliton polarity, c is a soliton velocity, and x_0 is a phase (initial position of the soliton).

The Mkdv-soliton is also highly localized in space. The soliton velocity does not depend on the soliton polarity and it always moves to the right side. The dependence of the soliton velocity of the soliton amplitude is stronger than in the Korteweg-de Vries equation: soliton of small amplitude is moving very slowly while large solitons move quickly.

The two-soliton solution has a more complex structure [Anco et al., 2011]:

$$u(x,t)=2\gamma\frac{s_1A_1\cosh(A_2(x-A_2t))+s_2A_2\cosh(A_1(x-A_1t))}{s_1s_2(\gamma^2-1)+\gamma^2\cosh(A_1(x-A_1t)-A_2(x-A_2t))+\cosh(A_1(x-A_1t)+A_2(x-A_2t))}, \quad (3.22)$$

$$\gamma=\frac{A_1+A_2}{A_1-A_2}>1.$$

The individual soliton phases are neglected here by the conversion of time and coordinates. When solitons are far from each other the solution of (3.22) can be presented as the sum of two non-interacting solitons:

$$u(x,t)=u_1(x,t)+u_2(x,t), \quad (3.23)$$

where $u_{1,2}$ is a one-soliton solution (3.21) with amplitudes $A_{1,2}$.

The case of the KdV-solitons in the case of the modified Korteweg-de Vries solitons the interaction of unipolar solitons leads to a nonlinear phase shift of faster (higher) solitons forward to [Slunyaev and Pelinovsky, 1999; Slunyaev, 2001]:

$$\Delta x_1=(2/A_1)\ln\left((A_1+A_2)/(A_1-A_2)\right)>0\,, \quad (3.24)$$

and slower (lower) solitons - back on

$$\Delta x_2=-(2/A_2)\ln\left((A_1-A_2)/(A_1+A_2)\right)<0\,. \quad (3.25)$$

Thus, the nonlinear interaction leads to "repulsion" of unipolar solitons from each other, as in the Korteweg-de Vries equation. However, for the solitons of different polarity the result is opposite – the solitons attract each other [Slunyaev, 2001].

The strongest interaction of solitons occurs at the time of their closest approach (t = 0). The shape of the resulting pulse is easily found from (3.22) explicitly

$$u(x,0)=2\gamma\frac{A_1\cosh(A_2x)+s_2A_2\cosh(A_1x)}{s_2(\gamma^2-1)+\gamma^2\cosh[(A_1-A_2)x]+\cosh[A_1+A_2)x]}. \quad (3.26)$$

We assume here that the largest soliton has a positive polarity, and the small soliton can have any polarity.

It is known that KdV-soliton impulse in the moment of soliton interaction will have a “one-humped” form (overtake interaction) if the amplitude of solitons are very different from each other, and a “two-humped” (exchange interaction) - if the amplitudes are similar. Similar results can be obtained for mKdV solitons, analyzing the second derivative of the function *u(x,0)* at *x=0*:

$$u_{xx}(x,0)\big|_{x=0} = (A_1 - A_2)\left(A_1 A_2 - (A_1 - s_2 A_2)^2\right). \qquad (3.27)$$

In the article [Anco, 2011] a similar expression for the modified Korteweg-de Vries equation (3.11) is obtained, but for the cubic nonlinearity coefficient equal to 24 instead of 6.

From (3.27) is clear that in case of interactions of heteropolar solitons (s_2 = - *1*), this value is always negative and, at least the central part of the resulting pulse is “one-humped”.

In the case of unipolar solitons, the sign of the second derivative (3.27) depends on

$$\frac{A_2}{A_1} = \frac{3-\sqrt{5}}{2} \cong 0.382\,, \qquad (3.28)$$

The critical value of the ratio of soliton amplitudes in the modified Korteweg-de Vries equation differs from the similar value in the Korteweg-de Vries equation.

Thus, there are three types of soliton interactions in the modified Korteweg-de Vries equation. For the positive solitons there are two types of interactions: overtake (A_2 <0.38 A_1) and exchange (A_2> 0.38A_1). In this sense there is a complete analogy with the soliton interaction in the framework of the Korteweg - de Vries equation. In the case of heteropolar solitons, the fast soliton always absorbs slowly one and then is restored. This type of interaction is called absorb-emit [Anco et al, 2011].

Different types of soliton interaction are shown in Fig. 3.9:

a)

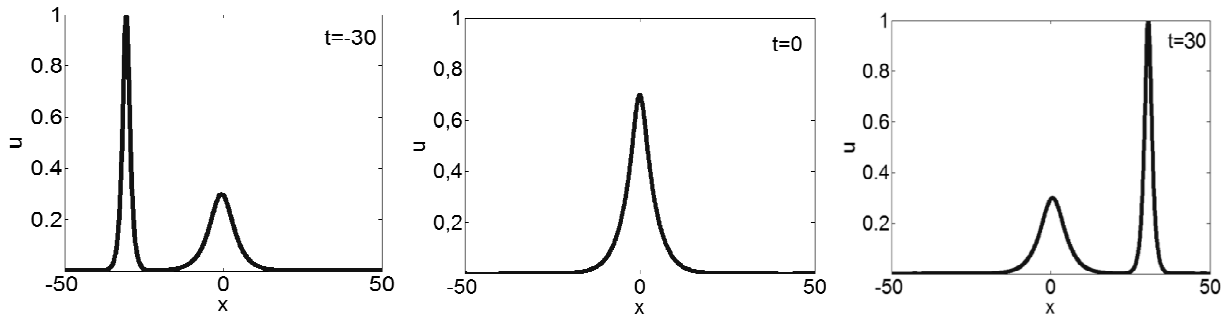

b)

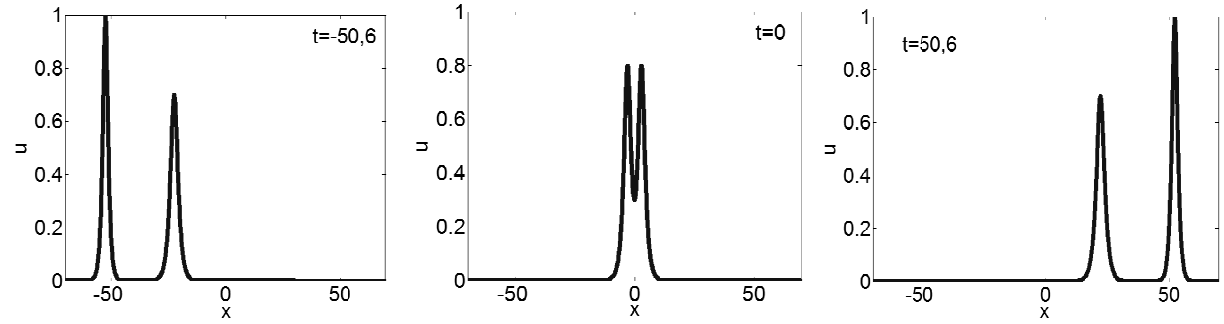

c)

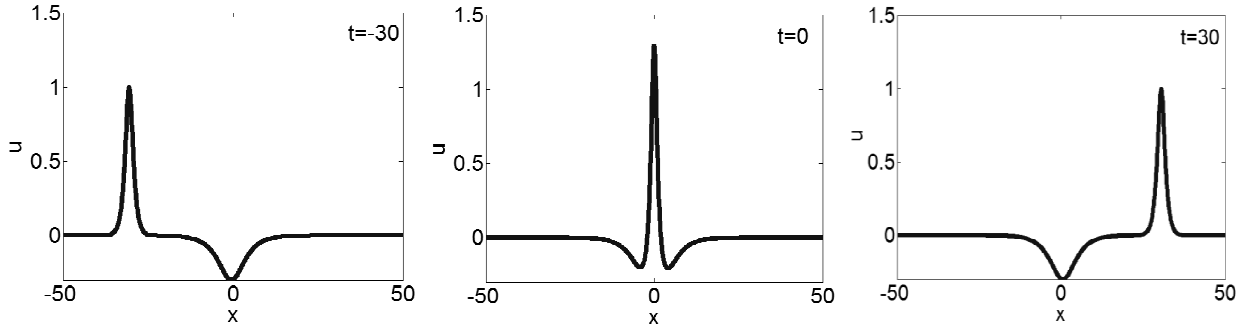

Figure 3.9 Different types of soliton interaction*: a), $s_1A_1=1$, $s_2A_2=0.3$, b) $s_1A_1=1$, $s_2A_2=0.7$ c) $s_1A_1=1$, $s_2A_2=-0.3$.*

The field value in the central part of the resulting impulse is easy to find from (3.2) at $x = 0$ [Pelinovsky and Slunyaev, 1999; Slunyaev, 2001]:

$$U_* = A_1 - s_2 A_2, \tag{3.29}$$

As in the case of KdV equation, this value corresponds to the amplitude of the resulting impulse if it is one-humped. Thus, the amplitude of the resulting impulse increases in the case of heteropolar soliton interactions and decreases in the case of unipolar soliton

interactions. In the case of two-humped resulting impulse, its maximum value is not located in the central point, and it cannot be found from (3.2) analytically.

The maximum and minimum amplitudes of the resulting impulse from the amplitude ratio of solitons for the four types of interactions are presented in Fig. 3.10 (the fourth type is for heteropolar solitons when the largest has a negative polarity - this case is added for generality). It is easy to see the symmetry of figures 3.10a and 3.10d, as well as 3.10b and 3.10c. This is due to the same soliton amplitudes, but opposite sign of both solitons.

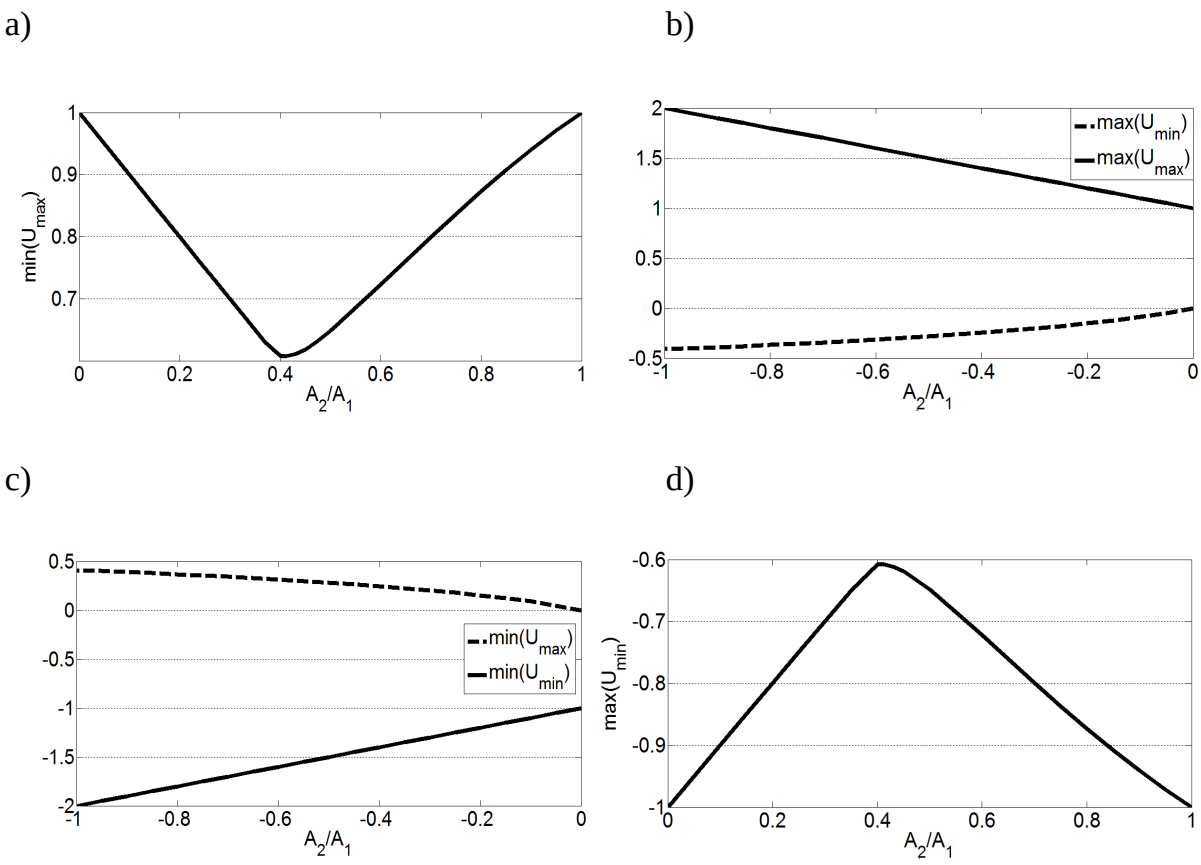

Figure 3.10 Extremes of wave fields: a) positive mKdV-solitons, b) heteropolar mKdV-solitons (bigger soliton has a positive polarity), c) heteropolar mKdV-solitons (bigger soliton has a negative polarity), d) negative mKdV-solitons.

Thus, in the cases 3.10a and 3.10d the amplitude of resulting impulse firstly monotonically decreases (increases) till the value $A_2 / A_1 = 0.41$ and this result is due to the formula (3.29). The extreme value of the maximum amplitude is about $|0.607|$.

Then the maximum amplitude monotonically increases (decreases) (when the amplitudes of the second soliton are large enough and when the resulting impulse is “two-humped”). This behavior is explained by the change of regimes from overtake to exchange for the amplitude ratio $0.38 < A_2/A_1 < 0.43$. In fact there is a complete analogy with the dynamics of the KdV-solitons, where there is a transition zone between two regimes of interaction as well.

Due to there existing only a regime of soliton interactions, in the case of heteropolar solitons (Fig. 3.10b, c) the curves of variation of positive and negative amplitudes of the total impulse are monotonous. The impulse maximum at the time of interaction on Fig. 3.10b and respectively the minimum on Fig. 3.10d, decreases (increases) linearly with decreasing of modulus of the second soliton amplitude, and it is equal to $s_1 A_1 - s_2 A_2$ by analogy with (3.29).

Let us consider the integral characteristics of the modified Korteweg-de Vries equation. Due to its complete integrability it has an infinite number of conserved invariants [Miura et al., 1968]. The first three of which correspond to the laws of conservation of mass, momentum and energy:

$$I_1 = \int_{-\infty}^{+\infty} u dx, \tag{3.30}$$

$$I_2 = \int_{-\infty}^{+\infty} u^2 dx, \tag{3.31}$$

$$I_3 = \int_{-\infty}^{+\infty} \left[u^4 - u_x^2\right] dx, \tag{3.32}$$

$$I_4 = \int_{-\infty}^{+\infty} \left[u^6 - 5u^2 u_x^2 + \frac{1}{2} u_{xx}^2\right] dx, \tag{3.33}$$

These invariants are saved during the evolution of the wave field and they are easily found analytically for the case when the solitons are separated in space:

$$I_1 = \pi\left(s_1 + s_2\right), \tag{3.34}$$

$$I_2 = 2\left(A_1 + A_2\right), \tag{3.35}$$

$$I_3 = \frac{2}{3}\left(A_1^3 + A_2^3\right) , \tag{3.36}$$

$$I_4 = \frac{A_1^5 + A_2^5}{5} . \tag{3.37}$$

The first invariant depends only on its polarity, and not on the amplitude of the soliton. Its value plays an important part in the evolution of the initial perturbation, determining the number of emerging solitons and breathers [Clarke et al., 2000]. Thus, in contrast to the Korteweg-de Vries equation, here solitons arise only from the perturbation with a mass greater than the critical value, not from any initial perturbations of "correct" polarity. Other invariants are positive definite and their values increase with increasing amplitudes of interacted solitons regardless of their polarity. Knowledge of these invariants is important primarily for the control of numerical solutions of the modified Korteweg - de Vries equation.

To investigate the contribution of two-soliton interactions to the total wave dynamics, we will investigate the integrals (moments) of the type

$$M_n(t) = \int_{-\infty}^{+\infty} u^n(x,t)dx . \qquad (n = 1,2,3\ldots) \tag{3.38}$$

The first two moments will be saved in time due to the integrability of the modified Korteweg-de Vries equation. However, the third and fourth moments corresponding to the coefficients of skewness and kurtosis in the theory of turbulence are not invariants and are changed in time (Fig. 3.11). In the case of two positive soliton interaction the third and fourth moments are decreased, as in the analogous problem for the KdV solitons (Fig.3.11a). Physically, this can be explained by the effect of reducing of the resulting impulse amplitude at the moment of interaction. In case of interaction of solitons of different polarities described by (3.22), when the larger soliton remains positive, and the smaller becomes negative – it is contrary; the amplitude of the resulting impulse grows significantly, and it gives a contribution to the change of third and fourth moments. Which both increase at the moment of interaction (Fig. 3.11b).

In the case of two negative soliton interactions, the third moment is negative and at the moment of interaction is increased, and the fourth moment is reduced (Fig.

3.11d). If the larger soliton is located on the left, has a negative amplitude, and the smaller soliton is positive, the third moment will remain negative and decreases in the moment of interaction, while the fourth moment increases (Fig. 3.11c).

a) b)

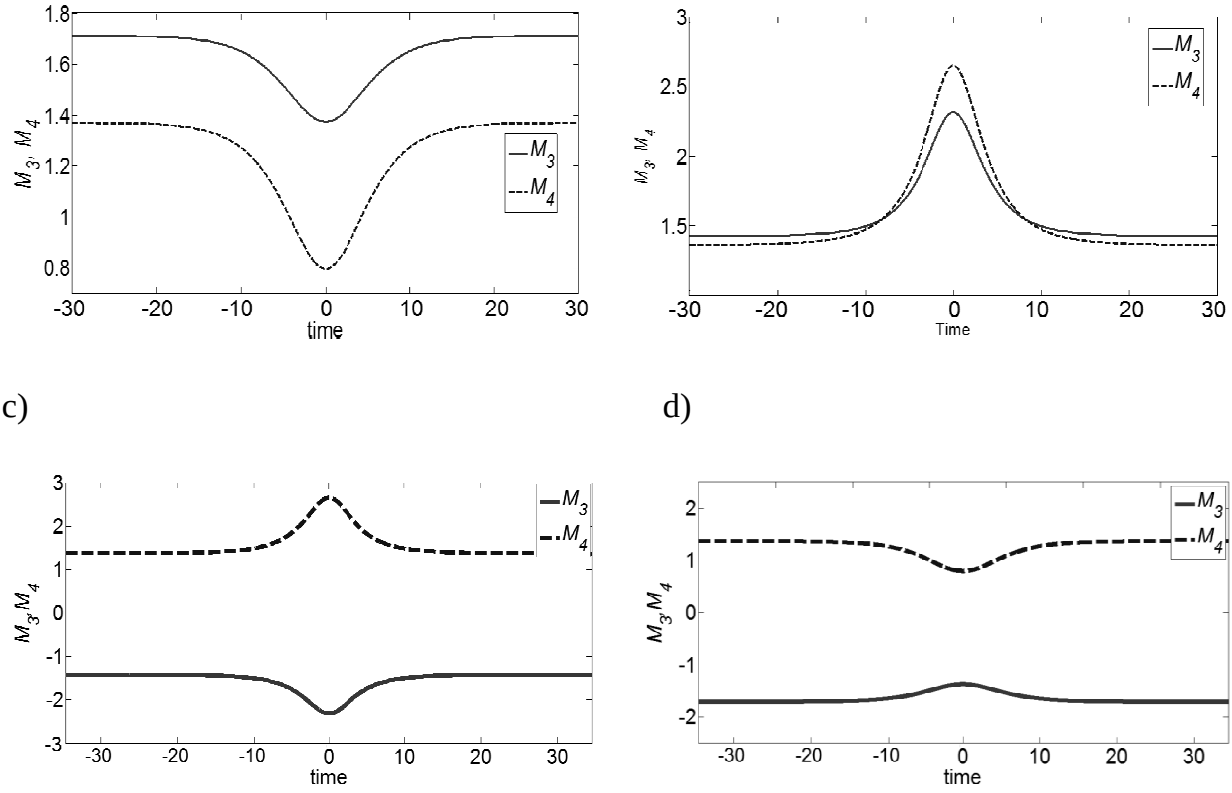

c) d)

Figure 3.11 Dependence of moments M_3 and M_4 on time in case of mKdV soliton interaction a) A_1=1, A_2=0.3, b) A_1=1, A_2=-0.3, c) A_1=-1, A_2=0.3, d) A_1=-1, A_2=-0.3.

For non-interacted solitons all moments can be calculated analytically:

$$M_1 = \pi(s_1 + s_2), \tag{3.39}$$

$$M_2 = 2(A_1 + A_2), \tag{3.40}$$

$$M_3 = \frac{\pi}{2}(s_1 A_1^2 + s_2 A_2^2), \tag{3.41}$$

$$M_4 = \frac{4}{3}(A_1^3 + A_2^3). \tag{3.42}$$

Formulas (3.39) - (3.42) determine the initial and final values of the moments when solitons are separated. Thus, the sign of the first and third moments depends on the polarity of the solitons.

To estimate the value of moment changing during the soliton interaction, we consider the changing the values of the third and fourth moments M_3^*, M_4^* depending on the ratio of the soliton amplitudes. Here $M_i^* = (M_{i\_\max} - M_{i\_\min})/M_{i\_0}$. There is a symmetry for the third moments on Fig. 3.12a and 3.12d and for 3.12b and 3.12c; the fourth moments are identical to the corresponding graphs.

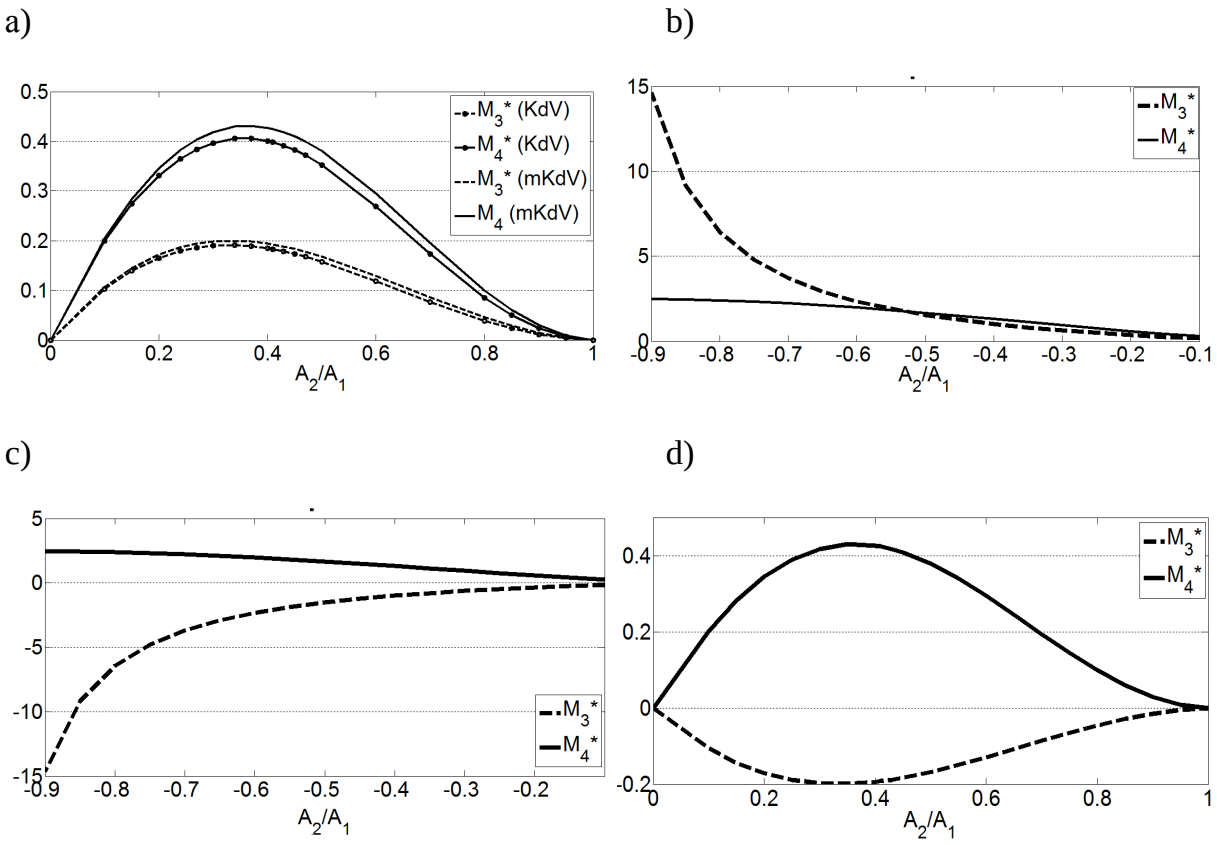

Figure 3.12 Changing of third and fourth moments M_3^*, M_4^* on amplitude soliton ratio: a) positive KdV and mKdV-solitons with corresponding amplitudes, b) heteropolar mKdV-solitons (bigger soliton has a positive polarity), c) heteropolar mKdV-solitons (bigger soliton has a negative polarity), d) negative mKdV-solitons.

For unipolar solitons (Fig. 3.12 a, d), the moment behavior is non-monotonic, and there is a regime change of soliton interactions. The value of the changing moment is maximum for solitons with the ratio A_2/A_1 corresponding to the transition zone, and the

changing moment in this case can reach 20% and 40% for the third and fourth moments respectively. Fig. 3.12a shows the corresponding curves for the KdV solitons, which are slightly lower than the mKdV-soliton curves, but, in principle, differ slightly.

In the case of heteropolar soliton interaction, the curve behavior is changes drastically (Fig. 3.12b, c). Curves are monotonic because in this case there is only one regime of interaction. It is important to note that the value of moment changes is quite significant in case of heteropolar solitons, especially when the soliton amplitudes are similar by the module.

Thus, the two-soliton interaction strongly influences the moments of the wave field, and this effect may be important for understanding the nature of soliton turbulence.

Material from this paragraph is presented in the article **E.N. Pelinovsky, E.G. Shurgalina, Two-soliton interaction in the frameworks of modified Korteweg – de Vries equation, Radiophysics and Quantum Electronics**, **2014, 57 (10).**

3.5 Conclusion

The features of two-soliton interactions in the framework of the Korteweg - de Vries equation and the modified Korteweg - de Vries equation are studied in this chapter. The criterion of transition of breaking bores to undular bores based on field data is analyzed and verified. It allows us to determine the applicability of soliton models in a particular case.

The process of two soliton collisions is studied in detail. The possible types of soliton interactions in the framework of both equations is discussed. The first four moments of the wave field, which play an important role in the theory of turbulence, are found. The first two of them are integrals of motion for the KdV and mKdV, and they are saved. It is shown that soliton interactions of the same polarity lead to a decrease of the third and fourth moments characterizing the coefficients of skewness and kurtosis of the wave process. On the other hand, soliton interactions of different polarity (in the case of the modified Korteweg-de Vries equation) lead to an increase of these moments of soliton field. In the case of unipolar soliton interactions, solitons with amplitudes corresponding to the transition regime between the exchange and overtake interactions made the greatest contribution to the dynamics of moments; for heteropolar solitons (in the case of mKdV) – the solitons with amplitude ratio close to one made the greatest contribution.

Thus, it is shown that two-soliton interactions strongly affect moments of a wave field, and it is an important factor for understanding soliton turbulence.

4 Soliton turbulence in the framework of some integrable long-wave models

4.1 Introductory remarks

4.2 Nonlinear dynamics of irregular soliton ensembles in the framework of the Korteweg – de Vries equation

4.3 Unipolar soliton gas in the framework of the modified Korteweg – de Vries equation

4.4 Freak waves in soliton fields in the framework of the modified Korteweg – de Vries equation

4.5 Conclusion

4.1 Introductory remarks

The theory of wave (weak) turbulence is presently well developed [Zakharov et al., 1992; Nazarenko, 2011]. Its experimental evidence is found in the ocean, atmosphere, plasma, and Bose-Einstein condensate. It is important to emphasize the works about one-dimensional wave turbulence, which to some extent retain the main features of water waves, but are much easier to compute [Majda et al, 1997; Cai et al, 2001; Zakharov et al, 2001].

Several decades ago soliton turbulence (or soliton gas) provoked scientific interest. These problems are also considered in one-dimensional formulations. The first theoretical description of soliton gas was proposed by V.E. Zakharov in 1971. In theoretical studies the investigations have been focused around the kinetic equation, which allows one to describe the spatial and temporal distribution of soliton gas characteristics [Zakharov, 1971; Gurevich et al., 2000; El et al., 2001, 2011]. However, the statistical dynamics of soliton ensemble (or more general problem of the evolution of a random wave field) at the moment is actually a problem left unsolved.

This chapter is devoted to the study of multi-soliton fields in the framework of some long-wavelength integrable models. Soliton fields and their statistical properties are studied in §4.2 in the framework of the Korteweg - de Vries equation. Similar field (consisting only of solitons of the same polarity) in the framework of the modified Korteweg - de Vries equation are studied in §4.3. There is also a comparison of the characteristics of a unipolar soliton gas within the KdV and mKdV equations. In §4.4, a numerical study of the dynamics of heteropolar soliton gas in the framework of the modified Korteweg - de Vries equation is presented. The occurrence of freak waves as a result of interaction of solitons of different polarity is demonstrated. The obtained results are summarized in the conclusion.

4.2 Nonlinear dynamics of irregular soliton ensembles in the framework of the Korteweg – de Vries equation

It is commonly known that the sea surface is a random surface due to the existence of waves with different wavelengths propagating in different directions on it. Their interference and interactions lead to a fast changing of sea surface. Therefore the wave turbulence is taken in consideration [Zakharov et al., 1992; Nazarenko, 2011]. The main idea is that the wave process is described by the interaction of a large number of sinusoidal waves with independent phases in the linear approximation, and a weak phase correlation is due to weak nonlinearity. Equations for the intensity are obtained by perturbation theory and statistical averaging. However, integrable systems have their own specifics which were formulated half a century ago as the problem of the Fermi-Pasta-Ulam [Riskin and Troubetzkov, 2010].

Instead of the initial perturbation energy being distributed over the spectrum, after a certain time it is then concentrated in a small number of harmonics. This was discovered by the example of a vibrating string (Boussinesq equations that for unidirectional waves lead to the Korteweg-de Vries equation). Thus it is clear that the wave turbulence can be very specific in integrable systems, discussed in [Zakharov, 2009].

Soliton turbulence in integrable systems has degenerated to some extent since there is a weak correlation between the spectral components. Solitons (representing strongly correlated clots) are stored in the interaction, and hence their characteristics (or discrete spectral values of the associated tasks in the inverse scattering method) are not changed. Soliton turbulence in the integral systems has degenerated to some extent, because solitons are conserved in the interacting process which is why their characteristics (more precisely discrete eigenvalues of the associated spectral problem) do not change. That is why the nonlinear Fourier transform for sea waves on shallow water (in the framework of KdV) was developed, which allows exploration of the "structure" of the observed random waves [Osborne, 1993, 1995, 2010; Osborne et al., 1991, 1998].

These components of the wave field (analogues of cnoidal waves and solitons if they exist independently) do not change over time, but their superposition leads to random changes on the water surface. In practice not only is it important to know the distribution and moments of the random wave field, but also the parameters of solitons and cnoidal waves.

Korteweg - de Vries equations is an etalon equation of nonlinear wave theory [Korteweg and de Vries, 1895; Zakharov et al., 1980]. With the help of the inverse scattering problem the occurrence of soliton solutions from random initial perturbations on an infinite interval in the framework of this equation were proved [Murray, 1978], and for the periodic interval is was shown in a series of papers by Osborne and colleagues [Osborne, 1993, 1995, 2010; Osborne et al, 1991, 1998]. The importance of this task to describe the random wind wave field in shallow water is demonstrated in the articles [Osborne, 1993, 1995; 2010; Osborne et al, 1991, 1998; Brocchini and Gentile, 2001; Pelinovsky and Sergeeva, 2006].

In this paragraph the nonlinear dynamics of an ensemble of solitons in the approximation of the Korteweg - de Vries equation are studied. It is studied numerically by using periodic boundary conditions. A random sequence of separated solitons with random amplitudes is chosen as the initial condition:

$$u(x,0)=\sum_{i=1}^{N}u_i=\sum_{i=1}^{N}A_i\operatorname{sech}^2\left[K_i\left(x-x_{0i}\right)\right],\qquad A_i=2K_i^2 \tag{4.1}$$

where N is the number of solitons in the computational domain.

Phases x_{0i} are chosen so that initially solitons do not interact with each other, hence they are not random. If they are randomly selected, a set of soliton amplitudes A_i (or K_i) are constant for all realizations, and the only change is the order of the solitons. In the initial experiments with 20 solitons their amplitudes in the computational domain vary from $A_{min} = 0.5$ to $A_{max} = 3.5$ (a full set of amplitudes for these realizations is presented in Table. 3.2.1 - 20 cells correspond to 20 soliton amplitudes) and the average value of the amplitude is equal to $\langle A \rangle = 1.73$. Two realizations of these fields are shown in Fig. 4.1:

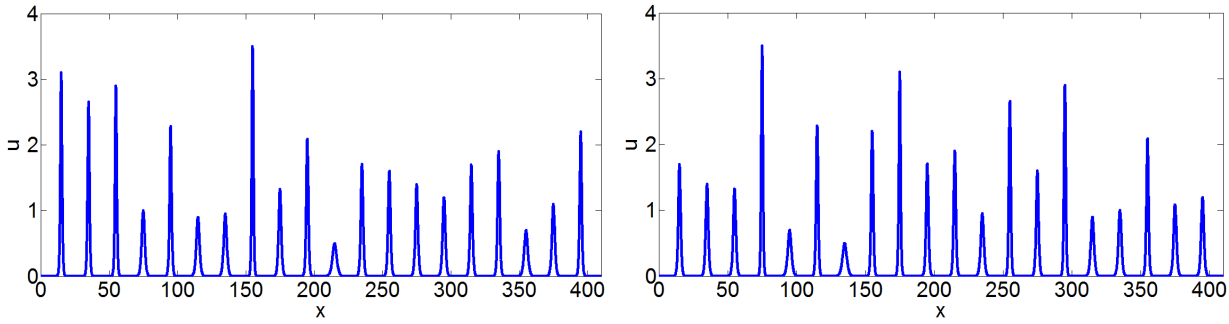

Figures 4.1. The initial soliton ensembles, two realisations.

Table 4.1 The initial soliton amplitudes from the realizations in Fig.4.1.

0.5	0.7	0.9	0.95	1	1.1	1.2	1.33	1.4	1.6
1.7	1.71	1.9	2.09	2.2	2.28	2.66	2.9	3.1	3.5

The solitons have different amplitudes and different speeds, hence they will interact over time. Wave field at the time moment t = 100 are presented in Fig. 4.2. Pair interactions that have been discussed in the second chapter are clearly distinguished on these figures. This is why the pair soliton interactions are the basis of soliton turbulence.

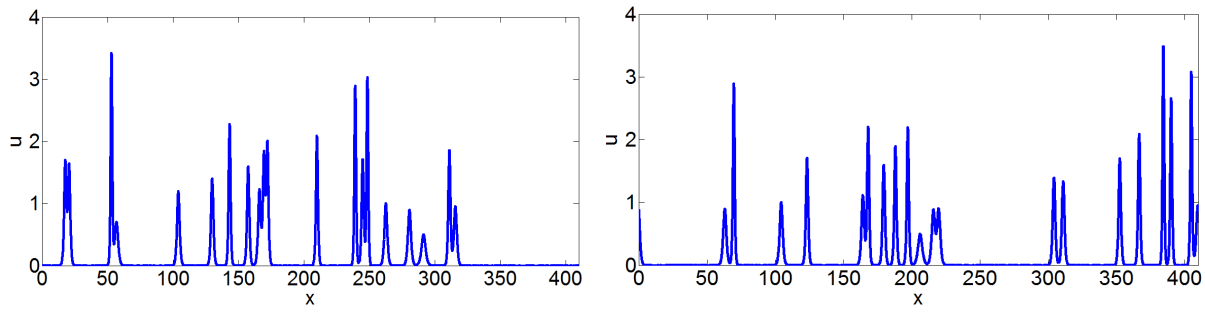

Figures 4.2 Ensembles of solitons at t = 100, two realizations.

Fig. 4.3a shows the evolution of the soliton field, represented in Fig.4.1, in *x-t* domain. The zoomes of the parts are marked by red squares are shown in Fig. 4.3b. Different slopes and trajectories correspond to different soliton speeds. Soliton trajectories do not lie only on straight lines after interacting, which demonstrates the phase shift is a result of nonlinear soliton interaction. Similar conclusions about the trajectories of the ensemble of solitons are made in [Salupere et al, 1996, 2002, 2003a, b].

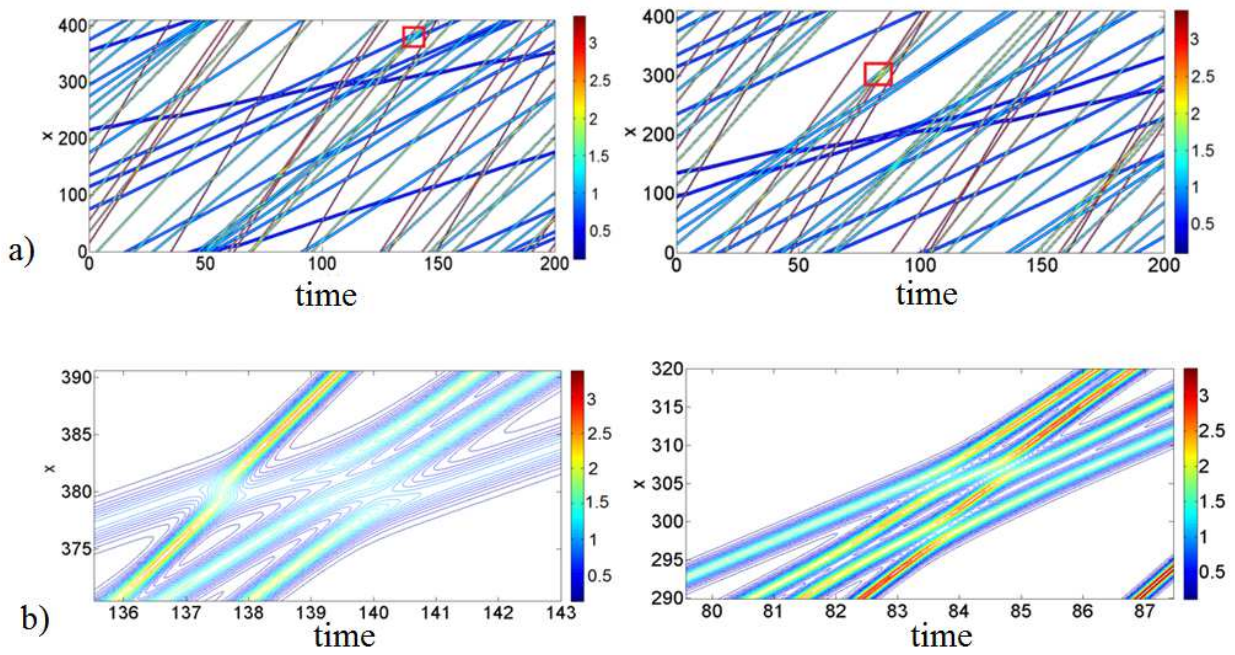

Figures 4.3 a - Space-temporal diagrams of the soliton fields, two realizations. b – zoom of red squares.

Some conclusions about the dynamics of the wave fields can be found by using field extreme graphs (Fig. 4.4). As shown in the previous chapter, since pairs of soliton interactions lead to a decrease in the amplitude of the resulting impulse, the maximum value of the extremum does not exceed the amplitude of the biggest soliton in the realisation. The maximum amplitude in the process of interaction is reduced by about 20% to 2.8-2.9 (A_{max} = *3.5*), while the minimum amplitude of the field does not change and coincides with the minimum amplitude of the soliton in the ensemble (A_{min} = *0.5*) . Thus the amplitude of the resulting wave field (not of solitons) changes over time, and on average it is less than in the initial time moment. Therefore the emergence of anomalously large impulses is not possible here.

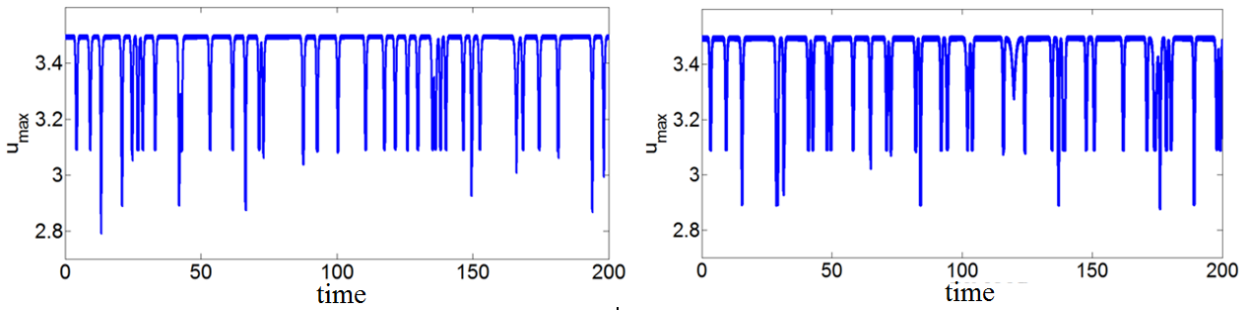

Figure 4.4 Temporal variability of the maximum value of the wave fields' extremes; two realizations.

These processes affect the distribution functions of the wave field and its statistical moments. At the initial moment the soliton amplitudes are chosen close to the Weibull distribution (Fig. 4.5):

$$F(A) = \exp\left(-k \cdot \left(\frac{A}{\sigma}\right)^{p}\right), \tag{4.2}$$

The distribution function of the wave amplitude (local maxima of the wave field) varies in each realization over time, and the examples of the distributions are shown in the same figure. Qualitative changes manifest in the same way: as the number of small amplitude impulses increases and the number of large waves decreases. As a result, the distribution function of the wave amplitudes becomes steeper in comparison to the initial distribution. In principle, the effect of steepening of the distribution function in the shallows is known (the empirical distribution of the Glukhovsky) [Massel, 1996]. However, in a field of purely solitons, this effect is weak, underlining the resilient nature of the soliton interaction and their ability to retain their parameters.

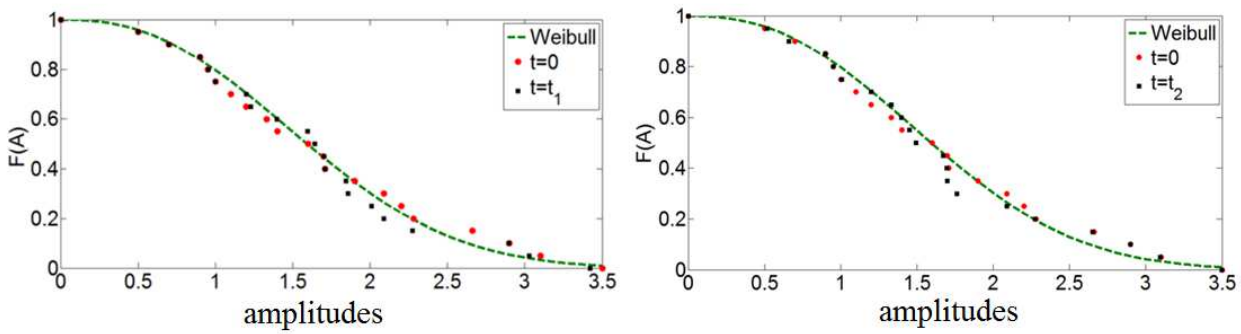

Figure 4.5 The distribution function of soliton amplitudes at the different moments of time (t_1 = 100, t_2 = 90): The dotted line is the approximation by the Weibull distribution with (p=2.4; k=0.11; σ =0.74)

Let's discuss the statistical characteristics of the soliton gas. We have a random wave field, which depends on two variables: the coordinates x and time t, which are not very convenient for the analysis. For simplicity, we will consider the statistical characteristics averaged over the computational domain:

$$M(t) = \frac{1}{L}\int_0^L f(x,t)dx \tag{4.3}$$

(f – any characteristic of the wave field), which are functions of the current time.

This procedure corresponds to the ergodic hypothesis, when the averaging over the ensemble of realizations is replaced by integration, in this case over the space. At the same time *M(t)* is a random function of time due to the random nature of the soliton interactions. Moments of a random function are the values averaged over the ensemble of realizations

$$< M >= \frac{1}{n}\sum_{j=1}^{n} M_j(t) \tag{4.4}$$

This value for a large number of realizations, in the limit $n \to \infty$ becomes independent of time and determines the statistical moment of integral characteristics of the wave field. We can again use the ergodic hypothesis and change the averaging over ensemble to integrate over time (which should be large enough). Below we will often call the integral characteristics (4.3) the moments of the wave field, as in (4.4), and we hope that in the text, the reader will not be confused between (4.3) and (4.4).

Most simply, all these moments are calculated at initial time, when all the solitons are isolated from each other (we have already demonstrated this in the second chapter in the example of two non-interacting solitons). In this case all the integral characteristics are calculated explicitly. The average value of the wave field over the computational domain is:

$$M_1 = \frac{1}{L}\int_0^L u(x,0)dx = \frac{1}{L}\sum_{i=1}^{N}\int_0^L u_i(x,0)dx = \frac{1}{L}\sum_{i=1}^{N} 2K_i \int_0^L \mathrm{sech}^2(y - y_{i0})dy \tag{4.5}$$

The integration can be carried out over an infinite limit and the last integral is trivial because of the narrowness of solitons in comparison with the size of the computational domain. Then the average field is

$$M_1 = \frac{4}{L}\sum_{i=1}^{i=N} K_i\,, \tag{4.6}$$

The sum can easily be expressed in terms of the average value of *K*:

$$M_1 = 4\frac{N}{L} < K > \ . \tag{4.7}$$

where $<K>$ is a statistical average over the ensemble of random amplitude solitons. M_1 does not depend on the realization of the soliton gas, thus its value will not change in case of averaging over realizations and it is the first statistical moment - the mean $<M_1> = <u(t=0)>$.

The coefficient N/L, included in (4.7), has a clear physical meaning of the density of the soliton gas

$$\rho = \frac{N}{L}. \tag{4.8}$$

Then (4.7) becomes

$$< u(t=0) >= 4\rho < K >= 2\sqrt{2}\rho < A^{1/2} > \tag{4.9}$$

As expected the mean increases with increasing of soliton gas density. $<A^{1/2}> \neq (<A>)^{1/2}$, thus the knowledge of the average soliton amplitude is not sufficient for the calculation of the average characteristics of the soliton gas.

The dispersion of the wave field at the initial moment is calculated similarly

$$\sigma^2(t=0) = < \left[u - < u >\right]^2 >= \frac{16}{3}\rho < K^3 > -16\rho^2 \left[< K >\right]^2. \tag{4.10}$$

or

$$\sigma^2(t=0) = \frac{8}{3\sqrt{2}}\rho < A^{3/2} > -8\rho^2 < A >. \tag{4.11}$$

Due to the positive dispersion of the wave field the limit of density of the soliton gas appears:

$$\rho < \rho_{cr} = \frac{< A^{3/2} >}{3\sqrt{2} < A >} \tag{4.12}$$

The critical density is easily understood from the following considerations. Assuming that all the amplitudes are the same, the critical density is $\rho_{cr} = K/3$. If we recall the definition of density as (4.8), the critical number of solitons is equal $N_{cr} = KL/3$. Yet, K^{-1} is the characteristic scale of the soliton, thus the critical condition corresponds to one or two solitons in the segment.

It is clear that in this case any averaging procedures lose any sense, and therefore the density of the solitons should always be less than critical. We are talking about a large number of random solitons initially separated from each other, and the density of the soliton gas should be much less than the critical value. It follows that our formula will work well only for a rarefied gas.

When the density of soliton gas is small, in (4.11) the second term can be neglected and retain only the linear density term. However we will not do this because in the numerical calculation the solition density is not very small and the second term is important to analyze the results of calculations.

Similarly, there are a third and fourth statistical moments, particularly coefficients of skewness and kurtosis:

$$Sk(t=0) = \frac{<[u-<u>]^3>}{\sigma^3} = \frac{<u^3> -3<u^2><u> +2<u>^3}{\sigma^3} = \\ = \frac{16\sqrt{2}\rho <A^{5/2}>}{15\sigma^3} - \frac{16<A>^2\rho^2}{\sigma^3} + \frac{32\sqrt{2}<A>^{3/2}\rho^3}{\sigma^3} \quad (4.13)$$

$$Kur(t=0) = \frac{<[u-<u>]^4>}{\sigma^4} = \frac{<u^4> -4<u^3><u> +6<u^2><u>^2 -3<u>^4}{\sigma^4} = \\ = \frac{32\sqrt{2}\rho <A^{7/2}>}{35\sigma^4} - \frac{256\rho^2 <A^3>}{15\sigma^4} + \frac{64\sqrt{2}<A^{5/2}>\rho^3}{\sigma^4} - \frac{192<A^2>\rho^4}{\sigma^4} \quad . \quad (4.14)$$

We present here the asymptotic formulas which are valid for a very rarefied gas: ($\rho \to 0$):

$$Sk(t=0) \approx \frac{2\sqrt{3}}{5\sqrt{\rho}} \frac{<K^5>}{(<K^3>)^{3/2}} = \frac{\sqrt{3}\sqrt[4]{2}<A^{5/2}>}{5\sqrt{\rho}(<A^{3/2}>)^{3/2}} \quad (4.15)$$

$$Kur(t=0) \approx \frac{18}{35\rho} \frac{<K^7>}{(<K^3>)^2} = \frac{9\sqrt{2}<A^{7/2}>}{35\rho(<A^{3/2}>)^2} \quad (4.16)$$

The coefficient of gas density is included in the denominators in (4.15) and (4.16), thus the coefficients of skewness and kurtosis are anomalously large for a very rarefied gas. Thus, a very rarefied soliton gas is not always Gaussian process.

Calculated at the initial time, the statistical moments of the ensemble of solitons do not depend on the number of realizations. Different average values included in there can be easily calculated for any distribution function of soliton amplitudes. For specific

calculations below: N = 20 and L = 410, thus the density of the soliton gas ρ = 0.048 is really small.

The initial values of the statistical moments for the selected amplitude distribution are:

$$< u > \approx 0.18\ ,\ \sigma \approx 0.45\ ,\ Sk \approx 3.53,\ Kur \approx 17.2. \qquad (4.17)$$

The positive sign of the skewness can be easily explained, since all the solitons are positive, and the average value is small.

As solitons begin to interact over time the formula given above becomes inapplicable. However the invariants of the Korteweg-de Vries equation are first two moments. Therefore in the process of nonlinear interaction the mean and the variance of the soliton gas does not change.

The third and fourth moments are not invariant, thus they will change over time. Fig. 4.6 shows the time evolution of the third and fourth moments of the soliton gas, calculated for one realisation according to (4.3) and the "real" statistical moments calculated by the formula (4.4) – in the last case the averaging over 50 realizations is used. Whereas in one realization they are random, the skewness and kurtosis averaged over realizations decrease over time and after a few collisions become almost fixed values.

The reason for this is the nature of the interaction of solitons, because such interactions lead only to a decrease of the third and fourth moments (integrals), as shown in the second chapter. A finite sum of random variables is also a random variable, therefore by averaging over the realizations, we get only an estimation of the coefficients of skewness and kurtosis.

Thus, the average value of skewness is equal to 3.45 with a standard deviation of 0.07. It is important to note that the average value of this ratio is less than the initial value of 3.53, demonstrating the contribution of the nonlinear interaction of solitons. The average value of kurtosis is equal to 16.6 with a standard deviation of 0.7, while the initial value is 17.2. The decrease of the average values can be characterized as a tendency to Gaussian soliton gas.

a) b)

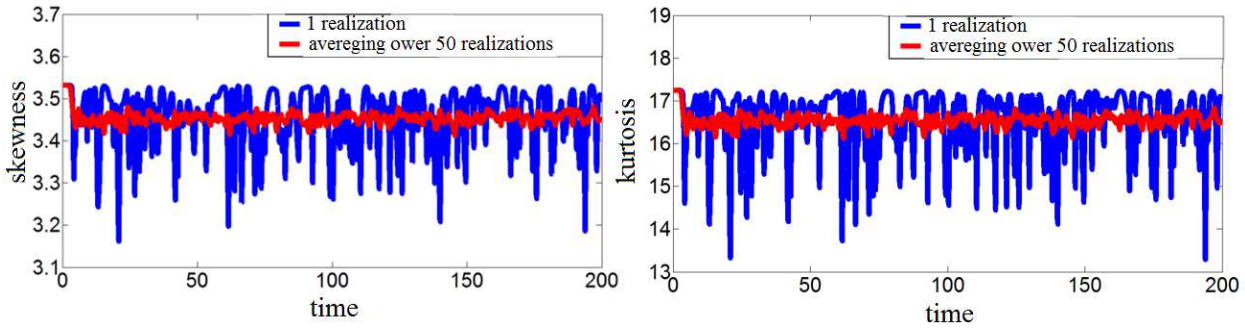

Figure 4.6 The temporal evolution of the skewness and kurtosis of the unipolar soliton gas.

From the above it can be concluded that the interaction of solitons in the framework of the Korteweg - de Vries equation leads to a change of the statistical characteristics of the soliton gas (distribution function of the wave amplitudes, skewness and kurtosis), but we have to admit that all of these changes are small enough. In each realization the soliton interactions do not lead to the formation of abnormally large waves, thus there are no freak waves.

A similar study with a large number of solitons in realization (200 solitons) fully confirmed the findings were carried out recently [Dutykh & Pelinovsky, 2014]. Moreover, the influence of non-integrability of the generalizations of the Korteweg-de Vries equation in the framework of the Benjamin-Bona-Macon equation on the soliton gas characteristics is analyzed. Although the interaction of solitons is inelastic in this model, the effect of the dispersion packets is sufficiently small [Dutykh & Pelinovsky, 2014].

4.3 Unipolar soliton gas in the framework of the modified Korteweg – de Vries equation

In this paragraph we solve the analogous problem for the modified Korteweg-de Vries equation, which we discussed earlier in the fourth paragraph of the third chapter. In the framework of modified Korteweg-de Vries equation there are solitons of different polarity, and the wave interaction is much richer than in the framework of the Korteweg - de Vries equation. In this paragraph we study the dynamics of the unipolar soliton gas in the framework of the modified Korteweg - de Vries equation and compare it with similar dynamics in the framework of the classical Korteweg-de Vries equation.

For unipolar solitons, as was shown in the previous chapter, in the framework of the modified Korteweg - de Vries equation there are two types of soliton interaction (overtake and exchange) which influence the overall dynamics of multi-soliton fields (as in the analogous problem for the Korteweg - de Vries equation). Random sequences of remote solitons with random amplitudes are chosen as the initial condition:

$$u(x,0)=\sum_{i=1}^{N}u_i=\sum_{i=1}^{N}A_i\operatorname{sech}\left[A_i\left(x-x_{0i}\right)\right]. \tag{4.18}$$

Initial soliton fields are the same as in the case of KdV-solitons (see the previous paragraph), their amplitudes are presented in Table 4.1; the order of solitons is changed. The realizations of such fields in the initial moment of time are shown in Fig. 4.7:

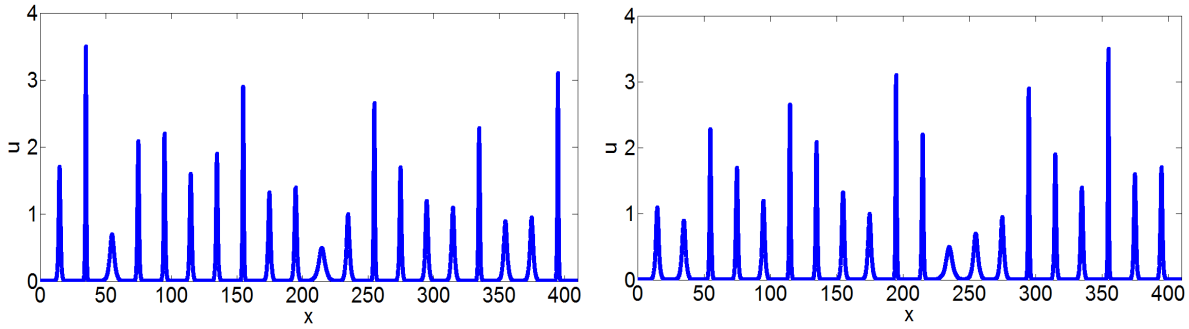

Fig. 4.7 Two realisations of initial soliton fields.

Solitons begin to interact over time. Fig. 4.8 shows the evolution of the soliton fields at the time moment t=80 (for the initial fields from Fig. 4.7). The dynamics of these solitons is very similar to the behavior of KdV-solitons.

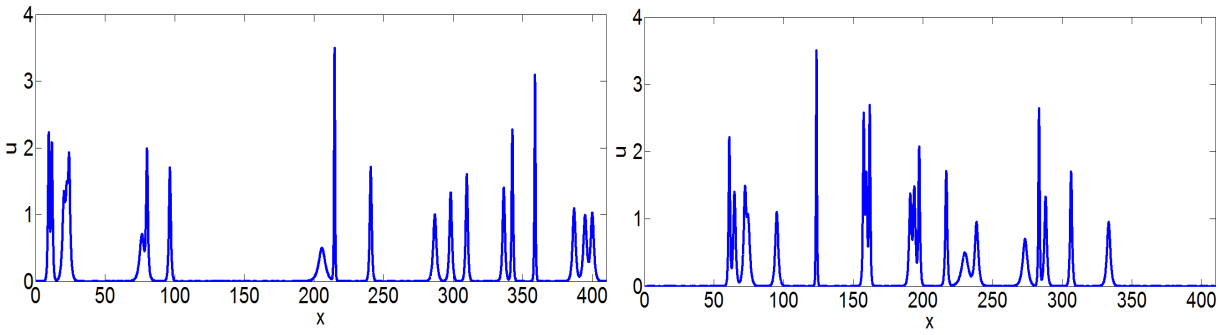

Figure 4.8 Two realizations of soliton gas at t=80.

Fig. 4.9a,b shows the evolution of the soliton field, represented in Fig. 4.7, in *x-t* domains. Here the different types of two-soliton interactions discussed below can be observed. Zooming in on the diagrams (Fig. 4.9c, d) interactions of larger numbers of solitons can be identified.

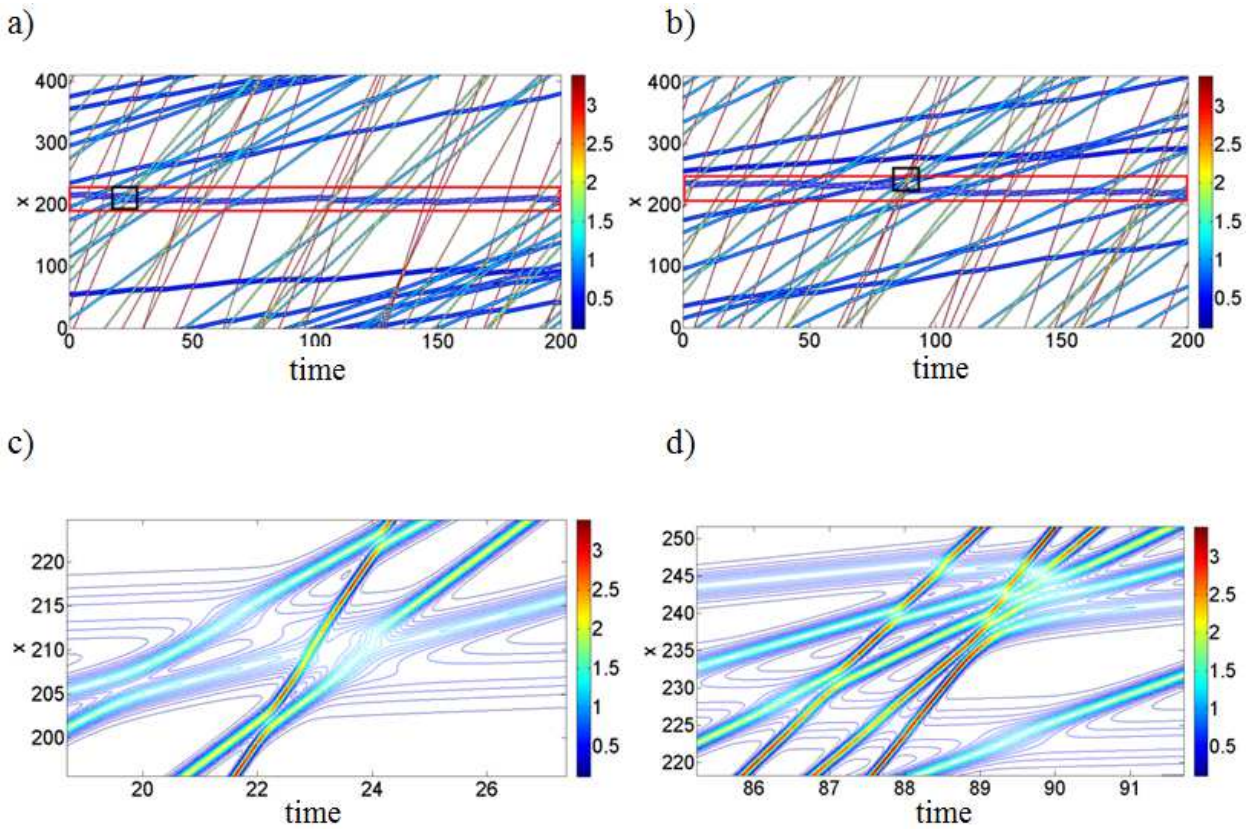

Figure 4.9 Space-temporal diagrams of the soliton fields (a, b - positive solitons, c,d - zoom of black rectangles).

All solitons move with positive velocity except one, which is marked with a red rectangle in Fig. 4.9a,b. In the present wave field its amplitute is the smallest and accordingly it moves with the smallest velocity between collisions. The slope of its trajectory line on Fig. 4.9b points on negative resulting velocity. Such an affect is seen

because of the large amount of collisions with others solitons, and each collision moves this small soliton slightly backward (which happens for solitons, yet for the solitons with large amplitude it is not significant). Hence we can conclude that strong nonlinear interaction can significantly influence the velocity and the trajectory of the soliton and this effect requires a more detailed investigation.

In the framework of the Korteweg - de Vries this effect was not observed. Since solitons have a higher speed than mKdV-solitons (their speed is proportional to the amplitude, while in mKdV equation is proportional to A^2), and this effect is not manifested, although in that case the interaction of solitons shifted the smaller soliton backwards. Thus the soliton gas in the modified Korteweg-de Vries equation has surprising properties when changes in weak particle direction is observed. This feature has not been previously noted in literature.

Some conclusions about the dynamics of wave fields can be given using the graphs of field extremes. The temporal variability of the maximum value of wave field (throughout the computational domain) is presented in Fig. 4.10.

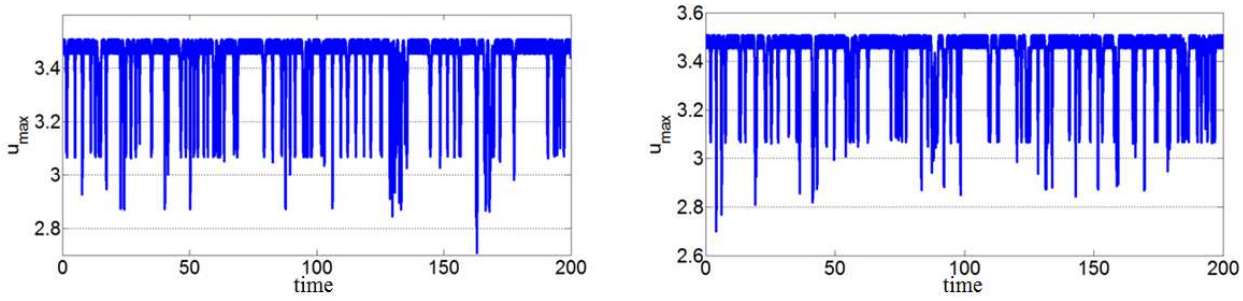

Figure 4.10 Temporal variability of the maximum value of the wave fields' extrema of two realizations.

In the case of the wave field which consists only of unipolar solitons (in this case they are positive), the maximum value of extrema do not exceed the amplitude of the biggest soliton ($A_{max}=3.5$). Since the maximum amplitude during the interaction process is decreasing, the values of the changes are not significant (up to 2.7).

The minimum amplitude of the field is the same as the amplitude of the minimum soliton ($A_{min} = 0.5$), which is a complete analogy to the changes of maximum amplitude within the Korteweg-de Vries equation.

These processes affect the distribution functions of the wave field and its statistical moments. In the initial moment the soliton amplitudes are chosen close to Weibull distribution (Fig. 4.11)

As in the case of the Korteweg - de Vries equation, the distribution function is shifted upward in the case of small wave amplitudes and downwards in the case of large amplitudes.

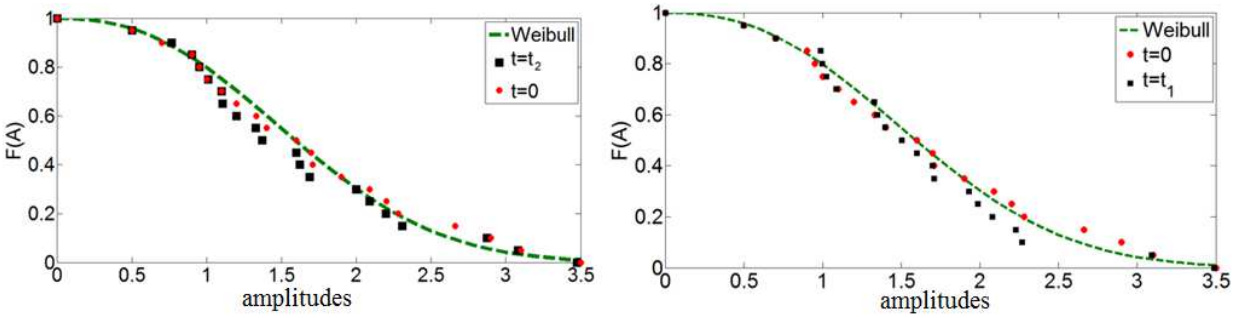

Figure 4.11 The distribution function of soliton amplitudes at different moments in time (t_1 = 110, t_2 = 100) for the wave fields presented in Fig. 4.7. The dotted line is approximated by the Weibull distribution with (p=2.4; k=0.11, σ =0.74).

Similarly in the KdV case, the analytical formulas for the statistical characteristics of the soliton gas can be obtained and the final expression takes the following forms:

$$< u(t=0) >= \frac{1}{L}\int_0^L u(x)dx = \pi\rho, \tag{4.19}$$

$$\sigma^2(t=0) = \frac{1}{L}\int_0^L u(x)^2 dx - < u(x) >^2 = 2 < A > \rho - \pi^2\rho^2 \ , \tag{4.20}$$

$$Sk(t=0) = \frac{\frac{1}{L}\int_0^L (u(x) - < u(x) >)^3 dx}{\sigma^3} = \frac{\pi\rho < A^2 >}{2\sigma^3} - \frac{6\pi\rho^2 < A >}{\sigma^3} + \frac{2\pi^3\rho^3}{\sigma^3} \ , \tag{4.21}$$

$$Kur(t=0) = \frac{\frac{1}{L}\int_0^L (u(x) - < u(x) >)^4 dx}{\sigma^4} = \tag{4.22}$$

$$= \frac{4\rho < A^3 >}{3\sigma^4} - \frac{2\pi^2\rho^2 < A^2 >}{\sigma^4} + \frac{12\rho^3\pi^2 < A >}{\sigma^4} - \frac{3\pi^4\rho^4}{\sigma^4} \ .$$

It is noteworthy that in contrast to the KdV moments, the mean does not depend on the amplitude distribution, and depends only on the gas density of soliton gas. Therefore, the dependence of the moments on the amplitude distributions is different for the KdV and mKdV, but the dependence on the density remains the same (in the limit of low density).

In our calculations of the initial moment the statistical moments are equal to the following values:

$$< u > \approx 0.15\ ,\ \sigma \approx 0.39\ ,\ Sk \approx 3.8\ ,\ Kur \approx 20.4. \qquad (4.23)$$

Thus the wave field is not symmetrical with skewness of 3.8.

As in the case of Korteweg-de Vries equation, the first two moments are the invariants of the modified Korteweg-de Vries equation, and therefore in the process of nonlinear interaction the mean and the variance do not change. The third and fourth moments will change over time. Also as time passes, the coefficients of skewness and kurtosis are reduced and after a few collisions are located on the stationary values (Fig. 3.3.6). As was shown in the previous chapter, the reason for this as well as earlier in the nature of the unipolar soliton interactions is because such interactions lead only to a decrease of the third and fourth moments.

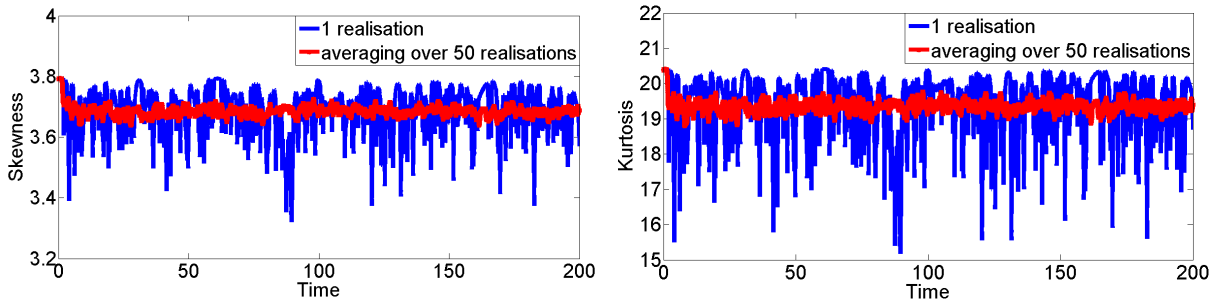

Figure 4.12 Temporal evolution of skewness and kurtosis.

The average value of kurtosis is equal to 19.4 with a standard deviation of 0.18; but the reduction of kurtosis is not very significant (19.4 with initial value of 20.4). Similarly with skewness: the average value is 3.7 (plus/minus 0.02) instead of its initial value of 3.8.

In the calculations 50 realizations are used where the average values of the statistical moments undergo small fluctuations. For comparison, we have done the estimation of the influence of the realization number on standard deviation of the kurtosis coefficient (Fig. 4.13). It is shown, that this value is slightly decreases with the growth of the realization number (for 20 realizations it is 0.0217, for 50 - 0.0169, for 100 - 0.0143). This is why it is sufficient to use only 50 realizations to save computational time.

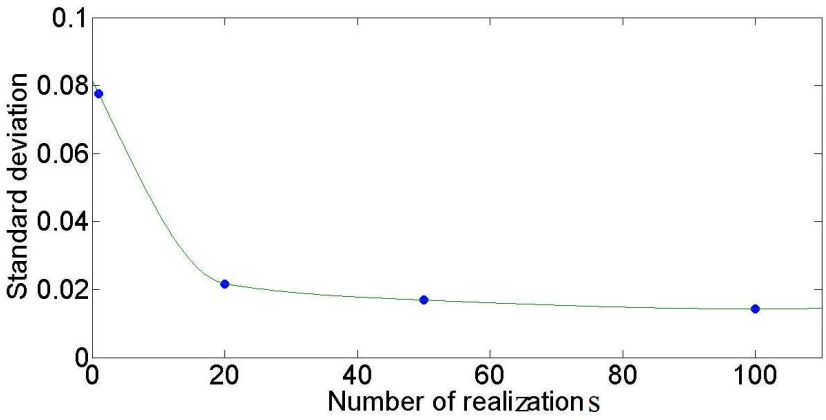

Figure 4.13 The dependence of the standard deviation of the average coefficient of kurtosis from the number of realizations.

The comparison of statistical characteristics of unipolar soliton gas in the framework of the Korteweg - de Vries equation and the modified Korteweg - de Vries equation is presented above. The distinguishing feature of solitons in these equations is that for amplitudes larger than ≈ 1.3 the KdV soliton is wider than the mKdV soliton (Fig. 4.14).

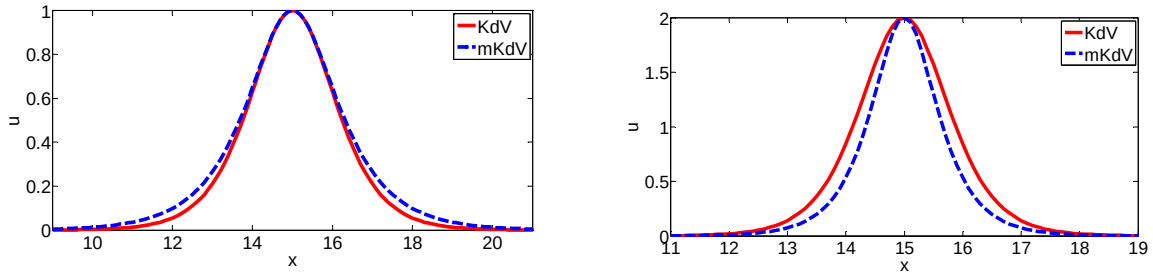

Figure 4.14 Comparison of KdV and mKdV solitons with different amplitudes.

Formally, the behavior of these moments reminds us of the behavior of analogous moments for positive mKdV fields, except the fact that the quantitative values are changing.

The comparison of numerical values of averaged moments for the identical distributions of soliton amplitudes is shown in Fig. 4.15 (the distribution function of soliton amplitudes are the same). The mean and variance of the wave fields are larger for KdV-fields (Table 4.2). This is confirmed by the fact that in realizations the solitons with amplitudes larger than 1.3 prevail (Table 4.2).

Table 4.2 Values of moments for KdV and mKdV soliton fields

	$<u>$	σ	*Sk*	*Kur*
KdV	0.18	0.45	3.5	17.2
mKdV	0.15	0.39	3.8	20.4

The initial values of skewness and kurtosis are presented by dotted lines in Fig. 4.15 (respectively, blue lines - for the case of mKdV and red lines - for the case of the KdV). Their initial values, found analytically, are presented in Table 4.2.

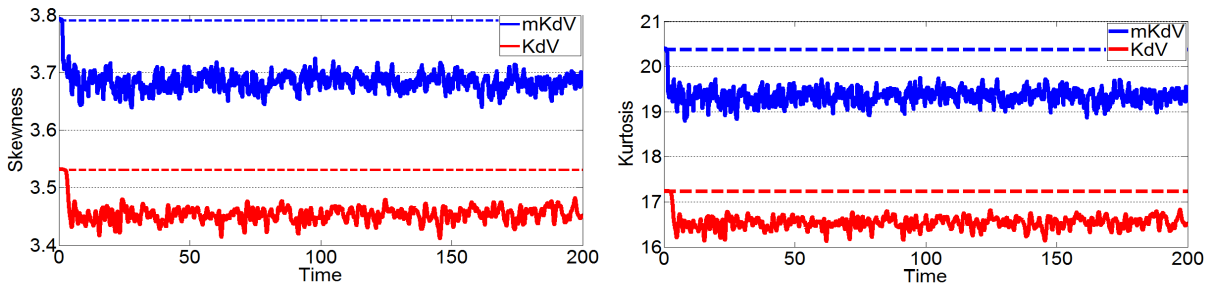

Figure 4.15 Averaged values of statistical moments over 50 realizations over time for mKdV and KdV fields.

The coefficients of skewness and kurtosis, in contrast to the mean and variance, are larger for the mKdV soliton gas for the given amplitude distribution. The similarity of the behavior of the third and fourth moments is obvious. However, if in the initial field the solitons with amplitudes less than 1.3 prevail, then the conclusions will be the opposite, and the values of skewness and kurtosis will be larger for the mKdV fields. This is due to the fact that the mean and the variance make "negative" contributions to the

value of the third and fourth statistical moments (see 4.21, 4.22), and therefore if the first and second moments are larger, then the third and fourth moments will be smaller.

Thus, the dynamics of the KdV and positive mKdV soliton fields is quite similar. However, in such unipolar fields abnormally large waves do not appear. Radically different situation exist for heteropolar soliton fields, and it will be discussed in the next paragraph.

4.4 Freak waves in soliton fields in the framework of the modified Korteweg – de Vries equation

The main difference between the Korteweg - de Vries equation and the modified Korteweg - de Vries equation is the presence of solitons of different polarity in mKdV case. Heteropolar solition iteractions make wave dynamics much richer. The interaction of two heteropolar solitons leads to the formation of abnormal pulses, as shown in paragraph 3.4. It can be expected that these effects will manifest in heteropolar soliton gases, leading to the appearance of the freak waves.

In this paragraph the dynamics of multisoliton fields consisting of solitons of different polarities with means equal to zero are studied. The initial soliton field consists of two components, positive and negative. In each component the amplitudes are distributed similarly such as in paragraphs 4.2 and 4.3. Also, each positive soliton's amplitude corresponds to the same negative amplitude. Soliton amplitudes are obtained using a random number generator and are taken from the interval |0.8-2|. A random sequence of separated solitons with random amplitudes and polarity is chosen as the initial condition:

$$u(x,0)=\sum_{i=1}^{N}u_i=\sum_{i=1}^{N}s_iA_i\operatorname{sech}\left[A_i\left(x-x_{0i}\right)\right]. \tag{4.24}$$

In our calculations, the size of the computational domain is constant and equal to 416. The number of solitons varies from 100 to 20, which allows us to change the soliton gas density up to 5 times. We consider the problem with periodic boundary conditions, thus the solitons pass the computational domain many times during the computation time.

Fig. 4.16 presents the soliton field at the initial time (left column) and at time moment of 500 (right column).

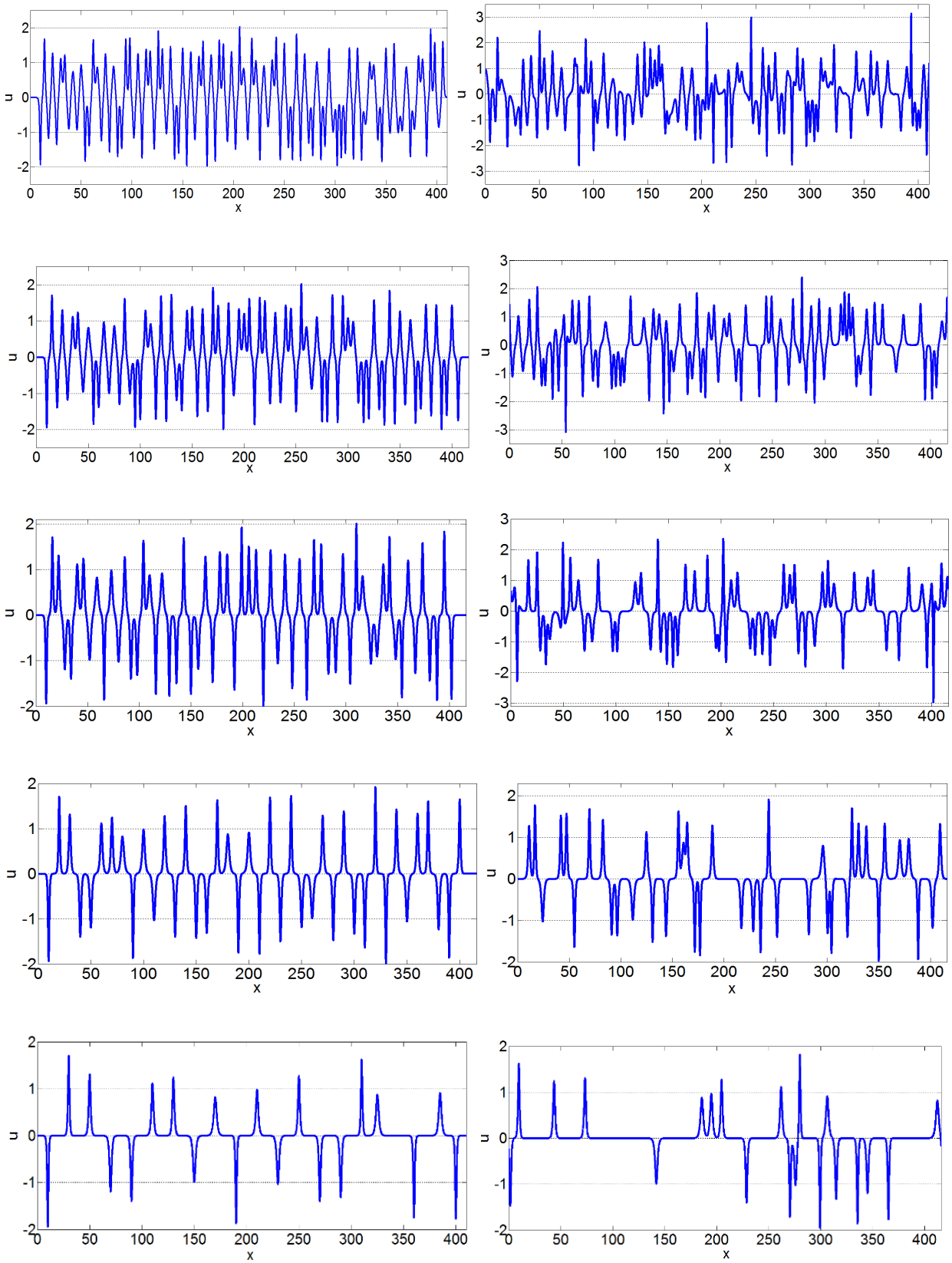

Figure 4.16 Initial multisoliton fields (left column) and t = 500 (right column). From the top to bottom $\rho = 0.24$, $\rho = 0.19$, $\rho = 0.14$, $\rho = 0.096$, $\rho = 0.048$.

Solitons interact over time and abnormal impulses sometimes appear (Fig. 4.17), with both polarities - positive and negative.

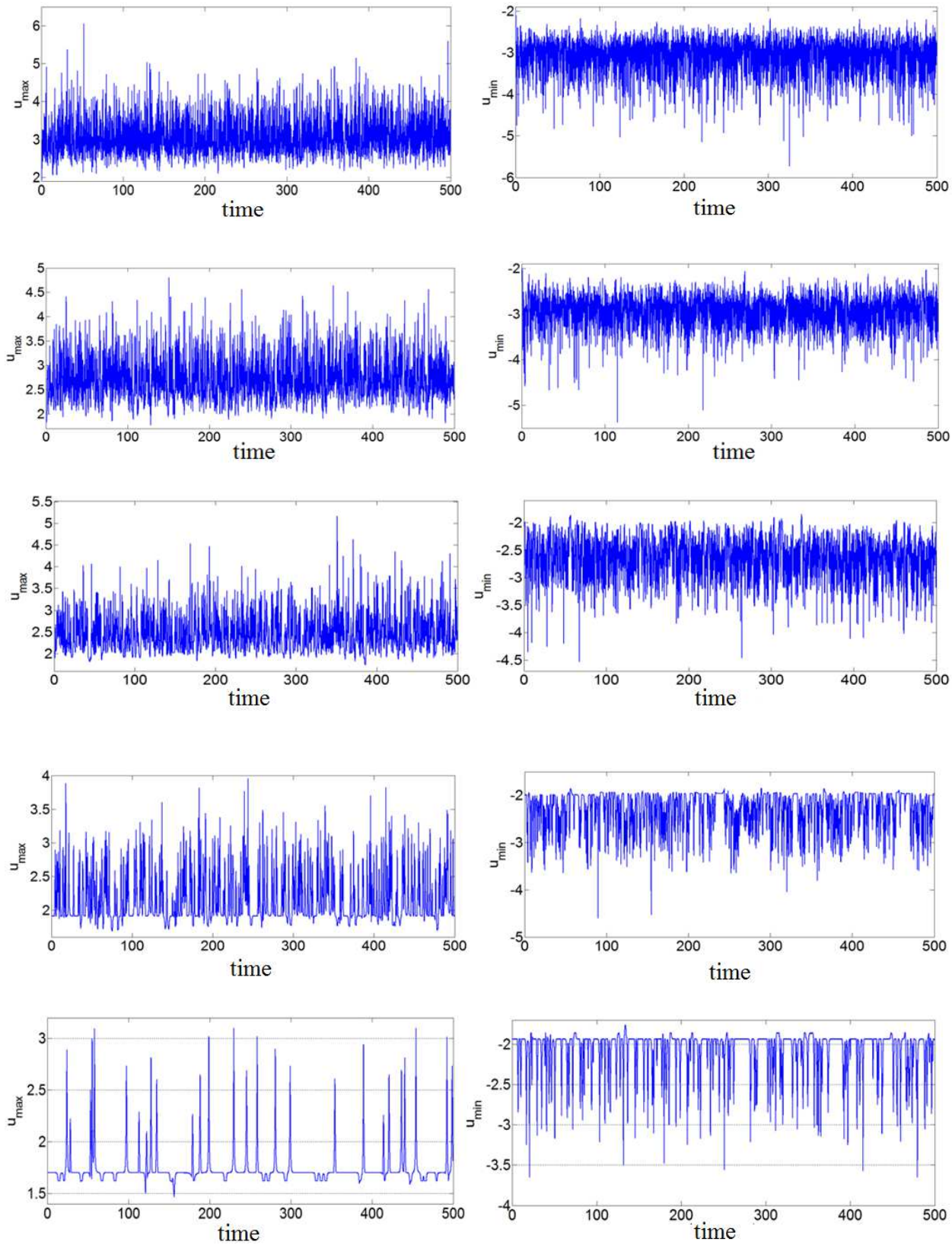

Figure 4.17 Extremes of wave fields: from the right - the maximums, from the left – the minimums. From the top to down: ρ =0.24, ρ =0.19, ρ =0.14, ρ =0.096, ρ =0.048.

In the soliton gas with bigger density the intensity (frequency) of interactions is larger and it is logical to assume that in such fields the anomalous amplitudes should have amplitudes larger than in the fields with a lower density. Fig. 4.18 shows the dependence of "the peak-peak" on the gas density. The trend of amplitude increasing by module is observed. However, this assumption is violated by two points on the graphs for ρ=0.19, ρ=0.14 in the first case and for ρ=0.14, ρ=0.096 – in the second. In this case we compare the specific realizations and there are not full statistics with many realizations, thus such deviations do not violate the general trend of maximums increasing and minimums decreasing.

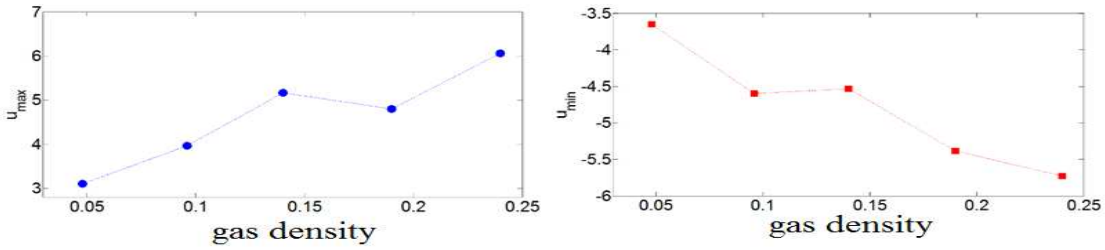

Figure 4.18 The dependence of the extremes (the peak-peak) on the gas density.

As noted previously, the nonlinear interaction leads to changing of the distribution function of the amplitude characteristics. However, in the case of heteropolar fields the effect will be opposite. In this case, the role of small-amplitude waves decreases, and role of waves with large amplitudes increases. Thus, in moments of strong nonlinearinteraction the tails of the distribution functions may increase significantly (Fig.4.19).

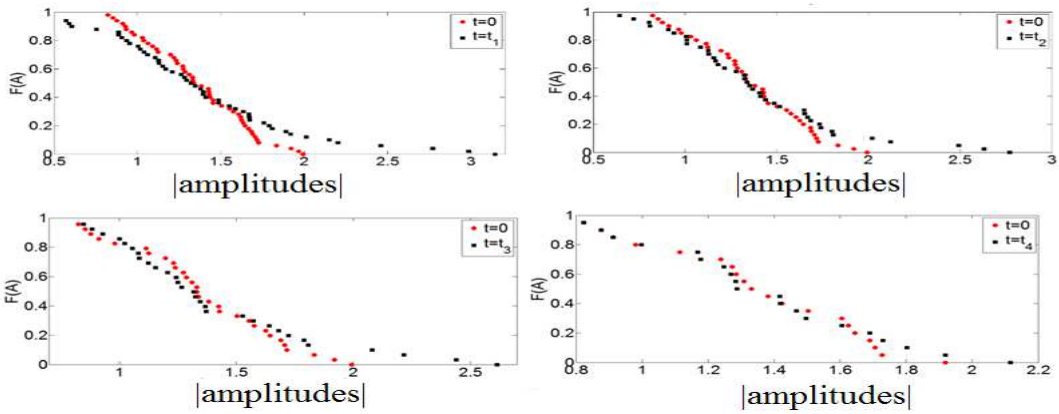

Figure 4.19 The distribution function of soliton amplitudes at the different moments in time From the top to bottom: ρ=0.24 (t_1=500), ρ=0.19 (t_2=2), ρ=0.14 (t_3=80), ρ=0.096 (t_4=40).

Abnormal peaks, currently appearing against the background of other waves can be considered from the point of view of the freak waves [Kurkin, Pelinovsky 2004, Kharif et al., 2009]. In the third paragraph of the first chapter we point out an amplitude criterion of freak waves when we considered the interference of swell and wind waves (2.32).

In this paragraph, we will use this criterion to detect freak waves. The value of A_s is the average value of the largest one third of waves in the realization. In wind wave theory, this definition has been proposed for 20 minute records containing about 3000 waves. In our case, the number of waves is much smaller, thus the A_s value will change over time for the concrete realization and not be the average characteristics of the process.

Therefore we will consider the specific realization at specific moment in time, and for each case we will determine the A_s (as an average of one-third of large waves). In Fig. 4.20 the wave fields containing abnormally large waves are shown. For density ρ=0.24, ρ=0.19, ρ=0.14, ρ=0.096 the amplitude criterion of freak waves is performed, and in the first case – the exceedance of the significant wave amplitude A_s is three fold.

The right column shows zoom of freak waves. In all cases, they have approximately the same shape corresponding to the resulting impulse in the case of unipolar soliton interaction (Fig. 3.9c).

a)

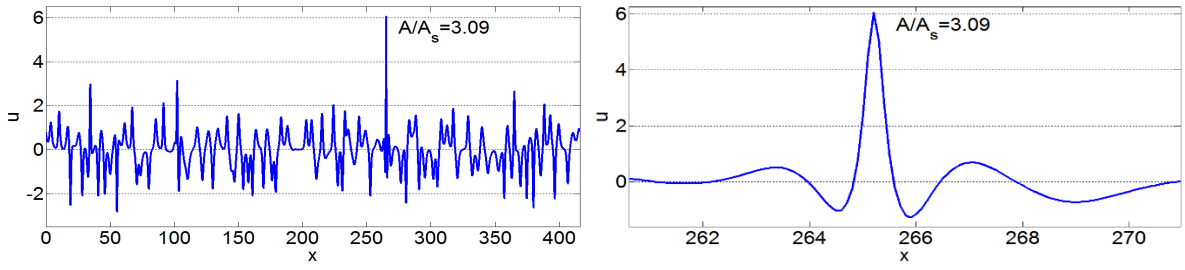

b)

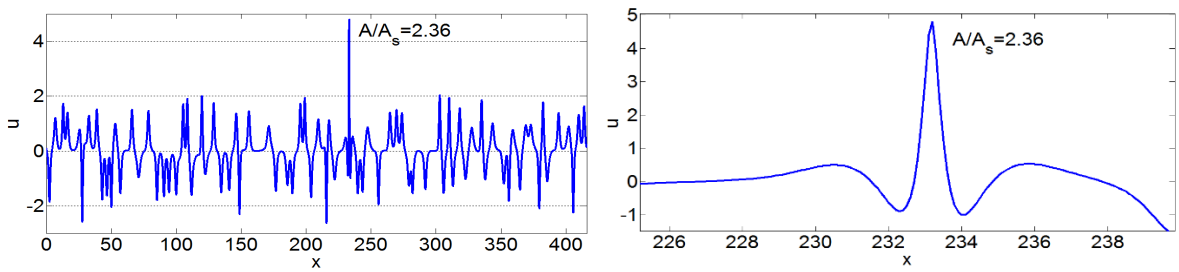

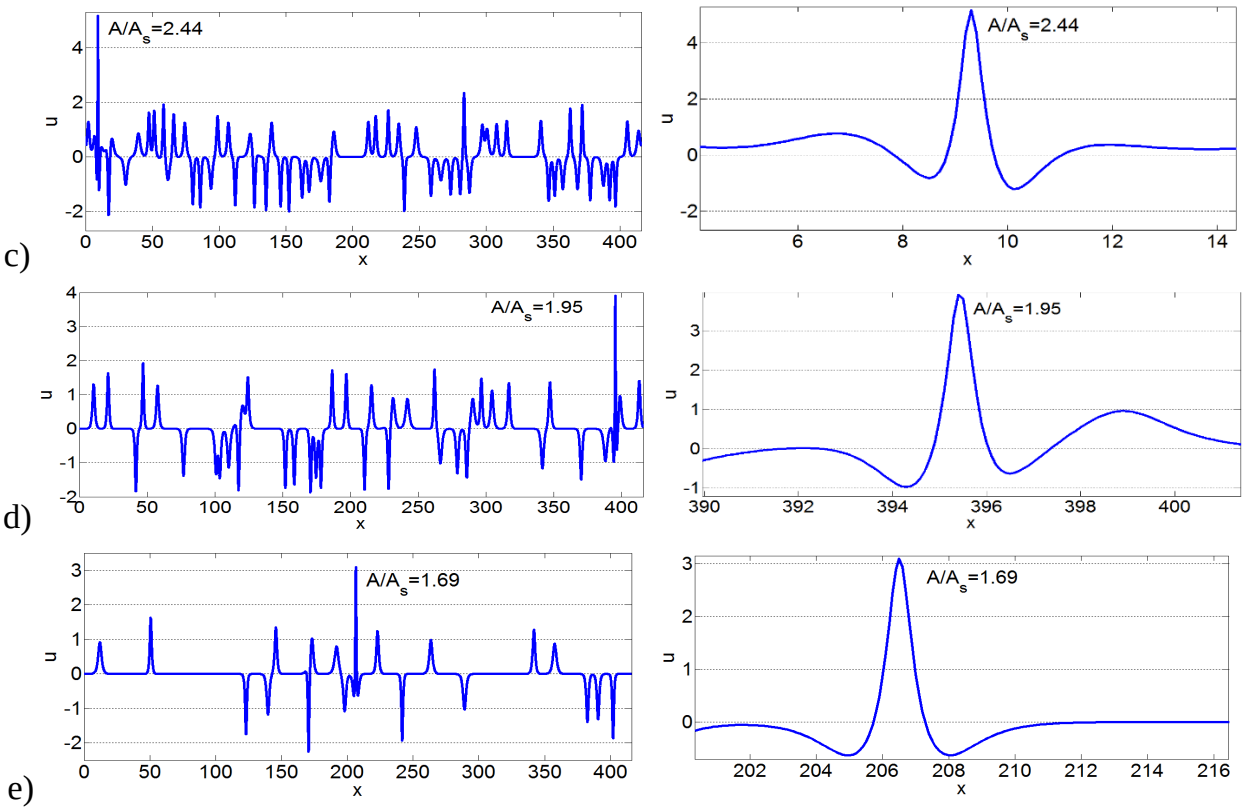

Figure 4.20. Wave fields that contain the abnormally large waves,the right column is zoom of freak wave: a) ρ =0.24,b) ρ =0.19, c) ρ =0.14, d) ρ =0.096,e) ρ =0.048.

For the analysis of the probability of occurrence of freak waves in the soliton fields statistical moments will be used. For separated solitons it is easy to analytically calculate the mean, variance, skewness, and the kurtosis. In this paragraph we consider the soliton fields with the same number of positive and negative waves. Therefore, the mean and the skewness will be equal to zero. Variance and kurtosis are calculated as follows:

$$\sigma^2 = 2 < A_i > \rho, \tag{4.25}$$

$$Kur = \frac{< A_i^3 >}{3\rho < A_i >^2}. \tag{4.26}$$

These formulas can only be used in cases where soliton gas has low density (for example ρ =0.048). However, in this paragraph we consider also a soliton gas with high density when solitons are already intersected at the initial time (Fig. 4.21) and in this case, the statistical moments must be found numerically.

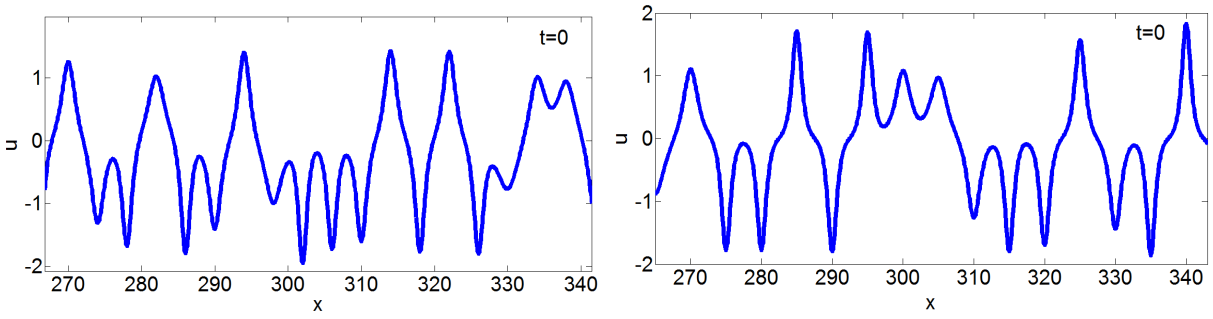

Figure 4.21 Zoom of initial field with ρ =0.24 and ρ =0.19.

Fig. 4.22 demonstrates the temporal evolution of the coefficients of skewness and kurtosis in one realization, and averages of these values over 50 realisations. Values of skewness changes in the realization from -1 to +1, but the ensemble of solitons is symmetrical in averages as expected. Kurtosis changes asymmetrically around the average, from 11 to 23. Average value of kurtosis tends to the value of 13.66 (plus/minus 0.315) after several interactions, which is larger than initial value of (13.1).

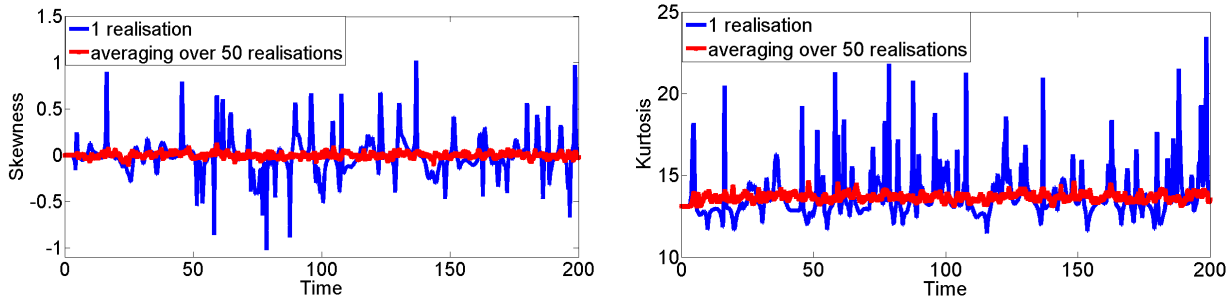

Figure 4.22 Temporal evolution of skewness and kurtosis in heteropolar soliton gas.

The coefficient of kurtosis advantageously increases, indicating an increase of the tail of the distribution function. Correspondingly, the skewness can take both negative and positive values at different times. However their averaging is close to zero due to the balance between positive and negative waves.

The kurtosis for soliton fields of different densities in one realization is presented in Fig. 4.23. With the gas density increasing the kurtosis decreases, however this effect can be seen from the analytical formulas for the initial state (4.26). As you know, this ratio shows the difference between the Gaussian distribution function, and if it is positive the probability of occurrence of large waves increases as compared with the normal stationary process.

As known, this coefficient shows the difference between of distribution function from the Gaussian, and if it is positive the probability of a freak wave is increased in comparison with the normal stationary processes. Therefore, it seems that the decreasing of kurtosis as gas density increasing means a reduction of the probability of freak wave occurrence, and that contradicts the results of direct calculations shown above. Changes of kurtosis characterize the excess of the distribution function from the Gaussian curve in an integral sense, but this does not say anything about the value of the distribution function at very large amplitudes.

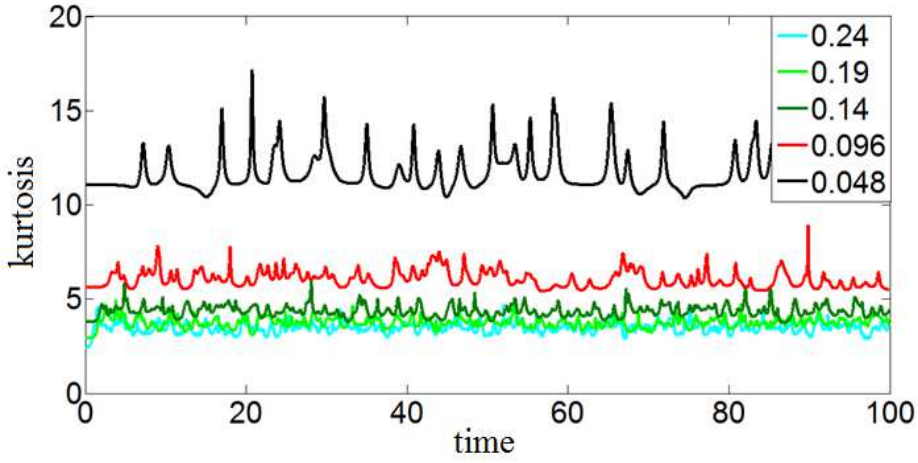

Figure 4.23 Kurtosis and skewness of soliton fields with different density.

It should be noted that freak waves in the framework of the modified Korteweg-de Vries equation have been studied previously in the case of narrowband initial conditions [Grimshaw et al, 2005, 2010; Talipova, 2011]. In this case, the mechanism of freak wave generation is modulation instability of modulated quasi-sinusoidal wave packets. We managed to find a mathematical work on the modulation instability of modulated cnoidal waves [Driscoll & O'Neil, 1976].

The main conclusion of this work is that if cnoidal waves have a mean of zero, then they are unstable. Yet if they are set on a pedestal, then the waves are stable. Soliton sequencing is a special case of a cnoidal wave. As already stated, the evolution of an ensemble of unipolar solitons does not lead to the formation of large waves, which is consistent with the stability of cnoidal waves having a non-zero average. At the same time, an ensemble of heteropolar soliton gas freak waves may appear, and this is correlated with the modulation instability of cnoidal waves with an average of zero. In

contrast to the cited work about instability of a cnoidal wave [Driscoll & O'Neil, 1976], our study shows the dynamic evolution of instability and makes it possible to quantify the characteristics of the soliton gas and probability of freak wave occurrence.

4.5 Conclusion

The dynamics of multi-soliton fields in the framework of the Korteweg - de Vries equation and the modified Korteweg - de Vries equation are studied in the present chapter. Four statistical moments (mean, variance, skewness and kurtosis) of soliton gas are investigated and analyzed. The distribution functions of soliton amplitudes are determined. It is shown that in the case of unipolar solitons the role of impulse with small amplitudes increases and with large amplitudes they are reduced.

The opposite result is obtained for heteropolar fields, in which the role of waves with large amplitudes increases, i.e. the tails of the distribution function increase. This means an increase of the probability of freak wave occurrence in the heteropolar fields. It is demonstrated that in a heteropolar field abnormally large waves (freak waves) may appear. The comparison of the dynamics of the unipolar soliton gas within the KdV and mKdV equations is given. In such fields, nonlinear interactions lead to an increase in the role of small-amplitude waves.

Chapter 5

Conclusions

The dynamics of random wave fields in the coastal zone in relation to the problem of freak wave occurrence is studied in this thesis. The following results are obtained:

1. It is demonstrated that the mechanism of dispersion focusing of freak wave formation "works" for waves interacting with a vertical barrier. It is shown that just before the maximum wave formation a freak wave quickly experiences a shape change from a high ridge to a deep depression. The lifetime of a freak wave increases with the growth of number of individual waves in anomalous wave packets, and the lifetime of a freak wave increases as water depth decreasing.

2. It is demonstrated that pair interaction of unipolar solitons lead to a decrease of the third and fourth moments of a wave field. It is shown that in the case of heteropolar soliton interactions the fourth moment increases.

3. The nonlinear dynamics of ensembles of random unipolar solitons in the framework of the Korteweg - de Vries equation and the modified Korteweg - de Vries equation is studied. It is shown that the coefficients of skewness and kurtosis of the soliton gas are reduced as a result of soliton collisions. The distribution functions of wave amplitudes are defined. The behavior of soliton fields in the framework of these models is qualitatively similar. It is shown that in these fields the amplitude of the large waves is decreased in average due to multi-soliton interactions.

4. A new breaking effect of solitons with small amplitudes and even changing of its direction in multi-soliton gas as a result of nonlinear interactions with other solitons is found in the framework of the modified Korteweg-de Vries equation.

5. It is shown that in heteropolar soliton gas abnormally large waves (freak waves) appear in the frameworks of the modified Korteweg - de Vries equation. With increasing of soliton gas density the probability and intensity of freak waves in such systems increases.

Chapitre A

Annexes

A.1 Publication dans le journal “Natural Hazards and Earth System Sciences”

Nat. Hazards Earth Syst. Sci., 11, 127–134, 2011
www.nat-hazards-earth-syst-sci.net/11/127/2011/
doi:10.5194/nhess-11-127-2011

Natural Hazards and Earth System Sciences

The scenario of a single freak wave appearance in deep water – dispersive focusing mechanism framework

E. Pelinovsky[1,2], **E. Shurgalina**[1,2], **and N. Chaikovskaya**[2]

[1]Department of Nonlinear Geophysical Processes, Institute of Applied Physics, Nizhny Novgorod, Russia
[2]Nizhny Novgorod State Technical University, Nizhny Novgorod, Russia

Received: 12 September 2010 – Revised: 6 November 2010 – Accepted: 16 November 2010 – Published: 11 January 2011

Abstract. One of the possible mechanisms of the emergence of freak waves in deep water, based on the dispersive focusing of unidirectional wave packets is analysed. This mechanism is associated with the frequency dispersion of water waves and manifested in the interference of many spectral components, moving with different velocities. Formation of a single freak wave in a random wind wave field is considered in the frame of linear theory. The characteristic lifetime of an abnormal wave in the framework of this mechanism for typical conditions is approximately two minutes, thus, a rapid effect is difficult to predict and prepare for. A rogue wave quickly changes its shape from a high ridge to a deep depression.

1 Introduction

The large-amplitude waves suddenly appearing for a short time on the sea surface (freak or rogue waves) attract the attention of professionals nowadays because of their danger to ships and oil platforms in sea, ports and tourist resorts on the coast. Numerous data of observing freak waves in different areas of the World Ocean can be found, for example, in books (Lavrenov, 2003; Kurkin and Pelinovsky, 2004; Kharif et al., 2009) and papers (Kharif and Pelinovsky, 2003; Didenkulova et al., 2006; Liu, 2007). Among the mechanisms of their appearance in the open sea the following ones are marked (Kharif et al., 2009): (a) a superposition of a large number of individual spectral components, which move with different speeds and in different directions (the dispersive and geometrical focusing); (b) nonlinear mechanisms of modulation instability, in particular, the Benjamin-Feir instability; and (c) interaction of sea waves with currents and wind flow. Each of these mechanisms has its own specificity, which is ultimately manifested in the probability of freak wave occurrence and the time of their life. It is possible that each mechanism leads to different forms of rogue waves and scenarios of their manifestation. All these important features have not been studied yet.

Here the possible scenario of the freak wave appearance in deep water, based on dispersive focusing of unidirectional wave packets is analysed. This mechanism is associated with the dispersion of water waves and is manifested in the interference of many spectral components, moving with different velocities. This mechanism "works" for both the deterministic (with certain conditions on the phases of spectral components) and random waves, leading to the appearance of abnormally high waves. It is possible in both, linear and nonlinear theories of water waves, although, of course, the nonlinearity leads to their peculiarities in the wave field (Pelinovsky and Kharif, 2000; Kharif et al., 2001; Pelinovsky et al., 2003; Shemer et al., 2007; Shemer and Dorfman, 2008). We also emphasize that the mechanism of dispersion focusing is very popular with experimentalists, because it allows generating a wave of huge height in a relatively short tank. The main attention in the laboratory experiments is paid to the description of the wave field (the displacement of water surface and particle velocities) at the focal point, which is essential for the subsequent assessment of the impact of extreme waves on ships and platforms (Brown and Jensen, 2001; Contento et al., 2001; Johannesen and Swan, 2001; Clauss, 2002; Touboul, 2006; Shemer et al., 2007; Shemer and Dorfman, 2008; Kharif et al., 2008, 2009; Shemer and Sergeeva, 2009).

Theoretical results for focusing wave packets in deep water are obtained mostly in the linear theory, in the framework of the so-called parabolic equation for the envelope of the wave packet (see, for example, Clauss and Bergmann, 1986; Magnusson et al., 1999; Pelinovsky and Kharif, 2000; Shemer et al., 2002; Pelinovsky et al., 2003; Shemer and

Correspondence to: E. Pelinovsky
(pelinovsky@hydro.appl.sci-nnov.ru)

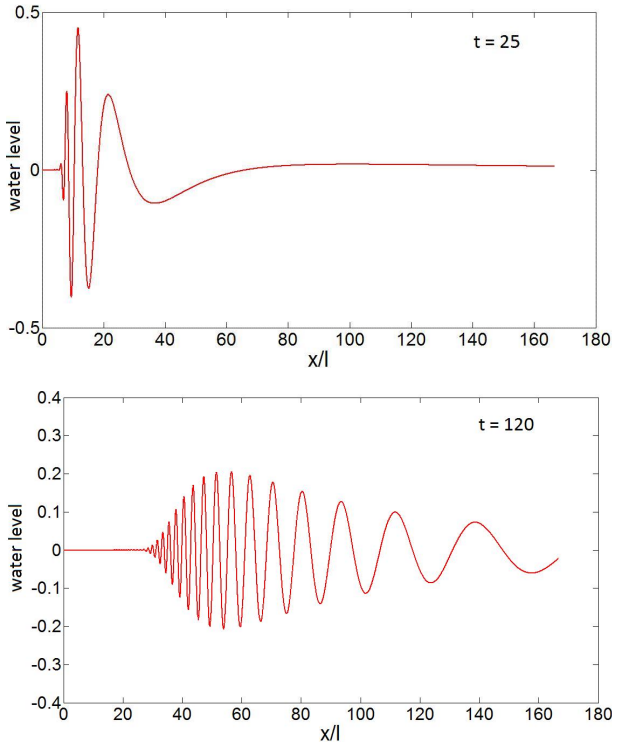

Fig. 1. Evolution of the Gaussian pulse in deep water for long times.

Dorfman, 2008). The particular analytical solution of this equation is the Gaussian packet, which demonstrates the process of the emergence of abnormally high waves and their disappearance. It is important to emphasize that the parabolic equation is valid for slow varying envelope on the scale of the carrier waves, so that the freak wave is a group of waves such as "Three Sisters" – a term often encountered in the witness descriptions of the phenomenon. However, it does not meet a single rogue wave, the description which is also present in the literature.

The aim of this work is to develop a scenario of appearance and disappearance of a single freak wave in the frame of the dispersive mechanism of focusing wave packets. Section 2 provides a solution to the Cauchy problem for waves in infinitely deep water, corresponding to the initial perturbation in the form of a single pulse. It is the basis for the demonstration of the occurrence of solitary freak waves in the deterministic wave field. The process of the appearing rogue waves in a random field of wind waves is considered in Sect. 3. It is shown that for typical conditions, the characteristic lifetime of a freak wave is about 2 min, demonstrating the difficulties in predicting this dangerous phenomenon. Features of the script of the development of abnormal pulse are discussed in Sect. 4. It is shown that the freak wave is not only there for a short time, but quickly changes its shape from a high ridge to a deep depression. The results are summarized in Sect. 5.

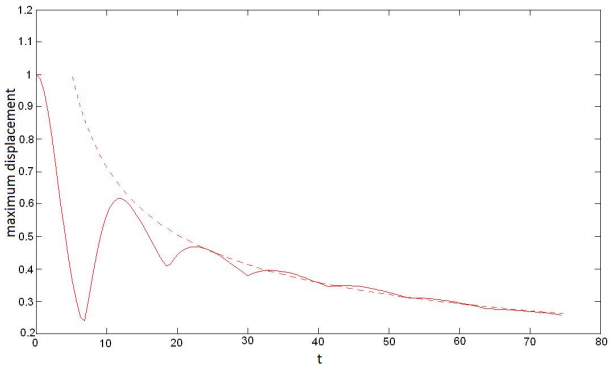

Fig. 2. The dependence of the maximum value of the wave field from dimensionless time (the solid line corresponds to the exact, and the dashed line – asymptotic solution).

2 Generation of "huge" wave in a frequency-modulated wave packet

The transformation of the wave packet into a single large-amplitude wave in the frame of the linear theory can be considered using the Fourier-superposition of spectral components. In practice, however, a different approach is used (Kharif et al., 2009): Cauchy problem is solved for the initial condition, which corresponding to the expected anomalous wave, and then the resulting solution is inverted in the space. As a result, possible forms of the wave packet can find the evolution of which leads to the formation of abnormal waves in a finite time, followed by its transformation back into the wave packet. Let us consider a classical solution of Cauchy problem for waves in deep water, written in the integral form

$$\eta(x,\tau) = \int_{-\infty}^{+\infty} A(k)\exp\{i\,[\omega(k)\tau - kx]\}dk, \qquad (1)$$

where $\eta(x,\tau)$ is a displacement of the water level, $A(k)$ is Fourier spectrum determined by the initial disturbance, corresponding to the expected anomalous wave $\eta_0(x)$

$$A(k) = \frac{1}{2\pi}\int_{-\infty}^{+\infty} \eta_0(x)\exp(ikx)dx, \qquad (2)$$

$\omega(k)$ is a wave frequency determined from the dispersion relation of waves in deep water

$$\omega(k) = \sqrt{gk}, \qquad (3)$$

where g is gravity acceleration. Integral Eq. (1) analytically is not calculated for "reasonable" initial disturbances, but at long times, its presented by a well-known expression obtained by the method of stationary phase (Whitham, 1977)

$$\eta(x,\tau) \approx Z(x,\tau)\cos\left[\omega(x,\tau)\tau - k(x,\tau)x + \varphi[k(x,\tau)] - \frac{\pi}{4}\right] \quad , \quad (4)$$

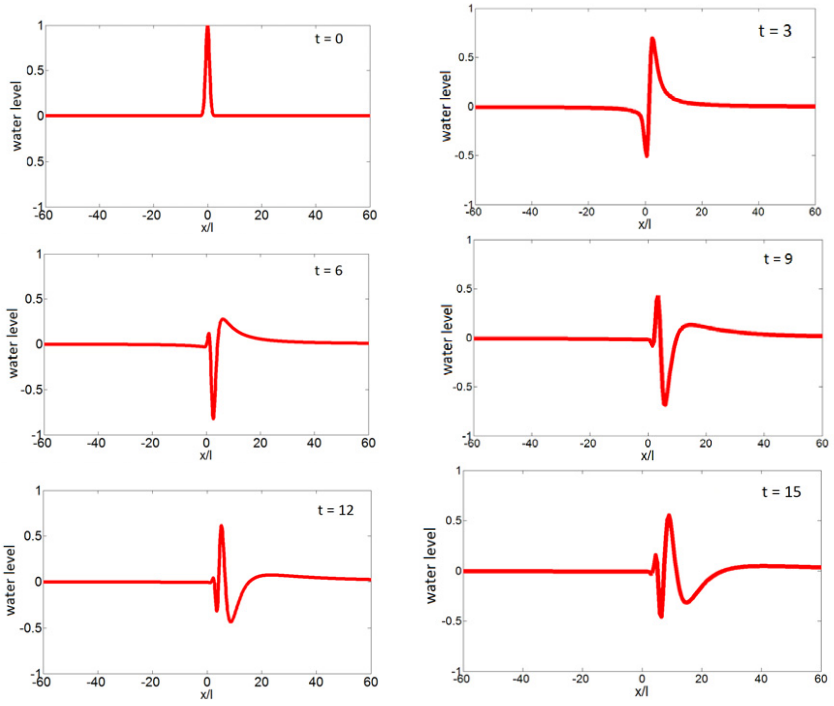

Fig. 3. Evolution of the pulse at short times.

$$Z(x,\tau) = 2\sqrt{\frac{2\pi}{|dC_{gr}/dk|}}\frac{|A(k)|}{\sqrt{\tau}},$$

$$C_{gr}(k) = \frac{d\omega}{dk} = \frac{1}{2}\sqrt{\frac{g}{k}} = \frac{x}{\tau}, \qquad (5)$$

$|A|$ and φ are module and an argument of the complex spectrum of $A(k)$. The last expression in Eq. (5) allows unambiguously to find the wave number $k(x,\tau) = g\tau^2/4x^2$, then from Eq. (3) the wave frequency $\omega(x,\tau) = g\tau/2x$. The final asymptotic expression for the wave field takes the following form

$$\eta(x,\tau) \approx 2\sqrt{\pi}|A(g\tau^2/4x^2)|\sqrt{\frac{g\tau^2}{x^3}}\cos\left[\frac{g\tau^2}{4x} + \varphi - \frac{\pi}{4}\right], \qquad (6)$$

it describes, at each moment in time, the wave packet with variable amplitude and length (frequency-modulated wave train), and ahead follow longer wavelengths, which have a great group velocity. Asymptotic solutions for waves of any physical nature are well-known (Whitham, 1977) and, therefore, the details of their derivation are not discussed here.

As an expected anomalous wave it is natural to choose a Gaussian pulse with a characteristic amplitude A_0 and half of a length l

$$\eta_0(x) = A_0 e^{-\frac{x^2}{l^2}}. \qquad (7)$$

Then at large distances ($x>>l$) it transforms into a wave packet

$$\eta(x,\tau) \approx A_0\frac{l\tau}{x}\sqrt{\frac{g}{x}}\exp\left(-\frac{g^2l^2\tau^4}{64x^4}\right)\cos\left[\frac{g\tau^2}{4x} - \frac{\pi}{4}\right]. \qquad (8)$$

The shape of the wave packet at different moments of the dimensionless time ($t = \tau\sqrt{g/l}$) is shown in Fig. 1. Over time a train stretches in the space (proportional to τ), and its amplitude decreases as $\tau^{-1/2}$, ensuring the conservation of wave energy. The number of individual waves increases linearly with time, the wave of maximum amplitude retaining its length and speed of propagation.

At short times the integral Eq. (1) is calculated numerically, which allowed us to define the limits of applicability of the asymptotic solutions. As it turned out, at values of dimensionless time ~20–25, the maximum water displacement (the amplitude of the high ridge) is well described by the asymptotic value (Fig. 2).

It is clearly seen that in the frame of the exact solution, the maximum of the field decreases sharply at times of ~5–10 and, consequently, the wave in the form of the hump disappears for a while. The evolution of the wave shape at short dimensionless times is shown in Fig. 3.

Initially, a positive bell-shaped pulse is transformed into a wave of depression and further into the wave train. The quick change of polarity of the pulse had not previously been noted in the literature, however, as we show below, it plays an important role in the scenarios of freak wave formation.

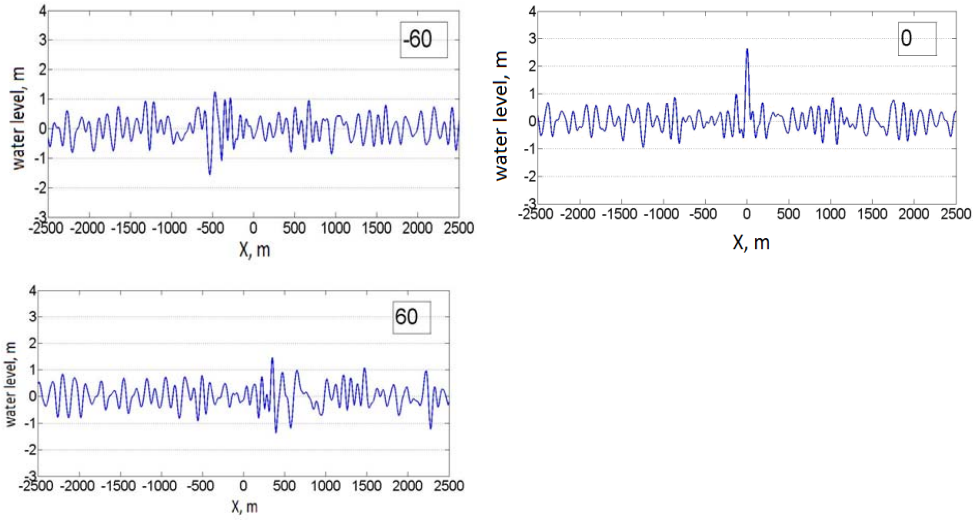

Fig. 4. Snapshots of the wave field at different times (s).

The solution given above describes the transformation of a solitary wave in the frequency modulated wave packet. If the wave packet is inverted in the space, so that now the short waves with small group velocity are ahead of the long ones, the wave packet will be transformed into a solitary wave of Gaussian shape. The property of inverting the solutions of linear equations of ideal hydrodynamics is used to find optimal conditions for the dispersive focusing. Nonlinearity, of course, affects the process of focusing. In particular, in the papers of Shemer et al. (2006, 2007) it was demonstrated that in an unidirectional focusing process nonlinear effects are essential in two important aspects. They may lead to a considerable modification of the complex amplitude spectrum in the course of evolution, affecting both absolute values of the amplitudes of various harmonics and their phases. The other aspect is related to the contribution of bound waves that changes considerably the amplitudes of troughs and crests and violates the symmetry between the two. But if the wave amplitude is relatively weak, this effect is not fundamental; it is just needed to make a few adjustments to the form of the wave packet (Johannesen and Swan, 2001; Clauss, 2002).

Concluding this section, we note that in laboratory conditions a single wave with a broad spectrum is generated by a wave maker with variable frequency, changing in finite limits according to the linear law (the optimal law for the generation of solitary waves through the mechanism discussed above) (see, for example, Brown and Jensen, 2001; Shemer et al., 2007; Shemer and Dorfman, 2008; Kharif et al., 2008). In this case, the signal spectrum is almost rectangular, while the wave itself (through the inverse Fourier transform) – crest of small, oscillating tails (like sin *(x)/x*); it is the shape of a focused wave observed in experiments (Kharif et al., 2008; Shemer and Dorfman, 2008).

3 Generation of a single pulse in a random field of wind waves

The mechanism of dispersion focusing described above must occur in a random field of wind waves, the spectral components of which move with different velocities. A simple statistical analysis of a random superposition of waves with a narrow spectrum in the linear approximation leads to the Rayleigh distribution, so that the freak wave should appear once every 10 h (Dysthe et al., 2008; Kharif et al., 2009). The simulation of the wave field for such long times is rather a difficult task, so we assume that, along with random components, there is a deterministic frequency-modulated packet of small amplitude, as described above. Then by the linearity the random and regular components of wind wave field do not interact with each other, so that the process of forming a single pulse from a frequency-modulated packet follows the scenario described above. The random disturbance, on average, does not change its energy and the possibility of a big wave in it is small at relatively short times. As a result, the initial wave field "looks" purely random, and then there comes a high ridge, which over time is again "dissolved" in random waves. Such processes of interference of random and deterministic fields have already been discussed in the literature (Kharif et al., 2009), but not for the formation of a single wave on deep water. Nonlinearity, if it is weak, can not prevent the dispersive focusing of a deterministic wave packet, so it can be ignored on the first stage.

In numerical experiments the random wave field is set by the superposition of spectral components with random phases

$$\eta(x,\tau) = \sum_{i=1}^{N} A_i \cos(\omega_i \tau - k_i x + \varphi_i), \tag{9}$$

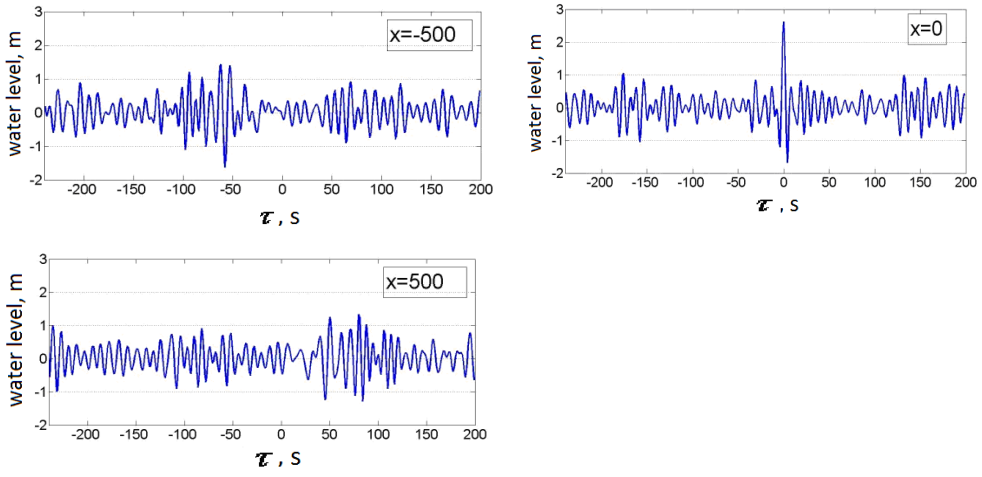

Fig. 5. Time series of the wave field at different distances (m) from the zone of anomalous wave.

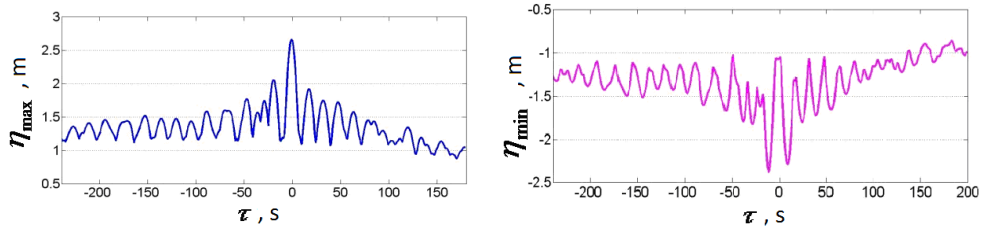

Fig. 6. Maximum values of positive and negative amplitudes versus time.

where the spectral amplitude $A_i = \sqrt{S(k)\Delta k}$, Δk is a sampling interval of the spectrum, $k_i = i\,\Delta k$, $\omega_i = \sqrt{g k_i}$, $N = 156$ is the total number of harmonics. Phases φ_i are evenly distributed and set with a random number generator, $S(k)$ is energetic spectrum, for example, the spectrum of the Pearson-Moskowitz or JONSWAP spectrum. In our calculations, we used a simpler Gaussian approximation of the wind wave spectrum

$$S(k) = B \exp\left(-\frac{(k-k_0)^2}{l^2}\right), \tag{10}$$

with $B = 0.05\,\mathrm{m}^3$, $l = 0.5\,\mathrm{m}^{-1}$, $k_0 = 0.063\,\mathrm{m}^{-1}$. In this case, the characteristic wavelength is 100 m and a significant height of the wave $H_s = 1.5$ m, thus, the rms value of the surface elevation variation as $\sigma = H_s/4$ yields to steepness $k_0\sigma \approx 0.025$. On the other hand the maximum height of the freak wave reaches $a_{\max} = 2.7$ m (see below) and, therefore, the steepness of the wave of maximum amplitude is $k_0 a_{\max} \sim 0.17$. This nonlinearity may probably be sufficiently small to justify linear analysis if we compare the experimental results with Shemer et al. (2007) where the nonlinear effects are manifested at $k_0 a_{\max} \sim 0.3$.

The superposition of deterministic and random components of the wave field at different times is illustrated in Fig. 4, where the time (s) is measured from the onset of solitary wave of large amplitude. As we see, even one minute before, the abnormal waves are not visible and they also almost disappear in 1 min, so the forecast of freak wave is indeed very difficult and, most importantly, there is little time to prepare for its appearance in such a short time. What is said above is also shown by the time series of the wave field at short distances (500 m) from the place of an abnormally large wave (Fig. 5).

A presentation of the typical lifetime of the rogue-wave is given in Fig. 6, which shows the maximum height of the ridges and deep depressions in the domain of 5 km versus time. As it can be seen, a significant change in the wave height occurs within about 2 min, and this value can be taken for the lifetime of the anomalous wave. We emphasize that the freak wave appears both in the form of a high ridge and in form of a deep depression, and near the estimated time the wave changed its polarity several times.

4 The scenario of a freak wave appearance

The calculations given above show that the freak wave exists about 2 min, and a detailed chronology during that time (the script of the process) will allow for the evolution of the freak

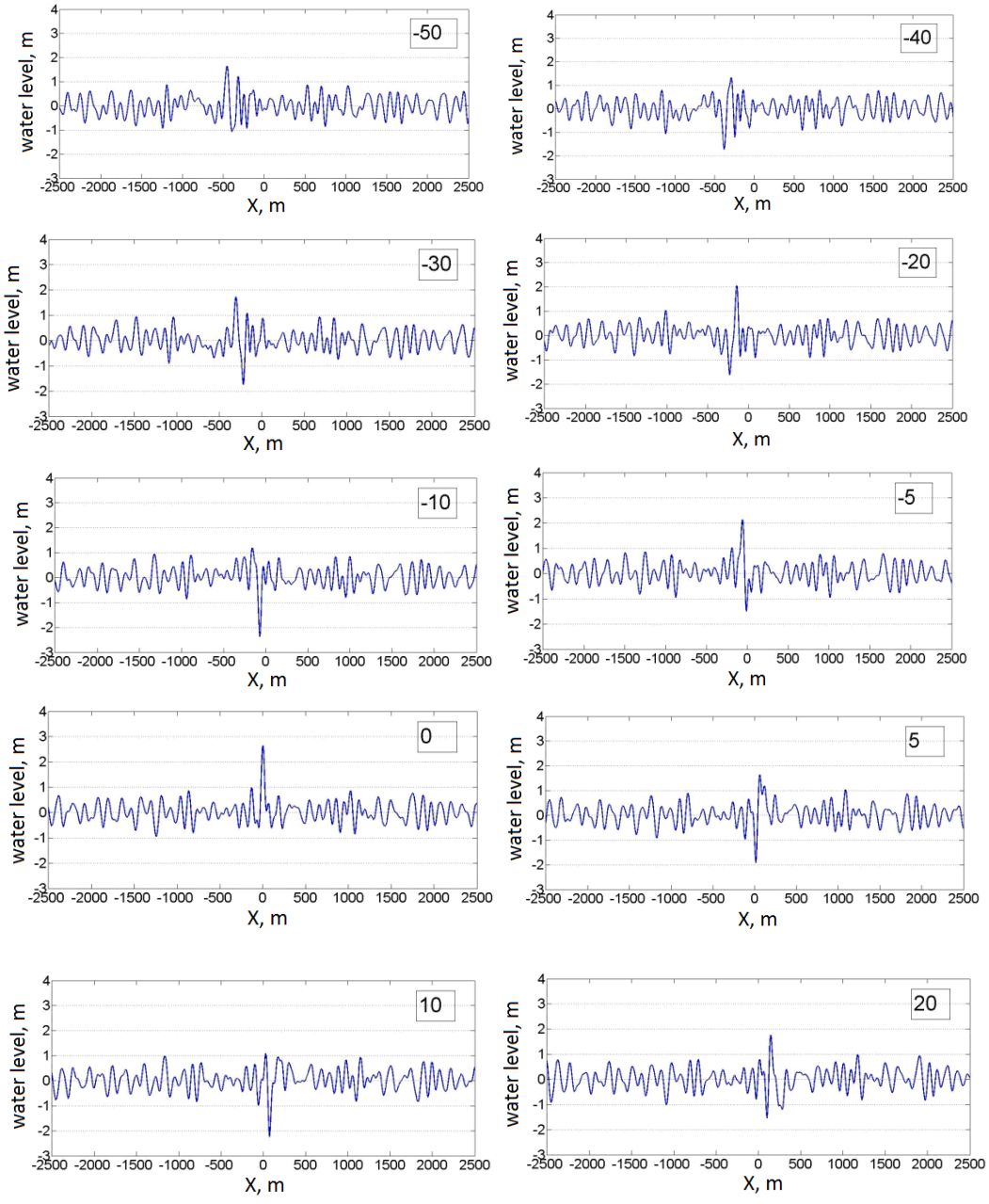

Fig. 7. Snapshots of water level for different times (s).

wave. Figure 7 shows the shape of the water surface at different times, calculated by the above formulas. At this time interval (about 2 min) an anomalous solitary wave is always visible in the background of random wind waves. Its shape is constantly changing from crest to trough and back quite quickly (within approximately 10 s).

Observability of the rogue waves depends on many factors. For example, if the observer is on the plane, he can only see one of the images shown in Fig. 7, and to estimate the height of the anomalous wave from its trough to the crest. In fact, such pictures of freak-waves have been received from space (Kharif et al., 2009) and are not discussed here. Freak waves were originally described in legends, transmitted orally from sailors who having survived the horror of meeting with this terrible phenomenon, hurried to share their impressions with others. Naturally, most of the stories contained a considerable exaggeration and fictitious descriptions. Having now a model of freak waves, it is possible to develop a "standardized" description schematizing the reaction of sailors to this phenomenon.

Thus, in the case of the focusing wave packets, as shown above, the apparent abnormal wave in the form of a crest appears in approximately 1 min prior to its approach to the ship at the distance about 600–700 m. If the observer is on board, who also "prescribes" water level fluctuations in pitching, he can only see a big crest. This crest can be seen a few times (2–4 times) for about 10 s, before it comes to the ship. In this case, the first not the highest ridges will hardly attract the attention of seafarers and, in fact, the freak waves will be visible for about 30 s before meeting with the biggest wave. And only when the wave appears just before the ship, the observer can see that the wave consists of a crest and trough or of trough/crest.

That is why phrases of the descriptions are typical: "crews do not have time to prepare for the meeting with the danger" (Kharif et al., 2009), which greatly aggravates the consequences of the meeting with the elements. The fact of the sudden appearance of the freak waves requires from the crew of any vessel not only professional knowledge, but also mental preparation. The reaction of seafarers, of course, depends on their experience related to stressful situations, such as during a storm. There are specific, purely psychological factors (the so-called sthenic or asthenic emotions, ability to anticipate situations in life and willingness to encounter them and so on). According to (Rogovin and Karpova, 1985), the willingness of action to external irritants is 0.5–2 s later, thus, there is no time to be prepared for a meeting with the freak wave. Therefore, one important task is to study the psychological characteristics of human behaviour in case of meeting with a freak wave and the development of special techniques and simulators for the crew of ships. In addition to purely technical issues (stability of the ship in large waves, a special lashing, etc.) this will prevent the severe consequences of this type of maritime disasters.

We should point out that in our study the temporal evolution problem is considered. The relation between the temporal and the spatial formulation was considered in detail in Shemer and Dorfman (2008). While the temporal approach is simpler and more "natural" for numerical simulations, it can not be realized in experiments where the evolution is spatial and the initial conditions are prescribed at $x = 0$ rather than at $t = 0$. It is possible that spatial formulation would be more appropriate from the point of view of the ship's captain watching the approaching waves, as attempted in the present manuscript. But in linear approximation, both approaches lead to the same results. The study by Shemer et al. (2010) indicated that for wider spectrum the importance of nonlinear effects seems to decrease and, therefore, we may use the temporal approach to analyse the scenario of appearance of the single freak wave.

Let us note that here we have considered the case when the wave of maximum amplitude is a ridge. Quite similarly, we can investigate a freak wave in the form of a deep depression. In the framework of linear theory, it is sufficient to change the sign in the Eq. (7). The scenario of the appearance of a freak wave in this case is almost not changed: waves of large amplitude are noticeable for about a minute and they change their polarity, appearing and disappearing at the sea surface for a short time. However, directly at the ship it will manifest itself in the form of a wave of deep depression and it will fail in trough. To predict the polarity of the freak wave (crest or trough), in the framework of this approach, is impossible if we use only the observation of waves in previous times.

5 Conclusions

The appearance of abnormally large waves on the sea surface is due to the different physical mechanisms. In this paper, we discuss the dispersive focusing scenario of a single freak wave formation. For typical conditions, it is shown that the characteristic lifetime of the freak waves is about two minutes. It is noted that at this time, the wave quickly (in about 10 s) changes its shape from crest to trough and back. At the same time, for an observer onboard a ship, when only the high ridges are seen, the appearance of a freak wave is always unexpected, especially because about a minute before a large wave, it appears only 2–4 times, each time for 10 s. The probability that the ship will rise to the top of the wave (if it is a crest), or fail in to the hole (if it has a negative polarity), is the same, and can not be determined in advance. All these points to the inherent difficulties in forecasting a freak wave, even a short time before when large waves become apparent on the sea surface.

Acknowledgements. The partial support of RFBR (08-05-00069), the European Programme FU-7 (No. 234175), State Contracts (No. 02.740.11.0732 and 01.420.1.2.0006) and RAS program "Nonlinear Dynamics" is used. Authors are also grateful to Lev Shemer (Tel-Aviv University, Israel) for the useful remarks.

Edited by: C. Kharif
Reviewed by: P. Liu and two other anonymous referees

References

Brown, M. G. and Jensen, A.: Experiments on focusing unidirectional water waves, J. Geophys. Research, 106, C8, 16917–16928, 2001.

Clauss, G.: Dramas of the sea: episodic waves and their impact on offshore structures, Appl. Ocean Res., 24, 147–161, 2002.

Clauss, G. and Bergmann, J.: Gaussian wave packets: a new approach to seakeeping tests of ocean structures, Appl. Ocean Res., 8, 190–206, 1986.

Contento, G., Codigla, R., and D'Este, F.: Nonlinear effects in 2D transient non-breaking waves in a closed flume, Appl. Ocean Res., 23, 3–13, 2001.

Didenkulova, I. I., Slunyaev, A. V., Pelinovsky, E. N., and Kharif, C.: Freak waves in 2005, Nat. Hazards Earth Syst. Sci., 6, 1007–1015, doi:10.5194/nhess-6-1007-2006, 2006.

Dysthe, K., Krogstad, H. E., and Muller, P.: Oceanic rogue waves, Annu. Rev. Fluid Mech., 40, 287–310, 2008.

Johannesen, T. B. and Swan, C.: A laboratory study of the focusing of transient and directionally spread surface water waves, Proc. Royal Soc. London, A457, 971–1006, 2001.

Kharif, C. and Pelinovsky, E.: Physical mechanisms of the rogue wave phenomenon, European J. Mechanics/B – Fluid, 22, 6, 603–634, 2003.

Kharif, C., Pelinovsky, E., and Slunyaev, A.: Rogue waves in the ocean, Springer, 196 pp., 2009.

Kharif, C., Pelinovsky, E., Talipova, T., and Slunyaev, A.: Focusing of nonlinear wave group in deep water, JETP Lett., 73, 4, 190–195, 2001.

Kharif, C., Giovanangeli, J.-P., Touboul, J., Grare, L., and Pelinovsky, E.: Influence of wind on extreme wave events: Experimental and numerical approaches, J. Fluid Mech., 594, 209–247, 2008.

Kurkin, A. A. and Pelinovsky, E. N.: Freak waves: facts, theory and modelling, Nizhny Novgorod, Nizhny Novgorod Technical University Press, 157 pp., 2004.

Lavrenov, I. V.: Wind waves in ocean: dynamics and numerical simulations, Springer, Heidelberg, 377 pp., 2003.

Liu, P. C.: A chronology of freaque wave encounters, Geofizika, 24, 1, 57–70, 2007.

Magnusson, A. K., Donelan, M. A., and Drennan, W. M.: On estimating extremes in an evolving wave field, Coast. Eng., 36, 147–163, 1999.

Pelinovsky, E. and Kharif, C.: Simplified model of the freak wave formation from the random wave field, Proc. 15th Int. Workshop on Water Waves and Floating Bodies, Israel, 142–145, 2000.

Pelinovsky, E. N., Slunyaev, A. V., Talipova, T. G., and Kharif, C.: Nonlinear parabolic equation and extreme waves on the sea surface, Radiophys. Quantum. El., 46, 7, 451–463, 2003.

Rogovin, M. S. and Karpova, E. V.: Content dynamics and tier organization of concepts in the psychological analysis of subjective time, Questions of Psychology, 3, 98–107, 1985 (in Russian).

Shemer, L., Goulitski, K., and Kit, K.: Steep transitional waves in tanks, Proc. 25^{th} OMAE, ASME paper OMAE2006-92547, Hamburg, 2006.

Shemer, L., Goulitski, K., and Kit, E.: Evolution of wide-spectrum wave groups in a tank: an experimental and numerical study, Eur. J. Mech. B/Fluids, 26, 193–219, 2007.

Shemer, L. and Dorfman, B.: Experimental and numerical study of spatial and temporal evolution of nonlinear wave groups, Nonlin. Processes Geophys., 15, 931–942, doi:10.5194/npg-15-931-2008, 2008.

Shemer, L., Kit, E., and Jiao, H.-Y.: An experimental and numerical study of the spatial evolution of unidirectional nonlinear water-wave groups, Phys. Fl., 14, 3380–3390, 2002.

Shemer, L. and Sergeeva, A.: An experimental study of spatial evolution of statistical parameters in a unidirectional narrow-banded random wavefield, J. Geophys. Res., 114, C01015, doi:10.1029/2008JC005077, 2009.

Shemer, L., Sergeeva, A., and Liberzon, D.: Effect of the initial spectrum on spatial evolution of the statistics of unidirectional nonlinear random waves, J. Geophys. Res., 115, C06326, doi:10.1029/2010JC006326, 2010.

Touboul, J., Giovanangeli, J. P., Kharif, Ch., and Pelinovsky, E.: Experiments and simulations of freak waves under the action of wind, Eur. J. Mech. B/Fluids, 25, 5, 662–676, 2006.

Whitham, G. B.: Linear and nonlinear waves, Wiley & Sons, New York, 635 pp., 1974.

A.2 Publication dans le journal “Fundamental and Applied Hydrophysics”

Shurgalina E., Pelinovsky E.

Development of freak waves swell in a weak wave field

Abstract:

Interference of unidirectional swell and wind waves in deep water in frameworks of linear potential theory is considered. Wind waves are described by Pierson–Moskowitz spectrum, and swell – by the frequency-modulated wave packet. It is noticed that in case of a variable wind in a storm area the swell waves can be focused on some distance from the origin area, forming abnormal big waves («freak waves»). A visibility of the freak wave swell of different shapes in wind wave field is examined.

Key words: water waves, wind waves, freak waves, dispersive focusing, life-time of freak waves

A.3 Publication dans le journal “Fundamental and Applied Hydrophysics”

Pelinovsky E., Shurgalina E.

Abnormal intensification of a wave near a vertical barrier

Abstract:

One of the possible mechanisms of emergence of freak-waves near a vertical barrier, based on the dispersive focusing of unidirectional wave packets is analyzed. This mechanism is associated with the frequency dispersion of water waves and manifested in the interference of many spectral components, moving with different group velocities. Formation of a single freak wave in a random wind wave field is considered in the frame of linear theory. The characteristic lifetime of an abnormal wave in the framework of this mechanism for typical conditions is approximately two minutes, so thus such a rapid effect is difficult to predict and prepare for. A rogue wave quickly changes its shape from a high ridge to a deep depression.

Keywords: water waves, wind waves, freak waves, dispersive focusing.

A.4 Publication dans le journal “Izvestiya, Atmospheric and Oceanic Physics”

On the criteria of the transition from breaking bore to undular bore

E. N. Pelinovsky[1-3], E. G. Shurgalina[1-2], A. A. Rodin[1,4]

1) Nizhny Novgorod State Technical University n.a. R. E. Alekseev, 6030950, Russia, Nizhny Novgorod, Minina street, 24

2) Institute of Applied Physics, Russian Academy of Sciences, 603950, Russia, Nizhny Novgorod, Ul'yanova street, 46

3) Higher School of Economics- National Research University,

603005, Russia, Nizhny Novgorod, Bolshaya Pecherskaya Street , 25/12

4) Institute of Cybernetics, Tallinn University of Technology, Akadeemia tee 21, EE-12618, Tallinn, Estonia

E-mail: pelynovsky@hydro.appl.sci-nnov.ru

E-mail: eshurgalina@mail.ru

E-mail: artem@cens.ioc.ee

Received 13.08.2014.

Field data of undular and breaking bores observed in a coastal zone and river estuaries are collected. Existing criteria of separation of these two regimes of bores which depend on the ratio between bore height and unperturbed water depth are applied to the collected data. It is shown that criterion $H/h > 1.5$ (H is a bore height, measured from the bottom, h is an unperturbed depth of reservoir) is sufficient for the bore separation by the regime.

Keywords: breaking bore, undular bore, shallow water theory, field data

A.5 Publication dans le journal “Physics Letters A”

Physics Letters A 377 (2013) 272–275

Contents lists available at SciVerse ScienceDirect

Physics Letters A

www.elsevier.com/locate/pla

Two-soliton interaction as an elementary act of soliton turbulence in integrable systems

E.N. Pelinovsky [a,b], E.G. Shurgalina [b,c], A.V. Sergeeva [b,c], T.G. Talipova [b,c], G.A. El [d,*], R.H.J. Grimshaw [d]

[a] Department of Information Systems, National Research University – Higher School of Economics, Nizhny Novgorod, Russia
[b] Department of Nonlinear Geophysical Processes, Institute of Applied Physics, Russian Academy of Sciences, Nizhny Novgorod, Russia
[c] Department of Applied Mathematics, Nizhny Novgorod State Technical University, Nizhny Novgorod, Russia
[d] Department of Mathematical Sciences, Loughborough University, UK

ARTICLE INFO

Article history:
Received 5 September 2012
Received in revised form 10 November 2012
Accepted 13 November 2012
Available online 19 November 2012
Communicated by C.R. Doering

Keywords:
KdV equation
Soliton
Turbulence

ABSTRACT

Two-soliton interactions play a definitive role in the formation of the structure of soliton turbulence in integrable systems. To quantify the contribution of these interactions to the dynamical and statistical characteristics of the nonlinear wave field of soliton turbulence we study properties of the spatial moments of the two-soliton solution of the Korteweg–de Vries (KdV) equation. While the first two moments are integrals of the KdV evolution, the 3rd and 4th moments undergo significant variations in the dominant interaction region, which could have strong effect on the values of the skewness and kurtosis in soliton turbulence.

1. Introduction

Solitons represent an intrinsic part of nonlinear wave field in weakly dispersive media and their deterministic dynamics in the framework of the Korteweg–de Vries (KdV) equation is understood very well (see e.g. [1–3]). At the same time, description of statistical properties of a random ensemble of solitons (or a more general problem of the KdV evolution of a random wave field) still remains to a large extent an unsolved problem, especially in the context of concrete physical applications. In particular, importance of this problem for the description of wind-generated waves on shallow water was demonstrated in [4–9]. From the theoretical point of view the description of a random soliton wave field is complementary to the "integrable wave turbulence" theory outlined in a recent paper by Zakharov [10].

The macroscopic dynamics of random soliton ensembles (soliton gases) in integrable systems are determined by the fundamental "microscopic" properties of soliton interactions: (i) soliton collisions are elastic, i.e. the interaction does not change the soliton amplitudes (or, more precisely, the discrete spectrum levels in the associated linear spectral problem); (ii) after the interaction, each soliton gets an additional phase shift; (iii) the total phase shift of a 'trial' soliton acquired during a certain time interval can be calculated as a sum of the "elementary" phase shifts in pairwise collisions of this soliton with other solitons during this time interval. Thus the dynamics of a soliton gas are essentially determined by two-soliton interactions.

The study of soliton gases was initiated by Zakharov in [11] where an approximate kinetic equation for random KdV solitons when their spatial density is small was derived. This equation describes spatio-temporal evolution of the distribution function of solitons over the (IST) spectrum. The full kinetic equation for the KdV soliton gas of arbitrary density was derived in [12] (see also [13]) using the thermodynamic limit of the Whitham modulation equations and then was generalized in [14] to other integrable systems. The kinetic description of a soliton gas makes an emphasis on the particle-like nature of solitons. At the same time, solitons represent nonlinear coherent wave structures so the total random nonlinear wave field associated with a soliton gas can be naturally interpreted as soliton turbulence [15]. In view of the outlined definitive role of two-soliton interactions, it is natural to ask: what is their specific (qualitative and quantitative) contribution to the statistical properties of soliton turbulence? In classical (both hydrodynamic and wave) turbulence theories the random field properties are usually described in terms of statistical moments (see e.g. [16,17]). This provides one with a natural motivation to start with the study of the properties of the spatial moments of the two-soliton KdV solution. In spite of the elementary nature of this problem it has apparently never been considered before. In the context of the soliton turbulence description, the knowledge of

* Corresponding author. Tel.: +44 1509 222869; fax: +44 1509 223969.
E-mail address: g.el@lboro.ac.uk (G.A. El).

0375-9601/$ – see front matter
http://dx.doi.org/10.1016/j.physleta.2012.11.037

"primitive" dynamics of the spatial moments of two-soliton solutions is a necessary ingredient in the understanding of the behavior of the statistical moments of the random KdV wave field.

Since the first and the second spatial moments of the two-soliton solution are conserved under the KdV evolution, our main focus in this Letter will be on the properties of the 3rd and 4th moments which vary with time and which, after appropriate ensemble averaging, will affect the behavior of the skewness and kurtosis of the probability distribution of the random wave field in the KdV soliton turbulence. These two statistical characteristics are also known to play important role in the theory of rogue waves [18].

2. Dynamics of two-soliton interactions

Although multisoliton solutions of the KdV equation had been known since the very beginning of the soliton theory creation [19,20], the nature of the mass/momentum/energy exchange occurring during the interaction of two solitons have been continued to be the subject of rather active study (see [21] and references therein). In view of the outlined in the Introduction key role of the two-soliton interactions in the formation of the structure of soliton turbulence we shall need to briefly revisit here some of their basic properties.

We shall use the canonical form of the KdV equation

$$u_t + 6uu_x + u_{xxx} = 0. \tag{1}$$

The two-soliton solution of (1) has the form (see e.g. [2,3])

$$u_2(x,t) = 2\partial_x^2 \ln\bigl[\tau(x,t)\bigr],$$
$$\text{where } \tau = 1 + e^{\phi_1} + e^{\phi_1} + \alpha^2 e^{\phi_1+\phi_2},$$
$$\alpha = \frac{\eta_2 - \eta_1}{\eta_1 + \eta_2}, \qquad \phi_i = -2\bigl(\eta_i x - 4\eta_i^3 t - \xi_i\bigr), \quad i = 1,2. \tag{2}$$

Here $-\eta_{1,2}^2$ are the discrete spectrum points in the associated IST formalism and ξ_i are the initial phases of solitons. When $t \gg 1$ solution (2) asymptotically (up to exponentially small terms) transforms into a superposition of two single-soliton solutions (see e.g. [1,3]):

$$u_2 \sim A_1 \operatorname{sech}^2\bigl[\eta_1 x - 4\eta_1^3 t - \xi_1 - \Delta_1\bigr] + A_2 \operatorname{sech}^2\bigl[\eta_2 x - 4\eta_2^3 t - \xi_2 - \Delta_2\bigr], \tag{3}$$

where the amplitudes $A_i = 2\eta_i^2$, $i = 1,2$ and the phase shifts $\Delta_{1,2}$ of the solitons due to the interaction are: $\Delta_{1,2} = \pm \ln|\alpha|$ assuming $A_1 > A_2$. We note that two-soliton KdV solution (2) can be represented in a number of equivalent forms emphasizing different aspects of the soliton interaction dynamics (see e.g. [21]).

Let at the initial moment the taller soliton with amplitude A_1 be located behind the shorter one with the amplitude A_2. Since the KdV soliton speed is proportional to its amplitude, the first soliton will catch up the second one and the nonlinear interaction will take place within certain space–time "dominant interaction region" (see [3]). There are three types of the behavior in the dominant interaction region depending on the amplitude ratio $r = A_1/A_2 > 1$ of the interacting solitons [22]:

(i) if $1 < r < \frac{3+\sqrt{5}}{2} \approx 2.62$, then the interacting solitons interchange their roles without passing through each other. They never "stick together" into a single unimodal pulse and always retain their "identity" during the interaction. This type of interaction is often called the "exchange interaction". At the moment when the strength of the interaction reaches its peak the double wave assumes a symmetric two-hump profile with the local minimum $u = u^* = A_1 - A_2$ at the centre (see e.g. [23]).

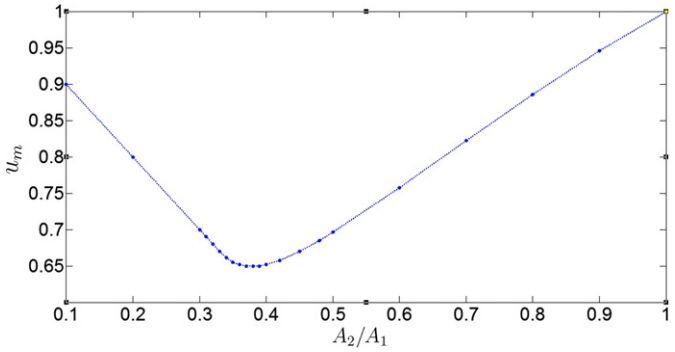

Fig. 1. Dependence of the minimum of the double wave amplitude $u_m = \min[\max\{u_2(x,t)\}: t > 0]$ on the soliton amplitude ratio A_2/A_1 in the two-soliton solution.

(ii) if $\frac{3+\sqrt{5}}{2} < r < 3$ the nature of the interaction changes so that the taller soliton first absorbs the shorter one and then re-emits it. Similar to the case (i) the solitons never merge into a single hump, but at the same time the double wave never assumes a symmetric shape. This scenario can be associated with the transition from the "exchange" to the "overtaking interaction". The amplitude of the shorter soliton grows during the absorption phase and assumes its maximum value $\frac{2}{5}[A_1 + A_2 + (A_1^2 + A_2^2 - 3A_1A_2)^{1/2}]$ at the moment of the strongest interaction, say $t = t^*$. At the same moment $t = t^*$ the value of the double wave amplitude reaches its minimum $u_m = \min[\max\{u_2(x,t)\}: t > 0]$.

(iii) if $r > 3$, then the soliton interaction mechanism is essentially the same as in case (ii) but now the solitons merge into a single unimodal hump in the dominant interaction region, before they separate again. This scenario is usually associated with the "overtaking interaction". The minimum of the resulting single pulse amplitude achieved at the moment of the strongest interaction is $u_m = A_1 - A_2$.

In all three above-mentioned scenarios, the resulting double wave in the dominant interaction region is wider than each of the interacting solitons and has a smaller amplitude than that of the taller soliton before the interaction. One can derive an ordinary differential equation describing the exact dynamics of the local maxima of the two-soliton solution (see [22]). However, for our purposes it is sufficient to present a simple plot of the value of the double wave minimal amplitude u_m defined above, versus the amplitude ratio $r^{-1} = A_2/A_1$ of the individual interacting solitons. The plot of $u_m(A_2/A_1)$ obtained from direct numerical simulations of the collisions of different pairs of the KdV solitons is presented in Fig. 1. It was assumed in the simulations that the initial amplitude of the taller soliton $A_1 = 1$.

As one can see, the absolute minimum of the function u_m is achieved at $A_2/A_1 = 1/2.62 \approx 0.38$, which is the upper boundary of the transition interval $0.33 < A_2/A_1 < 0.38$ between the exchange and overtaking soliton interaction scenarios (see previous section). This property of the two-soliton KdV solutions could have important implications for the analysis of the random soliton wave field, in particular, for establishing the relation between the distribution of the values of local extrema in the soliton turbulence and its spectral (IST) composition (we recall that the initial soliton amplitudes $A_{1,2}$ are directly related to the IST spectrum — see (2)).

3. Effect of soliton interactions on the integral characteristics of the wave field

Most of the features of the two-soliton interaction described in the previous section are known very well. However, the effect of the soliton interaction on the integral characteristics of the wave field to the best of our knowledge had not been considered before.

It is this effect that is of our primary concern in this Letter since it will have direct implications for the theory of the KdV soliton turbulence.

As is known, the KdV equation has an infinite number of conserved quantities (Kruskal integrals) (see e.g. [1–3]); below we present the first four of them:

$$I_1 = \int_{-\infty}^{\infty} u(x,t)\,dx, \tag{4}$$

$$I_2 = \int_{-\infty}^{\infty} u^2(x,t)\,dx, \tag{5}$$

$$I_3 = \int_{-\infty}^{\infty} \left[u^3 - \frac{1}{2}u_x^2\right] dx, \tag{6}$$

$$I_4 = \int_{-\infty}^{\infty} \left[u^4 - 2uu_x^2 + \frac{1}{5}(u_{xx})^2\right] dx. \tag{7}$$

The first three integrals (4)–(6) are usually associated with the "mass", "momentum" and "energy" conservation although they do not necessarily have physical meaning of the corresponding physical entities. All Kruskal integrals are conserved under the KdV evolution (assuming vanishing at infinity or periodic boundary conditions for the wave field) so it is clear from the very beginning that these quantities are not affected by the soliton interaction. Nevertheless, it is interesting to know their dependence on the soliton amplitudes since the higher integrals (starting from the 3rd) are not necessarily positive definite. Formally, one would need to use full two-soliton solution (2) in (4)–(7) but the calculation can be dramatically simplified in view of the conservation of I_1, I_2, I_3, I_4, so that one can use asymptotic expression (3) instead of the full solution (2) and all the integrals can be evaluated for each soliton separately. As a result, after somewhat lengthy calculation, we obtain:

$$I_1 = 4(\eta_1 + \eta_2) = 2\sqrt{2}\left(A_1^{1/2} + A_2^{1/2}\right), \tag{8}$$

$$I_2 = \frac{16}{3}\left(\eta_1^3 + \eta_2^3\right) = \frac{4\sqrt{2}}{3}\left(A_1^{3/2} + A_2^{3/2}\right), \tag{9}$$

$$I_3 = \frac{32}{5}\left(\eta_1^5 + \eta_2^5\right) = \frac{4\sqrt{2}}{5}\left(A_1^{5/2} + A_2^{5/2}\right), \tag{10}$$

$$I_4 = \frac{256}{35}\left(\eta_1^7 + \eta_2^7\right) = \frac{16\sqrt{2}}{35}\left(A_1^{7/2} + A_2^{7/2}\right). \tag{11}$$

Remarkably, all the integrals I_1, I_2, I_3, I_4 turn out to be positive definite so, taking into account the long-time asymptotic representation of the N-soliton solution as the sum of individual solitons, analogous to (3), one can conclude that their values increase as the number of solitons increases. As one could expect, the "higher" integrals have stronger dependence on the amplitude than the "lower" ones.

In turbulence theory one is usually interested in the standard moments of the form

$$M_n(t) = \int_{-\infty}^{\infty} u^n(x,t)\,dx, \quad n = 1, 2, 3, \ldots. \tag{12}$$

Obviously, for the two-soliton solution the first two moments (12) M_1 and M_2 coincide with the respective Kruskal integrals I_1 and I_2 and, therefore, are conserved. In turbulence theory M_1 and M_2 define the mean value and variance of the random wave field respectively, and their constancy means that nonlinear interactions do not affect these two important parameters (we note that in many problems nonlinearity leads to variations of the mean, e.g. in the so-called wave setup phenomenon in fluid dynamics).

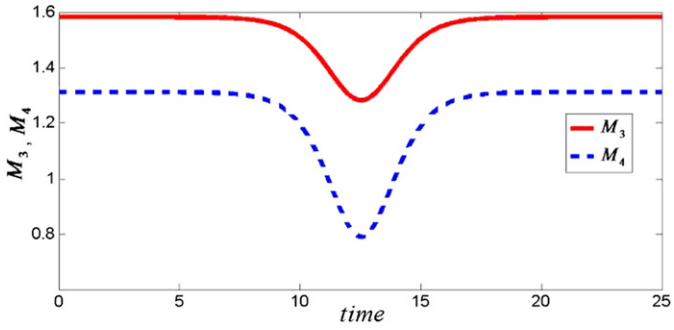

Fig. 2. The time dependence of the moments M_3, M_4 in the two-soliton interaction with $A_1 = 1$, $A_2 = 0.3$.

The next two moments, $M_3(t)$ and $M_4(t)$, are related to the skewness and kurtosis of the probability distribution of the turbulent field. They do not coincide with the Kruskal integrals I_3 and I_4 so one should not expect that they will be conserved in soliton turbulence. Numerical evaluation of M_3 and M_4 for the two-soliton solution (2) with $A_1 = 1$ and $A_2 = 0.3$ shows that these moments decrease in the dominant interaction region (see Fig. 2). Outside the interaction region M_3 and M_4 assume the values corresponding to the superposition of non-interacting solitons (3):

$$M_3^0 = \frac{8\cdot 16}{15}\left(\eta_1^5 + \eta_2^5\right) = \frac{16\sqrt{2}}{15}\left(A_1^{5/2} + A_2^{5/2}\right), \tag{13}$$

$$M_4^0 = \frac{16\cdot 32}{35}\left(\eta_1^7 + \eta_2^7\right) = \frac{32\sqrt{2}}{35}\left(A_1^{7/2} + A_2^{7/2}\right). \tag{14}$$

One can see that the variations of the 3rd and 4th moments are quite significant (up to 30%) which implies that soliton interactions can strongly affect the higher moments of the wave field, while the 1st and the 2nd moments remain unaffected. Physically, the decrease of the 3rd and 4th moments due to soliton interactions can be explained by the above-mentioned decrease of the resulting pulse amplitude during the interaction. Also, as one can see from the conservation of the third Kruskal integral (6), the decrease of the 3rd moment $\int u^3\,dx$ results in the decrease of the integral $\int (u_x)^2\,dx$ which implies smoothing of the monotone slopes of the pulse during the interaction. Our simulations of two-soliton collisions characterized by different values of the definitive interaction parameter $r = A_1/A_2$ show the same qualitative behavior of the higher moments in the dominant interaction region, while the amplitude of their variations depends on the value of r. In Fig. 3 we present the numerical results for the amplitudes of the relative variations, $\Delta M_i/M_i^0$, where $\Delta M_i = M_i^0 - M_i^{(min)}$, $i = 3, 4$, versus $r^{-1} = A_2/A_1$. Again, in our numerical simulations we have assumed that the amplitude of the greater soliton $A_1 = 1$. Both curves are nonmonotone and have their extremum (maximum) at the same value of the amplitude ratio $A_2/A_1 \approx 0.32$ which is close to the lower boundary of the transition region $0.33 < A_2/A_1 < 0.38$ separating the exchange and overtaking scenarios of the two-soliton interaction. Thus the two-soliton interactions with the amplitude ratio in the transition interval are expected to have greater impact on the higher moments in soliton turbulence.

To the best of our knowledge, the described effect of soliton interactions on the higher moments of multisoliton solutions has never been reported in the literature. Taking into account the key role of the higher moments in the characterization of the skewness and kurtosis of the turbulent field, an immediate implication of this effect in the context of soliton turbulence is that the pairwise interactions of solitons must decrease the skewness and kurtosis

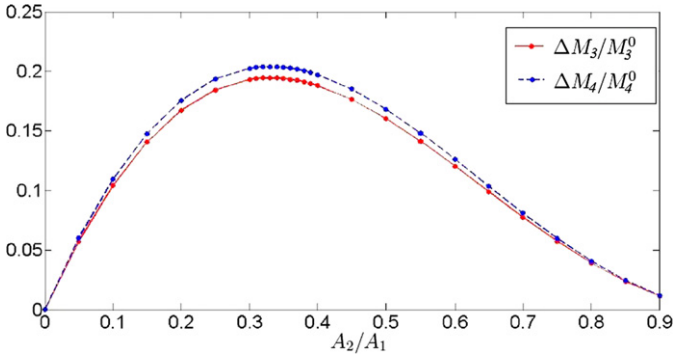

Fig. 3. Dependence of the relative variations $\Delta M_i/M_i^0$ of the 3rd and 4th moments of the two-soliton solution on the soliton amplitude ratio A_2/A_1.

(compared to their values for the gas of noninteracting solitons). It is clear the quantitative contribution of this effect will depend on the density of the soliton gas (frequency of soliton collisions) and on its spectral (IST) composition (the ratios A_1/A_2 involved), i.e. on the spectral distribution function of the soliton gas [14]. Thus, for *inhomogeneous* soliton turbulence, when the density of solitons depends on the spatial coordinate, the analysis of the higher statistical moments behavior will be coupled with the kinetic description of the associated soliton gas.

In conclusion of this section we note that in classical and wave turbulence theories, along with spatial moments, one is also interested in the Fourier transform of the velocity field, its power spectrum, etc. A similar description can be introduced for soliton turbulence as well and would require the knowledge of the Fourier spectrum evolution in the multisoliton solutions of integrable systems. The latter is also directly related to spectral algorithms of the numerical simulations of emergence, propagation and interaction of solitons in nonlinear dispersive media (see e.g. [24]).

4. Conclusions

We have shown that the two-soliton interaction in the framework of the KdV equation leads to the decrease of the 3rd and 4th moments $M_{3,4}$ of the nonlinear wave field while the 1st and the 2nd moments remain unchanged due to the conservation of the mass and momentum. The magnitudes of the relative variations of M_3, M_4 turn out to be nonmonotone functions of the soliton amplitude ratio A_2/A_1 each having a single maximum located at the point $A_2/A_1 \approx 0.32$, close the boundary of the transition region between the exchange and overtaking scenarios of two-soliton interactions. The qualitative implication of this dynamical effect for the soliton turbulence theory will be a decrease of the skewness and kurtosis of the turbulent wave field in the regions of higher density of solitons. The quantitative analysis of the effect of soliton interactions on the structure of soliton turbulence will be made in our future publications.

Acknowledgements

This work was supported by grants from the Volkswagen Foundation (E.N.P. and A.V.S.), Federal Target Programme “Research and scientific–pedagogical cadres of Innovative Russia” for 2009–2013 (E.N.P., E.G.S., A.V.S., T.G.T.), MK-4378.2011.5 (A.V.S.), RFBR 12-05-00472 and 12-05-33070 (T.G.T.), 11-05-00216 (E.N.P. and E.G.S.), 12-05-33087 (E.G.S. and A.V.S.), 01-02-00483 (A.V.S.), Dynastiya and MK-1440.2012.5 (E.G.S.), the Royal Society of London (E.N.P. and R.H.J.G.).

References

[1] S.P. Novikov, S.V. Manakov, L.P. Pitaevskii, V.E. Zakharov, The Theory of Solitons: The Inverse Scattering Method, Consultants, New York, 1984.
[2] A.C. Newell, Solitons in Mathematics and Physics, SIAM, Philadelphia, 1985.
[3] P.G. Drazin, R.S. Johnson, Solitons: An Introduction, Cambridge University Press, 1993.
[4] A.R. Osborne, Phys. Rev. Lett. 71 (1993) 3115.
[5] A.R. Osborne, Phys. Rev. E 52 (1995) 1105.
[6] A.R. Osborne, E. Segre, G. Boffetta, Phys. Rev. Lett. 67 (1991) 592.
[7] A.R. Osborne, M. Serio, L. Bergamasco, L. Cavaleri, Physica D 123 (1998) 64.
[8] M. Brocchini, R. Gentile, Cont. Shelf Res. 21 (2001) 1533.
[9] E. Pelinovsky, A. Sergeeva (Kokorina), Eur. J. Mech. 25 (2006) 425.
[10] V.E. Zakharov, Stud. Appl. Math. 122 (2009) 219.
[11] V.E. Zakharov, Sov. Phys. JETP 33 (1971) 538.
[12] G.A. El, Phys. Lett. A 311 (2003) 374.
[13] G.A. El, A.M. Kamchatnov, M.V. Pavlov, S.A. Zykov, J. Nonl. Sci. 21 (2011) 151.
[14] G.A. El, A.M. Kamchatnov, Phys. Rev. Lett. 95 (2005) 204101.
[15] G.A. El, A.L. Krylov, S.A. Molchanov, S. Venakides, Physica D Adv. Nonl. Math. Sci. 152–153 (2001) 653.
[16] A.S. Monin, A.M. Yaglom, Statistical Fluid Mechanics, vol. I, Dover Publications, 2007, 784 pp.
[17] S. Nazarenko, Wave Turbulence, Springer, 2011, 279 pp.
[18] Ch. Kharif, E. Pelinovsky, A. Slunyaev, Rogue Waves in the Ocean, Springer, 2009, 216 pp.
[19] N.J. Zabusky, M.D. Kruskal, Phys. Rev. Lett. 15 (1965) 240.
[20] C.S. Gardner, J.M. Greene, M.D. Kruskal, R.M. Miura, Phys. Rev. Lett. 19 (1967) 1095.
[21] N. Benes, A. Kasman, K. Young, J. Nonl. Sci. 16 (2006) 179.
[22] P.D. Lax, Comm. Pure Appl. Math. 21 (1968) 467.
[23] A.V. Slyunyaev, E.N. Pelinovsky, J. Exp. Theor. Phys. 89 (1999) 173.
[24] A. Salupere, in: E. Quak, T. Soomere (Eds.), Applied Wave Mathematics, Springer, 2009, pp. 301–333.

A.6 Publication dans le journal “Fundamental and Applied Hydrophysics”

Pelinovsky E., Shurgalina E.

Interaction of solitary internal waves of finite amplitude

Abstract:

The study of interaction of unidirectional one-mode solitary internal waves in a stratified ocean is done. The exact two-soliton solution of the Korteweg-de Vries equation, which is valid for internal waves of small amplitude, is used for the analysis. The role of this process in the dynamics of soliton turbulence which is important for understanding the oceanic turbulence in the range of long waves is discussed. It is shown that in the moment of interaction the third and fourth moments of the wave field, which play an important role in the theory of turbulence (skewness and kurtosis) decrease. The value of the relative changes of these moments is maximal for the amplitude ratio of solitons in the intermediate zone, where the exchange regime of soliton interaction changes to the overtake regime. The obtained results are compared with the linear dynamics of soliton-like pulses, for which the third and fourth moments grow in a collision.

Keywords: internal waves, the Korteweg–de Vries equation, soliton, turbulence

A.7 Publication dans le journal “Radiophysics and Quantum Electronics”

Two-soliton interaction in the frameworks of Modified Korteweg – de Vries equation

E.N. Pelinovsky, E.G. Shurgalina

Institute of Applied Physics RAS, 46 Uljanova street, Nizhni Novgorod 603950, Russia

Abstract

Interaction of two solitons of the same and different polarity in the framework of modified Korteweg-de Vries (mKdV) equation is studied. Three types of soliton interaction are considered: exchange and overtaking for positive solitons, and absorb-emit for solitons of different polarity. The intermediate case, which separates the different regimes of soliton interactions, is studied in details. Since the interaction of solitons is an elementary act of soliton turbulence, the moments of the wave field up to fourth are studied, which are usually considered in the turbulence theory. It is shown that in the case of interaction of solitons of the same polarity the third and fourth moments of the wave field, which determine the coefficients of skewness and kurtosis in the theory of turbulence, are reduced, while in the case of interaction of solitons of different polarity these moments are increased. The results are compared with the estimations for the two-soliton interaction in the framework of the Korteweg - de Vries (KdV) equation.

References

Abrashkin A. A., Oshmarina O. E. Pressure induced breather overturning on deep water: Exact solution. Physics Letters A, 2014, 378, 2866-2871.

Abrashkin A. A., Soloviev A. G. Vortical freak waves in water under external pressure action. Physical Review Letters, 2013, 110, 014501.

Abrashkin A.A., Solov'ev A.G. Gravitational waves in case of inhomogeneous pressure on the free surface: exact solutions. Izvestia RAS, Fluid and Gas Mechanics, 2013, 5, 125-133.

Akhmediev N., Pelinovsky E. Editorial – Introductory remarks on "Discussion & Debate: Rogue Waves – Towards a unifying concept?" European Physical Journal Special Topics, 2010, 185, 1 – 4.

Anco S.C., Ngatat N.T., Willoughby M**.** Interaction properties of complex mKdV solitons**,** Physica D, 2011, 240, 1378–1394.

Annenkov SY and Shrira V.I. Evaluation of Skewness and Kurtosis of Wind Waves Parameterized by JONSWAP Spectra. Journal of physical Oceanography, 2014, 44(6), 1582-1594.

Annekov, SY and Shrira VI. Large-time evolution of statistical moments of wind–wave fields. J Fluid Mechanics, 2013, 726, 517-546.

Apel J.R. A New Analytical Model for Internal Solitons in the Ocean. J. Phys. Oceanogr., 2003, 33, 2247–2269.

Apel J., Ostrovsky L.A., Stepanyants Y.A., Lynch J.F. Internal solitons in the ocean and their effect on underwater sound. J. Acoust. Soc. Am., 2007, 121, 695–722.

Badulin S., Babanin A., Zakharov V., Resio D. Weakly turbulent laws of wind-wave growth, J. Fluid Mech., 2007, 591, 339–378.

Badulin S. I., Pushkarev A. N., Resio D., Zakharov V. E. Selfsimilarity of wind-driven seas. Nonl. Proc. Geophys., 2005, 12, 891 - 946.

Badulin S., Ivanov A., Ostrovsky A. The influence of giant waves on the safety of offshore production and transportation of hydrocarbons. Technology of fuel-energy complex, 2005, 1 (20), 56-62.

Benes N., Kasman A., Young K. On decomposition of the KDV 2-soliton, Journal of Nonlinear Science, 2006, 2, 179-200.

Benney D.J. Long nonlinear waves in fluid flows. J. Math. Phys., 1966, 45, 52 - 63.

Bonneton P., Van de Loock J., Parisot J-P., Bonneton N., Sottolichio A., Detandt G., Castelle B., Marieu V., Pochon N. On the occurrence of tidal bores – The Garonne River case, Journal Coastal Research, 2011, 64, 1462–1466.

Brocchini M., Gentile R. Modelling the run-up of significant wave groups, Continental Shelf Research, 2001, 21, 1533–1550.

Brown M.G., Jensen A. Experiments on focusing unidirectional water waves. J. Geophys. Research, 2001, 106 (C8), 16917 – 16928.

Cai D., Majda A.J., McLaughlin D.W., and Tabak E.G. Dispersive wave turbulence in one dimension, Physica D, 2001, 152-153, 551-572.

Chanson H. An Experimental Study of Tidal Bore Propagation: the Impact of Bridge Piers and Channel Constriction, Hydraulic Model Report No. CH74/08, University of Queensland, Australia, 2009, 109 p.

Chanson H. Tidal Bores, Aegir, Eagre, Mascaret, Pororoca: Theory and Observations. World Scientific, 2012, 201p

Clarke S., Grimshaw R., Miller P., Pelinovsky E., Talipova T. On the generation of solitons and breathers in the modified Korteweg–de Vries equation, Chaos, 2000, 10, 383-392.

Clauss G. Dramas of the sea: episodic waves and their impact on offshore structures. Applied Ocean Research, 2002, 24, 147 – 161.

Clauss G., Bergmann J. Gaussian wave packets: a new approach to seakeeping tests of ocean structures. Applied Ocean Research, 1986, 8, 190-206.

Cun-Hong P., Hai-Yan L. 2d numerical simulation of tidal bore on Qiantang river using KFVS scheme. Coastal Engineering Proceedings, 2010, 32. doi:10.9753/icce.v32.currents.29

Dao, M. H., Tkalich P. Tsunami propagation modelling – a sensitivity study. Nat. Hazards Earth Syst. Sci., 2007, 7, 741–754.

Dean, R.G., Walton, T.L., Wave setup. In: Kim, Y.C. (Ed.), Handbook of Coastal and Ocean Engineering. World Sci, Singapore, 2009.

Didenkulova I., Pelinovsky E. Rogue waves in nonlinear hyperbolic systems (shallow-water framework). Nonlinearity, 2011, 24, R1-R18.

Didenkulova I.I., Slunyaev A.V., Pelinovsky E.N., Kharif Ch. Freak Waves in 2005. Natural Hazards and Earth System Sciences, 2006, 6, 1007 – 1015.

Dimakis A., Muller-Hoissen F. KdV soliton interactions: a tropical view. Journal of Physics: Conference Series, 2014, 482, 012010.

Divinsky B.V., Levin B.V., Lopatuhin L.I., Pelinovsky E.N., Slunyaev A.V. Anomalously high wave in the Black Sea: observations and modeling. DAN, 2004, 395, 690-695.

Docherty N.J., Chanson H. Characterisation of Unsteady Turbulence in Breaking Tidal Bores including the Effects of Bed Roughness. Hydraulic Model Report No. CH76/10. University of Queensland. Australia, 2010, 112 p.

Dobrohotov S.U., Tolstova O.L., Chudinovich I.U. Waves in a fluid over an elastic bottom. The existence theorem and exact solutions, Math. Notes, 1993, 54, 33–55.

Dotsenko S.F., Ivanov V.A. Freak waves. Modern problems in oceanology. Marine Hydrophysical Institute of National Academy of Sciences of Ukraine, 1, Sevastopol, 2006, 44 pp.

Driscoll F., O'Neil T.M. Modulational instability of cnoidal wave solutions of the modified Korteweg-de Vries equation. Journal of Mathematical Physics, 1976, 17 (7), 1196-1200.

Dutykh D., Chhay M., Fedele F. Geometric Numerical Schemes for the KdV Equation. Computational Mathematics and Mathematical Physics, 2013, 53 (2), 221-236.

Dutykh D., Pelinovsky E. Numerical simulation of a solitonic gas in KdV and KdV-BBM equations. Physical letters A, 2014, 378 (42), 3102-3110.

Dutykh D., Tobisch E. Observation of the inverse energy cascade in the modified Korteweg-de Vries equation, European Physical Letters, 2014a, 107 (1), 14001.

Dutykh D., Tobisch E. Direct dynamical energy cascade in the modified KdV equation, 2014b, https://hal.archives-ouvertes.fr/hal-00990724v2. Version 2, 33 p.

Dyachenko A. I., Zakharov V. E. On the Formation of freak waves on the surface of deep water. JETP Lett., 2008, 88 (5), 307-311.

Dysthe K.B., Trulsen K., Krogstad H.E., Socquet-Juglard H. Evolution of a narrow-band spectrum of random surface gravity waves. J.Fluid Mech., 2003, 478, 1-10.

Dysthe K., Krogstad H.E., Muller P. Oceanic rogue waves. Annual Review of Fluid Mechanics, 2008, 40, 287 – 310.

Efimov V.V., Polnikov V.G. Numerical simulation of wind waves. Kiev: Naukova Dumka, 1991, 239 pp.

El G.A., Kamchatnov A.M., Pavlov M.V., Zykov S.A. Kinetic equation for a soliton gas and its hydrodynamic reductions, J Nonlinear Sci, 2011, 21, 151–191.

El G., Krylov A.L., Molchanov S.A., Venakides S. Soliton turbulence as a thermodynamic limit of stochastic soliton lattices, Physica D, 2001, 152–153, 653–664.

Faulkner D. Rogue waves – defining their characteristics for marine design. Rogue Waves 2000 (Brest, France, 2000). Eds.: M. Olagnon, G.A. Athanassoulis. Ifremer. 2001, 3–18.

Favre H. Etude Théorique et Expérimentale des Ondes de Translation dans les Canaux Découverts (Theoretical and Experimental Study of Travelling Surges in Open Channels). Paris, France: Dunod Edition, 1935, 215 p.

Flatcher K. Numerical methods based on the Galerkin method, M.: Mir,1988, 353pp.

Fronberg B. A Practical Guide to Pseudospectral Methods, Cambridge Univ. Press, 1998.

Furgerot L., Mouaze D., Tessier B., Perez L., Haquin S. Suspended Sediment Concentration in Relation to the Passage of a Tidal Bore (Sée River Estuary, Mont Saint Michel, NW France). Proc. Coastal Dynamics. Arcachon, France, 24-28 June, 2013, 671-682.

Gardner C.S., Greene J.M., Kruskal M.D., Miura R.M. Method for solving the Korteweg-de Vries equation, Phys. Rev. Lett., 1967, 19, 1095-1097.

Grimshaw R., Pelinovsky D., Pelinovsky E., Talipova T. Wave group dynamics in weakly nonlinear long-wave models, Physica D, 2001, vol. 159, 35-57.

Grimshaw R., Pelinovsky E., Poloukhina O. Higher-order Korteweg-de Vries models for internal solitary waves in a stratified shear flow with a free surface. Nonlinear Processes in Geophysics, 2002, 9, 221-235.

Grimshaw R., Pelinovsky E., Talipova T. The modified Korteweg – de Vries equation in the theory of large –amplitude internal waves. Nonlin. Processes Geophys, 1997, 4, 237–250.

Grimshaw R., Pelinovsky E., Talipova T., Sergeeva A. Rogue internal waves in the ocean: long wave model. European Physical Journal Special Topics, 2010, 185, 195 - 208.

Grimshaw R., Pelinovsky E., Talipova T., Ruderman M. Erdelyi R. Short-lived large-amplitude pulses in the nonlinear long-wave model described by the modified Korteweg–de Vries equation. Studied Applied Mathematics, 2005, 114 (2), 189.

Grimshaw, R., Pelinovsky, E., Talipova, T. Modeling internal solitary waves in the coastal ocean. Survey in Geophysics, 2007, 28 (4), 273-298.

Gromov E.M., Tutin V.V. Drop waves in the extended nonlinear Schrödinger equation with allowance of induced scattering and nonlinear dispersion Radiophysics and Quantum Electronics, 2014, 57 (4), 311-318.

Grue, J., Pelinovsky, E. Fructus, D. Talipova, T., Kharif C, Formation of undular bores and solitary waves in the Strait of Malacca caused by the 26 December 2004 Indian Ocean tsunami, J. Geophys. Res., 2008, 113, C05008.

Gurevich A.V., Mazur T.G., Zybin N.G. Statistical limit in completely integrable system with deterministic initial conditions. JETP, 2000, 90, 797–817.

Haver S, Andersen O.J. Freak waves – rare realizations of a typical extreme wave population or typical realizations of a rare extreme wave population? Proc. 10th ISOPE Conference, Seattle, 2000, 123-130.

Johannessen T.B., Swan C. A laboratory study of the focusing of transient and directionally spread surface water waves. Proc. Royal Soc. London, 2001, A457, 971 – 1006.

Karpman V.I. Nonlinear waves in dispersive media. M.: Nauka, 1973, 175 pp.

Kharif C., Pelinovsky, E. Physical mechanisms of the rogue wave phenomenon. European J Mechanics / B – Fluid, 2003, 22, 603-634.

Kharif C., Pelinovsky E., Slunyaev A. Rogue Waves in the Ocean. Springer, 2009. 216 p.

Kharif C., Pelinovsky E., Talipova T., Slunyaev A. Focusing of nonlinear wave group in deep water. Письма в ЖЭТФ, 2001, 73 (4), 190-195.

Kharif, C., Giovanangeli, J-P., Touboul, J., Grare, L., and Pelinovsky, E.N. Influence of wind on extreme wave events: Experimental and numerical approaches. J Fluid Mech., 2008, 594, 209-247.

Kjerfve B., Ferreira H.O. Tidal bores: First ever measurements. Journal of the Brazilian Association for the Advancement of Science, 1993, 45 (2), 135-137.

Konyaev K.V., Sabinin K.D. Waves inside the ocean. St. Petersburg, Russia: Gidrometeoizdat, 1992, 271 pp.

Komen G.J., Cavaleri L., Donelan M et al, Dynamics and modeling of ocean waves. Cambridge University Press, 1994.

Korteweg D.J., de Vries G. On the change of form of long waves advancing in a rectangular canal, and on a new type of long stationary waves. Phil. Mag., 1895, 39, 422 — 443.

Kudryashov N.A. Methods of Nonlinear Mathematical Physics. M: MIFI, 2008, 362 pp.

Kurkin A.A., Pelinovsky E.N. Freak waves: facts, theory and modelling. Nizhny Novgorod, NNSU, 2004, 157 pp.

Kurkina O.E., Kurkin A.A., Soomere, T. Pelinovsky E.N., Ruvinskaya E.A. Higher-order (2+4) Korteweg-de Vries - like equation for interfacial waves in a symmetric three-layer fluid. Physics Fluids, 2011, 23, 116602.

Lamb D. Soliton theory. M.Nauka, 1983, 294 pp.

Lavrenov I.V. Mathematical modeling of wind waves in spatially inhomogeneous ocean. St. Petersburg: Gidrometeoizdat, 1998, 500 pp.

Lax P.D. Integrals of nonlinear equations of evolution and solitary waves. Communications on Pure and Applied Mathematics, 1968, 21, 467-490. Lavrenov I.V. Meeting with a freak wave. Morskoi flot, 1985, 12, 28-30.

Liu P.C. A chronology of freaque wave encounters. Geofizika, 2007, 24, 57–70.

Liu P.C. Brief Communication: Freaque wave occurrences in 2013. Nat. Hazards Earth Syst. Sci. Discuss., 2014, 2, 7017–7025.

Lopatuhin L.I., Buhanovsky A.V., Divinsky B.V., Rozhkov V.A. About unusual waves in the oceans and seas. Scientific and technical collection of Russian Maritime Register of Shipping, 2003, 26, 65-73.

Magnusson A.K., Donelan M.A., Drennan W.M. On estimating extremes in an evolving wave field. Coastal Engineering, 1999, 36, 147 – 163.

Majda A.J., McLaughlin D.W., Tabak E.G. A one-dimensional model for dispersive wave turbulence, J. Nonlinear Science, 1997, 6, 9-44.

Massel, S.R., Ocean Surface Waves: Their Physics and Prediction. World Scientific Publ, Singapore, 1996, 492 pp.

Miropolsky U.Z. The dynamics of internal gravity waves in the ocean. Leningrad, Gidrometeoizdat, 1981, 302 pp.

Miura R. M. Korteweg-de Vries Equation and Generalizations. I. A Remarkable Explicit Nonlinear Transformation. J. Math. Phys., 1968, 9, 1202-1204.

Monin A.S., Yaglom A.M. Statistical Hydromechanics., M.: Nauka. Fizmatgiz, 1,2, 1965, 1967, 784 pp.

Mori N., Liu P.C., Yasuda T. Analysis of freak wave measurements in the Sea of Japan. Ocean Engineering, 2002, 29, 1399–1414.

Morozov E.G. Ocean internal waves / ed. Kort V.G. Moscow, USSR: Nauka, 1985, 151 pp.

Mouaze D., Chanson H., Simon B. Field measurements in the tidal bore of the sélune river in the bay of Mont Saint Michel (September 2010). Report CH81/10, University of Queensland, Australia, 2010, 72 p.

Murray A.C. Solutions of the Korteweg – de Vries equation from irregular data, Duke Mathematical Journal, 1978, 45, 149-181.

Nakamura S.O. On hydraulic bore and applying of the results of its study to the problem of emergence and tsunami propagation. Tsunami waves, Trudy SahkNII, Yuzhno-Sakhalinsk. 1973, 32, 129–151.

Nazarenko S. Wave Turbulence, Springer, 2011, 279 pp.

Newell A., Solitons in mathematics and physics. M.:Mir, 1989, 323 pp.

Nikolkina I., Didenkulova I. Catalogue of rogue waves reported in media in 2006-2010. Nat. Hazards, 2012, 61, 989-1006.

Nikolkina I. Didenkulova I. Rogue waves in 2006–2010. Nat. Hazards Earth Syst. Sci., 2011, 11, 2913-2924.

Onorato M., Ambrosi D., Osborne A.R., Serio M. Instability of two quasi-monochromatic waves in shallow water, Phys. Fluids, 2003, 15, 3871-3874.

Onorato M., Osborne A.R., Serio M., Cavaleri L. Modulational instability and non-Gaussian statistics in experimental random water-wave trains, Phys.Fluids, 2005, 17, 078101-1-078101-4.

Onorato M., Osborne A.R., Serio M., Bertone S. Freak wave in random oceanic sea states. Phys. Review Letters, 2001, 86, 5831-5834.

Onorato M., Osborne A.R., Serio M. Extreme wave events in directional, random oceanic sea states, Phys. Fluids, 2002, 14, L25-L28.

Osborne A.R. Behavior of solitons in random-function solutions of the periodic Korteweg – de Vries equation. Phys. Rev. Lett., 1993, 71, 3115-3118.

Osborne A.R. Solitons in the periodic Korteweg – de Vries equation, the Θ-function representation, and the analysis of nonlinear, stochastic wave trains, Phys. Review E, 1995, 52, 1105-1122.

Osborne A.R. Nonlinear Ocean Waves and the Inverse Scattering Transform. Academic Press, 2010.

Osborne A.R., Segre E., Boffetta G. Soliton basis states in shallow-water ocean surface waves. Phys. Rev. Lett., 1991, 67, 592-595.

Osborne A.R., Serio M., Bergamasco L. Cavaleri L. Solitons, cnoidal waves and nonlinear interactions in shallow-water ocean surface waves. Physica D, 1998, 123, 64-81.

Ostrovsky L., Stepanyants Yu. Do internal solitons exist in the ocean? Rev. Geophys., 1989, 27, 293-310.

Ostrovsky L.A., Stepanyants Y.A. Internal solitons in laboratory experiments: Comparison with theoretical models. Chaos, 2005, 15, 037111.

Pelinovsky E.N. Nonlinear dispersive wave theory tsunami: looking after the tsunami disaster in the Indian Ocean. Nonlinear waves 2006, Nizhny Novgorod: IAP RAS, 2007, 393-407.

Pelinovsky E.N., Kharif Ch. Dispersion compression of wave packets as the mechanism of abnormally high wave occurrence of on the ocean surface. Izvestia Akademii of Engineering Sciences, 2000, 1, 50 - 61.

Pelinovsky E., Kharif C., Talipova T. Large-amplitude long wave interaction with a vertical wall. European J. Mechanics – B/Fluids, 2008, 27, 409-418.

Pelinovsky E.N., Polukhina O.E., Lamb K. Nonlinear internal waves in the ocean, stratified by density and flow. Oceanology, 2000, 40, 805 - 815.

Pelinovsky E.N., Rodin A.A. Transformation of strongly nonlinear waves on shallow water. Izvestiya, Atmospheric and Oceanic Physics, 2012, 48 (3), 343-349.

Pelinovsky E., Sergeeva (Kokorina) A. Numerical modeling of the KdV random wave field. Europ. J. Mechanics, 2006, 25, 425-434.

Pelinovsky E.N., Shurgalina E.G. Abnormal wave amplification near a vertical barrier. Fundamental and Applied Hydrophysics, 2010, 4 (10), 29-38.

Pelinovsky E.N., Shurgalina E.G., Interaction of internal solitary waves of small amplitude, Fundamental and Applied Hydrophysics, 2013, 2 (6), 78-86.

Pelinovsky E.N., Shurgalina E.G., Sergeeva A.V., Talipova T.G., El G.A., Grimshaw R.H.J. Two-soliton interaction as an elementary act of soliton turbulence in integrable systems, Physics Letters A, 2013, 377 (3-4), 272–275.

Pelinovsky E., Shurgalina E., Chaikovskaya N. The scenario of a single freak wave appearance in deep water – dispersive focusing mechanism framework. Nat. Hazards Earth Syst. Sci., 2011, 11, 127–134.

Pelinovsky E.N., Slunyaev E.N., Talipova T.G., Kharif Ch. Nonlinear parabolic equation and extreme waves on a sea surface. Radiophysics and Quantum Electronics, 2003, 46, 499-512.

Pelinovsky E.N., Sokolov V.V. Nonlinear theory of propagation of electromagnetic waves in size and quantum membranes. Radiophysics and Quantum Electronics, 1976, 19, 536 -542.

Pelinovsky E., Talipova T., Kharif C. Nonlinear dispersive mechanism of the freak wave formation in shallow water. Physica D, 2000, 147 (1-2), 83-94.

Perelman T.L., Fridman A.H., Elyashevich M.M. Modified Korteweg – de Vries equation in electrodynamics. JETP, 1974, 66, 316.

Reungoat D., Chanson H., Caplain B. Sediment Processes and Flow Reversal in the Undular Tidal Bore of the Garonne River (France). Environmental Fluid Mechanics, 2014, 14 (3), 591-616.

Rogovin M.S., Karpova E.V. The content, dynamics and level organization of concepts in psychological analysis of subjective time. Questions of psychology, 1985, 3, 98-107.

Ruderman M.S., Talipova T., Pelinovsky E. Dynamics of modulationally unstable ion-acoustic wavepackets in plasmas with negative ions. Journal of Plasma Physics, 2008, 74, 639-656.

Ryskin N.M., Trubetskov D.I. Nonlinear waves, M.: Nauka. Fizmatlit, 2000, 272 pp.

Salupere A. The pseudospectral method and discrete spectral analysis, in: E. Quak, T. Soomere (Eds.), Applied Wave Mathematics: Selected Topics in Solids, Fluids, and Mathematical Methods, Springer, Berlin, 2009, 301–333.

Salupere A., Peterson P., Engelbrecht J. Long-time behaviour of soliton ensembles. Part 1 – Emergence of ensembles, Chaos, Solitons and Fractals, 2002, 14, 1413-1424.

Salupere A., Peterson P., Engelbrecht J. Long-time behaviour of soliton ensembles. Part 2 – Periodical patterns of trajectorism, Chaos, Solitons and Fractals, 2003a, 15, 29-40.

Salupere A., Peterson P., Engelbrecht J. Long-time behavior of soliton ensembles, Mathematics and Computers in Simulation, 2003b, 62, 137-147.

Salupere A., Maugin G.A., Engelbrecht J., Kalda J. On the KdV soliton formation and discrete spectral analysis, Wave Motion, 1996, 123, 49-66.

Sergeeva, A., Pelinovsky, E., and Talipova T. Nonlinear random wave field in shallow water: variable Korteweg – de Vries framework. Natural Hazards and Earth System Science, 2011, 11 (1), 323-330.

Sergeeva A., Slunyaev A. Rogue waves, rogue events and extreme wave kinematics in spatio-temporal fields of simulated sea states. Nat. Hazards Earth Syst. Sci., 2013, 13, 1759-1771.

Shamin R.V. Water waves: modeling and statistical characteristics. Mathematical modeling and boundary value problems, 2009, 2, 214–215.

Shamin R.V., Gorlenko A.V., Smirnova A.I. Questions on stability of freak waves. Computational Technologies, 2013, 18, 96-105.

Shamin R.V., Zakharov V.E., Udin A.V. Energetic portrait of freak waves. LETP Letters, 2014, 99, 597 – 600.

Shamin R.V., Udin A.V. The processes of energy concentration in the formation of freak waves, Nonlinear dynamics, 2014, 10, 49-58.

Shamin R.V., Udin A.V. Modeling of spatial-temporal propagating of freak waves. Doklady Akademii Nauk. 2013, 448, 592-594.

Shemer L. and Dorfman B. Experimental and numerical study of spatial and temporal evolution of nonlinear wave groups. Non-lin. Processes Geophys., 2008, 15, 931–942.

Shemer L., Goulitski K., Kit E. Evolution of wide-spectrum unidirectional wave groups in a tank: an experimental and numerical study. European Journal of Mechanics B/Fluids, 2007, 26, 193-219.

Shemer, L. and Sergeeva, A. An experimental study of spatial evolution of statistical parameters in a unidirectional narrow-banded random wavefield, J. Geophys. Res., 2009, 114, C01015.

Shemer L., Sergeeva A., Slunyaev A. Applicability of envelope model equations for simulation of narrow-spectrum unidirectional random field evolution: experimental validation. Phys. Fluids, 2010, 22, 016601-1–9.

Shurgalina E.G., Pelinovsky E.N. Dynamics of random ensembles of surface gravity waves with applications to freak waves in the ocean, Lampert–Academic Publishing, 2012, 119. ISBN 978-3-659-18883-1

Simon B., Lubin P., Reungoat D., Chanson H. Turbulence measurements in the Garonne River tidal bore: First observations, Proc. 34th IAHR World Congress, Engineers Australia, 2011, 1141-1148.

Simpson J.H., Fisher N.R., Wiles P. Reynolds stress and TKE production in an estuary with a tidal bore. Estuarine, Coastal and Shelf Science, 2004, 60, 619-627.

Slunyaev A., Didenkulova I., Pelinovsky E. Rogue waters. Contemporary Physics, 2011, 52 (6), 571 – 590.

Slunyaev A., Pelinovsky E., Sergeeva A., Chabchoub A., Hoffmann N., Onorato M., Akhmediev N. Super rogue waves in simulations based on weakly nonlinear and fully nonlinear hydrodynamic equations. Physical Review E, 2013, 88 (1), 012909.

Slunyaev A.V. Dynamics of localized large-amplitude waves in weakly dispersive medium with quadratic and positive cubic nonlinearities., JETP, 2001, 19, 606-612.

Slunyaev A.V., Pelinovsky E.N. Dynamics of large amplitude solitons. JETP, 1999, 116, 318 – 335.

Slunyaev A.V., Sergeeva A.V. Stochastic simulation of unidirectional intense waves in deep water in the relation to the anomalous ocean waves. JETP Letters, 2011, 94, 850-858.

Slunyaev A.V., Sergeeva A.V. Numerical simulation and analysis of spatio-temporal fields of abnormal waves. Fundamental and Applied Hydrophysics, 2012, 5(1), 24-36.

Snodgrass F.E., Groves G.W., Hasselmann K.F., Miller G.R., Munk W.H., Powers W.H. Propagation of ocean swell across the Pacific. Phil. Trans. R. Soc. Lond., 1966, A 259, 431–497.

Stocker J.J. Water waves. M.: IL. 1959, 618 pp.

Talipova T.G. Mechanisms of internal freak waves, Fundamental and Applied Hydrophysics, 2011, 4(4), 58–70.

Talipova T.G., Pelinovsky E.N. Modelling of “Lavrenov wave” on the surface on shallow sea. Fundamental and Applied Hydrophysics. 2009, 2, 30-36.

Talipova T.G., Pelinovsky E.N., Hollovey P.A. Nonlinear transformation models of internal tides on the shelf. In the book: The surface layer of the ocean. Physical processes and remote sensing. Nizhny Novgorod: Institute of Applied Physics RAS. 1999, 1, 154 – 172.

Teles Da Silva A.F., Peregrine D.H. Nonsteady computations of undular and breaking bores. Proc. 22nd Int. Cong. Coastal Eng. ASCE Publ., Delft, Netherlands, 1990, 1, 1019–1032.

Trubkin I.P. Wind waves (relation and calculation of probability characteristics). M.: Scientific World, 2007. 264 pp.

Tsai Ch.-H., Su M.-Y., Huang Sh.-J. Observations and conditions for occurrence of dangerous coastal waves. Ocean Engineering, 2004, 31, 745–760.

Tsuji Y., Yanuma T., Murata I., Fujiwara C. Tsunami ascending in rivers as an undular bore. Natural Hazards, 1991, 4, 257-266.

Uizem J. Linear and nonlinear waves, M.: Mir, 1977, 624 pp.

Vlasenko V., Stashchuk N., Hutter K. Baroclinic Tides: Theoretical Modeling and Observational Evidence. Cambridge, UK: Cambridge University Press, 2005, 351.

Vorob'ev U.M., Dobrohotov S.U. Basis systems on the torus generated by finite integration of the Korteweg-de Vries equation. Math. Notes, 1990, 47, 47–61.

Zahibo, N., Pelinovsky, E., Talipova, T., Kozelkov, A., Kurkin, A. Analytical and numerical study of nonlinear effects at tsunami modelling. Applied Mathematics and Computation, 2006, 174 (2), 795-809.

Zakharov V.E. Turbulence in integrable systems, Stud. Appl. Math., 2009, 122, 219–234.

Zakharov V.E. The kinetic equation for solitons. JETP, 1971, 60, 993-1000.

Zakharov V.E., Guyenne P., Pushkarev A.N., Dias F. Wave turbulence in one-dimensional models, Physica D, 2001, 152-153, 573-619.

Zakharov V.E., L'vov V.S., Falkovich G. Kolmogorov Spectra of Turbulence, Springer-Verlag, 1992, 264 p.

Zakharov V.E., Manakov S.V., Novikov S.P., Pitaevsky L.P. The theory of solitons, M.:Nauka, 1980, 319 pp.

Zakharov V.E., Shamin R.V., Udin A.V. Energetic portrait of freak waves. JETP Letters, 2014, 99, 597 – 600.

Zhu X.-H. Observation and dynamics of the tidal bore in the Qiantang River, China. Int. Conference on Mechanic Automation and Control Engineering, 2011, 7496 - 7499.

List of Presentations and Publications

Monograph:

1) **E.G. Shurgalina,** E.N. Pelinovsky Dynamics of random ensembles of surface gravity waves with applications to freak waves in the ocean, 120 p. LAMBERT Academic Publishing, ISBN 978-3-659-18883-1, Russia.

Articles:

2) E.N. Pelinovsky, **E.G. Shurgalina.** Abnormal wave amplification near a vertical barrier. *Fundamental and Applied Hydrophysics*, 2010, No. 4 (10), 28-37. Partical access (first and last pages) http://www.nsgf.narod.ru/trudu_6/txt/10_nomer.pdf

3) E. Pelinovsky, **E. Shurgalina,** N. Chaikovskaya. The scenario of a single freak wave appearance in deep water: Dispersive focusing mechanism framework. *Natural Hazards and Earth System Sciences*, 2011, vol. 11, No. 1, 127-134 (impact-factor 1.792). Open access: http://www.nat-hazards-earth-syst-sci.net/11/127/2011/nhess-11-127-2011.pdf

4) **E.G. Shurgalina,** E.N. Pelinovsky Manifestation of abnormal swell on weak wind waves *Fundamental and Applied Hydrophysics*. 2012, Vol 5, № 1, 77–88. Open access: http://nsgf.narod.ru/trudu_6/txt/15_nomer.pdf

5) E.N. Pelinovsky, **E.G. Shurgalina**, A.V. Sergeeva, T.G. Talipova, G.A. El and R.H.J. Grimshaw, **Two-soliton interaction as an elementary act of soliton turbulence in integrable systems, *Physics Letters A*, 2013,** Volume 377, Issues 3–4, 272–275, http://dx.doi.org/10.1016/j.physleta.2012.11.037

6) E.N. Pelinovsky, **E.G. Shurgalina**, Interaction of internal solitary waves of small amplitude, *Fundamental and Applied Hydrophysics*, 2013, 2 (6), 78-86

7) E.N. Pelinovsky, **E.G. Shurgalina**, Two-soliton interaction in the frameworks of modified Korteweg – de Vries equation, *Radiophysics and Quantum Electronics*, **2014, 57 (10).**

8) E.N. Pelinovsky, **E.G. Shurgalina**, Rodin A.A. On the criteria of the transition from breaking bore to undular bore. *Izvestiya, Atmospheric and Oceanic Physics*, 2015, 51 (2).

Theses:

9) T. Talipova, E. Pelinovsky, **E. Shurgalina,** Nonlinear Dispersive Focusing Mechanism of Rogue Wave Formation, International Workshop on Anomalous Waves in the Ocean, 2010. 29 november - 1 Desember, Taiwan

10) **E.G. Shurgalina,** E.N. Pelinovsky Mathematical model of freak wave on the wall and its numerical implementation, XVI Nizhny Novgorod session of young scientists, Nizhny Novgorod, 15-19 February, 2011, 250-253

11) E.Pelinovsky, A.Slunyaev, I.Didenkulova, A.Sergeeva, T.Talipova, I.Nikolkina, A.Rodin, **E. Shurgalina** Shallow rogue waves: Observations, Laboratory Experiments, Theories and Modelling, VI-th international conference “Solitons, Collapses and Turbulence: Achievements, Developments and Perspectives”, Russia, Novosibirsk, 4-8 June 2012, 212-213 p

12) **E.G. Shurgalina** Soliton turbulence of wave motions in shallow water in the frameworks of Korteweg-de Vries equation, XI International Youth Scientific - Technical Conference "The Future of Technical Sciences" 18 May 2012 , Nizhny Novgorod, Russia, 428

13) **E. Shurgalina**, E. Pelinovsky, A.Sergeeva, T.Talipova, A.Litra KdV–turbulence and extreme waves in shallow water, Geophysical Research Abstracts Vol.14, EGU2012-603, 2012, EGU General Assembly 2012

14) **E. Shurgalina** Life-time of freak waves of different shapes: Dispersive focusing framework, ROGUE WAVES International Workshop — 07 - 11 November 2011, Max Planck Institute for the Physics of Complex Systems , (Dresden)

15) E. Pelinovsky, Ch. Kharif , A.Slunyaev, I.Didenkulova, A.Sergeeva, T.Talipova, I.Nikolkina, A.Rodin, **E. Shurgalina** Rogue Waves in the Ocean as a Part of Marine Natural Hazards, 19ème Conférence Géologique de la Caraïbe – Guadeloupe, 21 - 26 March 2011, 174.

16) **E.G. Shurgalina** The dynamics of the freak waves in canals and rivers, the International Scientific Conference "Information Systems and Technology (IST-2012)", April 20, 2012

17) E. Pelinovsky, **E. Shurgalina** Approximated solutions in the theory of the wave

focusing in deep water, Geophysical Research Abstracts Vol.12, EGU2010-2480, 2010, EGU General Assembly 2010

18) E. Pelinovsky, **E. Shurgalina** Formation of an abnormal wave in case of interaction with a vertical barrier, Geophysical Research Abstracts Vol.13, EGU2011-44, 2011, EGU General Assembly 2011

19) **E. Shurgalina,** E. Pelinovsky Life-time of freak waves of different shapes: dispersive focusing framework, Geophysical Research Abstracts Vol.13, EGU2011-42, 2011, EGU General Assembly 2011

20) **E. Shurgalina,** E. Pelinovsky**,** Swell freak wave manifestation on the background weak wind wave field, Geophysical Research Abstracts Vol.14, EGU2012-128, 2012, EGU General Assembly 2012

21) **Shurgalina E.**, Pelinovsky E. Statistical moments of soliton field in shallow water. Geophysical Research Abstracts, 2013, 15, EGU2013-168.

22) **Shurgalina E.**, Pelinovsky E. Features of two-soliton interaction in shallow water, Geophysical Research Abstracts, 2013, 15, EGU2013-169.

23) Pelinovsky E., **Shurgalina E.** Dynamics of soliton fields in the framework of modified Korteweg – de Vries equation. Geophysical Research Abstracts, 2014, 16, EGU2014-1451.

24) **Shurgalina E.**, Kimmoun O., Kharif Ch., Pelinovsky E. Experimental study of soliton interaction with a vertical wall. Geophysical Research Abstracts, 2014, 16, EGU2014-3950.

25) **Shurgalina E.**, Pelinovsky E. Soliton turbulence and freak waves in shallow water. NZCS 22ND Annual conference: Raglan 2014, 78.

26) **Shurgalina E.**, Pelinovsky E. Freak waves in modified KdV soliton gas. Geophysical Research Abstracts, 2015, 17, EGU2015-1014.